

APPLICATIONS OF MODERN QUANTUM MECHANICAL THEORIES:
FROM PROPARGYL AND HYDROXYFORMYL RADICALS TO ADAMANTANE

by

GE YAN

(Under the Direction of Henry F. Schaefer III)

ABSTRACT

Modern quantum mechanical theories, including high-level *ab initio* methods and density functional theory, have been applied to a variety of molecular systems.

The first work performs a comprehensive anharmonic vibrational analysis of propargyl radical. A highly-accurate quartic force field was constructed with coupled-cluster including singles and doubles and perturbatively applied triple excitations [CCSD(T)] using the aug'-cc-pVTZ basis set, complemented with a quadratic force field extrapolated to the complete basis set limit using cc-pVXZ (X=T, Q, 5) basis sets. Fundamental vibrational frequencies were computed with the complete quartic force field based on vibrational perturbation theory.

In the second work, accurate electron affinities and ionization potentials of *trans*- and *cis*-hydroxyformyl radicals were determined via systematic *ab initio* investigations. State-of-the-art *ab initio* electronic structure theories combined with aug-cc-p(C)VXZ (X=2-6) basis sets were utilized to extrapolate to the complete basis set full configuration interaction limit via the focal point analysis method. Core-correlation effects, special relativity, zero-point vibrational energy, and diagonal Born-Oppenheimer corrections were explicitly incorporated in the results to provide accuracy to the level of 0.1 kcal mol⁻¹.

The last work examines optimal structures, energetics, and harmonic vibrational frequencies of adamantane and a variety of its derivatives using four different density functional methods and the DZP++ basis set. Electronic affinities, ionization potentials and other properties have been predicted.

INDEX WORDS: *ab initio* Method, Coupled-cluster Theory, Density Functional Theory, Quartic Force Field, Propargyl Radical, Electron Affinity, Ionization Potential, Hydroxyformyl Radical, Adamantane

APPLICATIONS OF MODERN QUANTUM MECHANICAL THEORIES:
FROM PROPARGYL AND HYDROXYFORMYL RADICALS TO ADAMANTANE

by

GE YAN

B.S., Tsinghua University, China, 2001

A Dissertation Submitted to the Graduate Faculty of The University of Georgia in Partial
Fulfillment of the Requirements for the Degree

DOCTOR OF PHILOSOPHY

ATHENS, GEORGIA

2005

© 2005

Ge Yan

All Rights Reserved

APPLICATIONS OF MODERN QUANTUM MECHANICAL THEORIES:
FROM PROPARGYL AND HYDROXYFORMYL RADICALS TO ADAMANTANE

by

GE YAN

Major Professor: Henry F. Schaefer III

Committee: Nigel G. Adams
Geoffrey D. Smith

Electronic Version Approved:

Maureen Grasso
Dean of the Graduate School
The University of Georgia
Aug 2005

To my parents,

ACKNOWLEDGEMENTS

Looking back into my 20 years of education, there are too many people that I wish to thank for their continuous support, help, and encouragement throughout my life.

First of all, I want to thank my parents, who brought me up, educated me, and encouraged me to pursue my career in science.

I am fortunate to have so many great teachers during my early days. I am especially grateful to my primary school mathematics teacher, Mrs. Zhou, my middle school mathematics teacher, Mrs. Yi, and my high school chemistry teacher, Dr. Wang, who supported my participation in the mathematics and chemistry Olympic competition and initiated my interest in science.

During my undergraduate study at the chemistry department of Tsinghua University, I have learned both fundamental and advanced knowledge of mathematics, physics, chemistry and so on from many passionate and knowledgeable professors. I am particularly thankful to my undergraduate advisor Dr. YU Jianyuan, who not only helps me carrying out independent research, but also cares my life and future as a good friend.

It is not possible for me to finish my doctoral study without so many wonderful professors, tutors, and friends at Center for Computational Chemistry. I am indebted to Professor Schaefer, one of the best advisors one could possibly have, who recruited me from China, provided me with a world-class research environment and resources, and oversaw my healthy growth as a scientist. Dr. Allen, Dr. Yamaguchi and Dr. Xie are all great teachers in teaching us the details in quantum mechanics, and more importantly, the way of independent and logic thinking. I also

want to thank my committee members, Prof. Adams, Prof. Smith, and Prof. Babcock, who spent their time on various stages of my pursuit of doctoral degree. I also want to thank many of the past and present CC(Q)C members. My tutor Dr. Barden led me into the door of computational chemistry. Ankan and Nate are wonderful colleagues for many helpful and fruitful discussions. Dr. Schuurmann has always been helpful in solving our computer problems and answering many scientific questions. Both Dr. Woodcock and Dr. Brinkmann have been great officemates to teach me how to conduct computational chemistry research. The support staff of CCC, Linda, Amy, Karen, and Richard, are greatly appreciated for their hard work to insulate us from all kinds of unrelated disturbance and help us better focus on our research.

My life will not be so meaningful and colorful without the countless friends I am fortunate to have both at United States and China. This is a long list but I do want to mention their names here: Li Mo, Xu Jinna, Sun Feng, Cao Jinghua, Wu Qi, Dr. Zhao, Xu Jie, Xu Dan, Hou Wei, Fan Lijun, He Yu, Wang Hao, Chen Chong, Chen Guo, Liu Niya, Ye Na, Xiong Maojun, Zhang Jun, Shen Shiming, Li Xinyu, Lie Yan, so on and on...

Finally, I truly thank my girlfriend, Yuan Cao, for sharing the joy and pain of being graduate students in a foreign country, and supporting each other during this hard but memorable stage in our lives.

TABLE OF CONTENTS

	Page
ACKNOWLEDGEMENTS.....	v
LIST OF TABLES.....	ix
LIST OF FIGURES.....	xii
CHAPTER	
1 INTRODUCTION AND BACKGROUND MATERIALS	1
1.1 AB INITIO METHODS	2
1.2 DENSITY FUNCTIONAL THEORY	4
1.3 LITERATURE REFERENCES.....	5
2 ANHARMONIC VIBRATIONAL ANALYSIS OF PROPARGYL RADICAL USING HIGHLY- ACCURATE AB INITIO QUARTIC FORCE FIELD.....	9
2.1 ABSTRACT	10
2.2 INTRODUCTION	10
2.3 THEORETICAL METHODS	15
2.4 RESULTS AND DISCUSSIONS	17
2.5 CONCLUSIONS.....	26
2.6 ACKNOWLEDGMENTS	26
2.7 REFERENCES.....	27
2.8 APPENDIX.....	33

3	STRUCTURES AND ENERGETICS OF HOCO RADICAL, ANION, AND CATION: HIGH-ACCURACY AB INITIO INVESTIGATION VIA FOCAL POINT ANALYSIS.....	58
	3.1 ABSTRACT	59
	3.2 INTRODUCTION	59
	3.3 COMPUTATIONAL METHODS.....	61
	3.4 RESULTS AND DISCUSSIONS	63
	3.5 SUMMARY	68
	3.6 ACKNOWLEDGMENTS	69
	3.7 REFERENCES.....	69
4	ENERGETICS AND STRUCTURES OF ADAMANTANE AND THE 1- AND 2-ADAMANTYL RADICALS, CATIONS AND ANIONS	86
	4.1 ABSTRACT	87
	4.2 INTRODUCTION	87
	4.3 METHODS	89
	4.4 RESULTS AND DISCUSSION	91
	4.5 CONCLUSIONS.....	96
	4.6 ACKNOWLEDGMENTS	97
	4.7 REFERENCES.....	97
5	CONCLUDING REMARKS	129

LIST OF TABLES

	Page
Table 2.1: Optimized geometry of propargyl radical (C_3H_3 , C_{2v})	35
Table 2.2: Symmetry internal coordinate definition for propargyl radical.....	36
Table 2.3: Harmonic vibrational frequencies of propargyl radical computed with different basis sets	37
Table 2.4: Anharmonic constants (in cm^{-1}) of propargyl radical.....	39
Table 2.5: Final vibrational frequency (in cm^{-1}) analysis of HCCCH ₂ , DCCCH ₂ , HCCCD ₂ , and DCCCD ₂	40
Table 2.6: Rotation-vibration interaction constants (in $10^{-3} cm^{-1}$) of propargyl radical	44
Table 2.7: Spectroscopic constants of propargyl radical	45
Table 2.8: Quadratic force constants (F_{ij}) extrapolation of propargyl radical	46
Table 2.9: Cubic force constants (F_{ijk}) extrapolation of propargyl radical	48
Table 2.10: Quartic force constants (F_{ijkl}) of propargyl radical.....	53
Table 3.1: The optimized geometrical parameters and rotational constants of <i>trans</i> - and <i>cis</i> -HOCO radical, anion, and cation	76
Table 3.2: Vibrational frequencies of <i>trans</i> - and <i>cis</i> -HOCO anion, radical, and cation.....	78
Table 3.3: Valence focal point analysis for adiabatic electron affinity (in eV) of <i>trans</i> - and <i>cis</i> -HOCO radicals.	80
Table 3.4: Valence focal point analysis for vertical detachment energy (in eV) of <i>trans</i> - and <i>cis</i> -HOCO radicals.	81

Table 3.5: Valence focal point analysis for adiabatic and vertical ionization potential (in eV) of <i>trans</i> -HOCO radical	82
Table 3.6: Determination of adiabatic electron affinity (AEA), vertical detachment energy (VDE), adiabatic and vertical ionization potentials (AIP, VIP) of <i>trans</i> - and <i>cis</i> -HOCO radicals.....	83
Table 3.7: Focal point analysis of core-correlation effects (in eV) for adiabatic electron affinity, vertical detachment energy, and ionization potentials of <i>trans</i> - and <i>cis</i> -HOCO radicals.....	84
Table 4.1: Optimized geometry of adamantane (C ₁₀ H ₁₆ , T _d).....	103
Table 4.2: Optimized structures of the 1-adamantyl radical (C ₁₀ H ₁₅ , C _{3v}).....	104
Table 4.3: Optimized structures of the 1-adamantyl cation (C ₁₀ H ₁₅ , C _{3v}).....	105
Table 4.4: Optimized structures of the 1-adamantyl anion (C ₁₀ H ₁₅ , C _{3v}).....	106
Table 4.5: Optimized structures of the 2-adamantyl radical (C ₁₀ H ₁₅ , C _s)	107
Table 4.6: Optimized structures of the 2-adamantyl cation (C ₁₀ H ₁₅ , C _s).....	109
Table 4.7: Optimized structures of the 2-adamantyl anion (C ₁₀ H ₁₅ , C _s)	111
Table 4.8: Total electronic energies in hartrees and relative electronic energies in kJ mol ⁻¹ of the 1-adamantyl cation, anion, and radical.....	113
Table 4.9: Total electronic energies in hartrees and relative electronic energies in kJ mol ⁻¹ of the 2-adamantyl cation, anion, and radical.....	114
Table 4.10: Adiabatic ionization potentials (in eV) of the 1- and 2-adamantyl radicals	115
Table 4.11: Adiabatic electron affinities (in eV) of the 1- and 2-adamantyl radicals	116
Table 4.12: Observed and computed vibrational wavenumbers ω_e (in cm ⁻¹) for adamantane. ..	117

Table 4.13: Harmonic vibrational wavenumbers ω_e (in cm^{-1}) for the 1-adamantyl radical, anion, and cation by the B3LYP method	120
Table 4.14: Harmonic vibrational wavenumbers ω_e (in cm^{-1}) for the 2-adamantyl radical, anion, and cation by the B3LYP method	124

LIST OF FIGURES

	Page
Figure 2.1: Propargyl radical, C_3H_3 , C_{2v} symmetry	34
Figure 3.1: Equilibrium geometries of <i>trans</i> - and <i>cis</i> -isomers of HOCO species, C_s symmetry .	75
Figure 4.1: Adamantane ($C_{10}H_{16}$), T_d symmetry	100
Figure 4.2: 1-Adamantyl radical, 1-adamantyl cation, and 1-adamantyl anion ($C_{10}H_{15}$), C_{3v} symmetry	101
Figure 4.3: 2-Adamantyl radical, 2-adamantyl cation, and 2-adamantyl anion ($C_{10}H_{15}$), C_s symmetry	102

CHAPTER 1

INTRODUCTION AND BACKGROUND MATERIALS

Modern chemistry, apart from its original white-coat and lab-bench image, has evolved into an era where theoretical computations are as important as experiments. With the continuously increasing computing power and development of various methods for different situations, computational chemistry has become an indispensable component in modern chemistry by not only confirming or challenging experimental results, but also predicting properties that cannot be easily determined by experiments. Applications of computational chemistry range from the determination of optimal ground and transition state geometries, mapping of potential energy surfaces, to the assignment of vibrational frequencies and prediction of many other physical and chemical properties.

Two approaches of computational chemistry methods, *ab initio* and density functional theory, were routinely utilized in my doctoral research and will be presented here. Choice of specific theoretical methods usually depends on the size and accuracy requirement of the system under investigation.

1.1 AB INITIO METHODS

Traditional *ab initio* quantum mechanical methods aim at the computation of electronic energy of molecular systems from first principles. Since it is impossible to solve Schrödinger's equation exactly for most practical chemical systems with current computing power, different levels of approximations have made it possible to carry out practical computations with control over both accuracy and computing cost.

Most commonly used *ab initio* methods in computational chemistry include Hartree-Fock,^{1,2} Møller-Plesset perturbation theory,^{3,4} configuration interaction,² and coupled-cluster theory.⁵⁻⁹ Combination of large basis sets and high-level *ab initio* theories can usually yield results that achieve chemical or even subchemical accuracies.

In Chapter 2, a comprehensive anharmonic vibrational analysis has been performed on propargyl radical, a key intermediate in the soot formation process.¹⁰ A highly-accurate quartic force field was constructed with coupled-cluster including singles and doubles and perturbatively applied triple excitations [CCSD(T)] using the correlation-consistent basis set denoted as [C/H=aug-cc-pVTZ/cc-pVTZ], complemented with a quadratic force field extrapolated to the complete basis set limit using cc-pVXZ (X=T, Q, 5) basis sets.^{11,12} Based on vibrational perturbation theory,¹³ spectroscopic properties including the fundamental vibrational frequencies, vibration-rotation constants, rotational constants with zero-point corrections, centrifugal distortion constants and so on can be predicted which will help its identification in future studies.

In Chapter 3, highly-accurate focal point analysis method developed by Allen and coworkers¹⁴⁻¹⁷ has been applied to the *trans*- and *cis*-HOCO cation, radical, and anion systems. HOCO radical was shown as a critical intermediate in the OH + CO → H + CO₂ reaction, a key reaction for the production of CO₂ in combustion.¹⁸ State-of-the-art *ab initio* electronic structure theories including Hartree-Fock, second order Møller-Plesset perturbation theory, CCSD, CCSD(T), and CCSDT combined with aug-cc-p(C)VXZ (X=2-6) basis sets were utilized to extrapolate electronic energies to the complete basis set full configuration interaction limit. Accurate electron affinities and ionization potentials of *trans*- and *cis*-HOCO radicals were determined by including additional core-correlation effects, special relativity, zero-point vibrational energy, and diagonal Born-Oppenheimer corrections to provide accuracy to the level of 0.1 kcal mol⁻¹.

The *ab initio* calculations were carried out with Molpro,¹⁹ NWChem,^{20,21} ACESII,²² and PSI²³ computational chemistry software packages.

1.2 DENSITY FUNCTIONAL THEORY

Although *ab initio* method can usually yield highly accurate results, its large scaling limits its applications to large molecular systems. For example, CCSD(T) method formally scales as N^7 , where N is the number of basis functions, making it prohibitively expensive to be applied to systems containing more than five heavy atoms. Density functional theory (DFT), on the other hand, has been shown to be a relatively inexpensive yet reliable theoretical method. It has been successful in predicting many physical and chemical properties of larger molecular systems which cannot be handled by current high level *ab initio* methods, at the cost of less accuracy. For example, using a moderate DZP++ basis set,²⁴⁻²⁶ DFT has been exhaustively tested and shown to predict the electron affinity of many molecules to within 0.2eV of the experimentally reported values.²⁷

In DFT, the electronic energy depends on electron density instead of the wave function in the Schrödinger equation. DFT energy functional can be divided into several components:

$$E[\rho(r)] = E_T + E_V + E_J + E_X + E_C$$

where the five terms represent the kinetic energy of the non-interacting electrons, the nuclear-electron interaction, the classical electron-electron repulsion, the correction to the kinetic energy deriving from the interacting nature of the electrons (exchange correction), and all non-classical corrections to the electron-electron repulsion energy (correlation correction), respectively.

The exchange and correlation functionals are more difficult terms and various exchange and correlation functionals have been proposed in DFT. One of the earliest and most widely used is the Local Spin Density Approximation (LSDA) which treats electron density locally as a uniform electron gas. This functional employs the 1980 correlation functional of Vosko, Wilki, and

Nusair²⁸ and the exchange functional of Slater.²⁹ This functional was known to over-bind molecules. There are two types of functionals which added correction terms to LSDA: the Generalized Gradient Approximation (GGA) which introduces the derivative of the density as a non-local component, and the Hybrid functionals which includes some mixing with Hartree-Fock. Typical functionals used in DFT include B3LYP^{30,31}, BHLYP³², BLYP³³ and BP86.³⁴

In Chapter 4, four different DFT methods were applied to study the geometries, vibrational frequencies, and energies of adamantane and its radicals, cations, and anions. Adamantane and its derivatives have found a broad range of chemical, polymer, and pharmaceutical applications after Schleyer's innovative synthesis in 1957.³⁵ Electron affinities, vertical detachment energies, and ionization potentials were reported to assist future studies on these species. The DFT calculations were carried out with the Gaussian 94 software package.³⁶

1.3 LITERATURE REFERENCES

- (1) Roothaan, C. C. J. *Rev. Mod. Phys.* **1951**, 23, 69.
- (2) Szabo, A.; Ostlund, N. S. *Modern Quantum Chemistry*; McGraw-Hill: New York, 1989.
- (3) Moller, C.; Plesset, M. S. *Phys. Rev.* **1934**, 46, 618.
- (4) Pople, J. A.; Binkley, J. S.; Seeger, R. *Int. J. Quantum Chem. Symp.* **1976**, 10, 1.
- (5) Purvis, G. D.; Bartlett, R. J. *J. Chem. Phys.* **1982**, 76, 1910.
- (6) Raghavachari, K.; Trucks, G. W.; Pople, J. A.; Head-Gordon, M. *Chem. Phys. Lett.* **1989**, 157, 479.
- (7) Scuseria, G. E.; Lee, T. J. *J. Chem. Phys.* **1990**, 93, 5851.
- (8) Scuseria, G. E. *Chem. Phys. Lett.* **1991**, 176, 27.
- (9) Scuseria, G. E.; Schaefer, H. F. *Chem. Phys. Lett.* **1988**, 152, 382.

- (10) Westmoreland, P. R.; Dean, A. M.; Howard, J. B.; Longwell, J. P. *J. Phys. Chem.* **1989**, *93*, 8171.
- (11) Dunning, T. H. *J. Chem. Phys.* **1989**, *90*, 1007.
- (12) Kendall, R. A.; Dunning, T. H.; Harrison, R. J. *J. Chem. Phys.* **1992**, *96*, 6769.
- (13) Watson, J. K. G. *J. Chem. Phys.* **1968**, *48*, 4517.
- (14) East, L. L. A.; Allen, W. D. *J. Chem. Phys.* **1993**, *99*, 4638.
- (15) Kenny, J. P.; Allen, W. D.; Schaefer, H. F. *J. Chem. Phys.* **2003**, *118*, 7353.
- (16) Schuurman, M. S.; Muir, S. R.; Allen, W. D.; Schaefer, H. F. *J. Chem. Phys.* **2004**, *120*, 11586.
- (17) Wheeler, S. E.; Allen, W. D.; Schaefer, H. F. *J. Chem. Phys.* **2004**, *121*, 8800.
- (18) Smith, I. W. M. *Chem. Phys. Lett.* **1977**, *49*, 112.
- (19) MOLPRO is a package of ab initio programs written by H.-J. Werner, P. J. Knowles, M. Schütz, R. Lindh, P. Celani, T. Korona, G. Rauhut, F. R. Manby, R. D. Amos, A. Bernhardsson, A. Berning, D. L. Cooper, M. J. O. Deegan, A. J. Dobbyn, F. Eckert, C. Hampel, G. Hetzer, A. W. Lloyd, S. J. McNicholas, W. Meyer, M. E. Mura, A. Nicklaß, P. Palmieri, R. Pitzer, U. Schumann, H. Stoll, A. J. Stone, R. Tarroni, and T. Thorsteinsson.
- (20) Straatsma, T.P.; Aprà, E.; Windus, T.L.; Bylaska, E.J.; de Jong, W.; Hirata, S.; Valiev, M.; Hackler, M. T.; Pollack, L.; Harrison, R. J.; Dupuis, M.; Smith, D.M.A; Nieplocha, J.; Tipparaju V.; Krishnan, M.; Auer, A. A.; Brown, E.; Cisneros, G.; Fann, G. I.; Fruchtl, H.; Garza, J.; Hirao, K.; Kendall, R.; Nichols, J.; Tsemekhman, K.; Wolinski, K.; Anchell, J.; Bernholdt, D.; Borowski, P.; Clark, T.; Clerc, D.; Dachsel, H.; Deegan, M.; Dyllal, K.; Elwood, D.; Glendening, E.; Gutowski, M.; Hess, A.; Jaffe, J.; Johnson, B.; Ju, J.; Kobayashi, R.; Kutteh, R.; Lin, Z.; Littlefield, R.; Long, X.; Meng, B.; Nakajima, T.; Niu, S.; Rosing, M.; Sandrone, G.; Stave, M.; Taylor, H.; Thomas, G.;

van Lenthe, J.; Wong, A.; Zhang, Z.; "NWChem, A Computational Chemistry Package for Parallel Computers, Version 4.6" (2004), Pacific Northwest National Laboratory, Richland, Washington 99352-0999, USA.

(21) Kendall, R.A.; Aprà, E.; Bernholdt, D.E.; Bylaska, E.J.; Dupuis, M.; Fann, G.I.; Harrison, R.J.; Ju, J.; Nichols, J.A.; Nieplocha, J.; Straatsma, T.P.; Windus, T.L.; Wong, A.T. *Computer Phys. Comm.*, **2000**, *128*, 260

(22) ACES II is a program product of the Quantum Theory Project, University of Florida. Authors: J. F. Stanton, J. Gauss, J. D. Watts, M. Nooijen, N. Oliphant, S. A. Perera, P. G. Szalay, W. J. Lauderdale, S. R. Gwaltney, S. Beck, A. Balkova D. E. Bernholdt, K.-K Baeck, P. Rozyczko, H. Sekino, C. Hober, and R.J. Bartlett. Integral packages included are VMOL (J. Almlöf and P. R. Taylor); VPROPS (P. Taylor); ABACUS (T. Helgaker, H.J. Aa. Jensen, P. Jørgensen, J. Olsen, and P. R. Taylor).

(23) T. Daniel Crawford, C. David Sherrill, Edward F. Valeev, Justin T. Fermann, Rollin A. King, Matthew L. Leininger, Shawn T. Brown, Curtis L. Janssen, Edward T. Seidl, Joseph P. Kenny, and Wesley D. Allen, PSI 3.2, 2003.

(24) Huzinaga, S. *J. Chem. Phys.* **1965**, *42*, 1293.

(25) Dunning, T. H. *J. Chem. Phys.* **1970**, *53*, 2823.

(26) Lee, T. J.; Schaefer, H. F. *J. Chem. Phys.* **1985**, *83*, 1784.

(27) Rienstra-Kiracofe, J. C.; Tschumper, G. S.; Schaefer, H. F.; Nandi, S.; Ellison, G. B. *Chem. Rev.* **2002**, *102*, 231.

(28) Vosko, S. H.; Wild, L.; Nusair, M. *Can. J. Phys.* **1980**, *58*, 1200.

(29) Slater, J. C. *Quantum Theory of Molecules and Solids: The Self-Consistent Field for Molecules and Solids*; McGraw-Hill: New York, **1974**; Vol. IV.

- (30) Becke, A. D. *J. Chem. Phys.* **1993**, 98, 5648.
- (31) Lee, C.; Yang, W.; Parr, R. G. *Phys. Rev. B.* **1988**, 37, 785.
- (32) Becke, A. D. *J. Chem. Phys.* **1993**, 98, 1372.
- (33) Becke, A. D. *Phys. Rev. A.* **1988**, 38, 3098.
- (34) Perdew, J. P. *Phys. Rev. B.* **1986**, 33, 8822.
- (35) Schleyer, P. v. R. *J. Am. Chem. Soc.* **1957**, 79, 3292.
- (36) Gaussian 94, Revision C.3, M. J. Frisch, G. W. Trucks, H. B. Schlegel, P. M. W. Gill, B. G. Johnson, M. A. Robb, J. R. Cheeseman, T. Keith, G. A. Petersson, J. A. Montgomery, K. Raghavachari, M. A. Al-Laham, V. G. Zakrzewski, J. V. Ortiz, J. B. Foresman, J. Cioslowski, B. B. Stefanov, A. Nanayakkara, M. Challacombe, C. Y. Peng, P. Y. Ayala, W. Chen, M. W. Wong, J. L. Andres, E. S. Replogle, R. Gomperts, R. L. Martin, D. J. Fox, J. S. Binkley, D. J. Defrees, J. Baker, J. P. Stewart, M. Head-Gordon, C. Gonzalez, and J. A. Pople, Gaussian, Inc., Pittsburg, PA, U.S.A., 1995.

CHAPTER 2

ANHARMONIC VIBRATIONAL ANALYSIS OF PROPARGYL RADICAL USING HIGHLY-ACCURATE AB INITIO QUARTIC FORCE FIELD

¹Yan, G.; Allen, W. D.; Schaefer, H. F.; *To be submitted*

2.1 ABSTRACT

A complete and highly-accurate *ab initio* anharmonic quartic force field for the ground electronic state of the propargyl radical (\tilde{X}^2B_1 HC₃H₂) has been constructed by means of [C/H]=[aug-cc-pVTZ/cc-pVTZ] CCSD(T) methodology. Combined with a complete basis set limit quadratic force field including core-correlation effect, a comprehensive anharmonic vibrational analysis of propargyl radical was carried out based on second-order vibrational perturbation theory. A complete set of harmonic and fundamental frequencies, Coriolis, vibration-rotation interaction, and centrifugal distortion constants have been predicted. The linear bending vibrational modes are found to be extremely sensitive to the size of the correlation consistent basis sets used in the calculations. This analysis removes previous discrepancies in vibrational frequency assignments and assists further study for this important soot formation intermediate. The final harmonic frequencies for propargyl radical (in cm⁻¹) with associated anharmonic corrections in parentheses, are: $\omega_1(a_1)=3458.2$ (-122.1), $\omega_2(a_1)=3168.5$ (-123.5), $\omega_3(a_1)=1991.5$ (-63.1), $\omega_4(a_1)=1467.8$ (-18.4), $\omega_5(a_1)=1064.1$ (-1.6), $\omega_6(b_1)=674.4$ (14.5), $\omega_7(b_1)=498.4$ (26.6), $\omega_8(b_1)=391.6$ (6.0), $\omega_9(b_2)=3271.6$ (-147.4), $\omega_{10}(b_2)=1036.3$ (-6.2), $\omega_{11}(b_2)=626.9$ (20.3), $\omega_{12}(b_1)=334.2$ (6.7).

2.2 INTRODUCTION

Propargyl radical (H₂CC≡CH) has long been recognized as a fundamental species in combustion processes.¹ Many studies have shown the importance of propargyl radical reaction routes in the formation of large polyaromatic hydrocarbons (PAHs) and soot.²⁻¹⁰ For example, *ab initio* investigation⁴ as well as shock-tube study of hydrocarbon pyrolysis⁵ have provided compelling experimental evidence that propargyl radical is a possible precursor to benzene formation.

However, spectroscopic studies on the propargyl radical were rather incomplete and inconclusive. Ramsay and Thistlethwaite¹¹ observed and tentatively assigned diffuse gas-phase electronic absorption bands around 30000 cm^{-1} to propargyl radical during the flash photolysis of propargyl bromide, propargyl chloride, methylacetylene, allene, and other compounds in 1966. Early electron spin resonance (ESR) spectrum of propargyl radical obtained by Fessender and Schuler¹², Kochi and Krusic¹³ and Kasai¹⁴ confirmed its planar structure with a C_{2v} symmetry. Jacox and Milligan¹⁵ carried out an early argon matrix isolation study on the vibrational assignment of C_3H , C_3H_2 , and C_3H_3 radicals produced by the vacuum ultraviolet (VUV) photolysis of methylacetylene, allene and their deuterated isotopomers in 1974, and have assigned four vibrational frequencies at 3310 , 688 , 548 , and 484 cm^{-1} to the propargyl radical. Based on the isotopic effect, bands at 3310 and 688 cm^{-1} were assigned to the C-H stretching and C-C-H bending vibrations, respectively, while the 484 cm^{-1} band was attributed to the skeletal bending vibration. They have also observed the electronic transition reported earlier in the gas phase by Ramsay and Thistlethwaite.¹¹ Later Huang and Graham¹⁶ performed Fourier transform infrared (FT-IR) study on tricarbon hydride species prepared by similar methods, and they have only been able to confirm the vibrational frequency assignment of ν_1 band at 3308.8 cm^{-1} to propargyl radical that was observed for different isotopomers. Owing to the observed discrepancy in the intensity of the 686.5 cm^{-1} absorption relative to the 3308.8 cm^{-1} band on annealing and irradiation with light, they have reassigned the vibration of 686.5 cm^{-1} to the $\nu_{12}(a')$, C-H bending mode of ethylenic cyclopropenyl, which was predicted by Chipman and Miller¹⁷ at 616 cm^{-1} with their 3-21G MCSCF calculation. Huang and Graham¹⁶ have also reassigned the 547.3 cm^{-1} band to triplet propargylene, which was reported earlier by Maier and co-workers¹⁸ at 550.4 cm^{-1} in their argon matrix isolation infrared spectroscopy study on

propargylene prepared by photolysis of diazopropyne or cyclopropenylidene. The assignment of the 483.5 cm^{-1} band was left undetermined by Huang and Graham, because the observed small shifts ($2\text{-}4\text{ cm}^{-1}$) in vibrational frequencies for deuterated propargyl radical was inconsistent with their approximate calculations, which yields shifts of $\sim 80\text{-}100\text{ cm}^{-1}$ using 4-31G MCSCF optimized geometry of Honjou, Yoshimine, and Pacansky¹⁹ and empirical force constants. The adiabatic ionization potential of propargyl radical was determined in 1972 by Lossing²⁰ to be 8.68 eV from electron impact experiment, which was later confirmed by Minsek and Chen²¹ who obtained $8.67\pm 0.02\text{ eV}$ from laser photo ionization mass and photoelectron spectroscopy in 1990.

More recently, Morter and co-workers²² investigated the ν_1 acetylenic CH stretch band of the propargyl radical by means of infrared laser kinetic spectroscopy at Doppler limited resolution. The radical was prepared by flash photolysis of propargyl bromide or chloride at 193 nm and the band origin was determined to be $3322.287(2)\text{ cm}^{-1}$. Ground and excited state rotational constants were determined as $B''=0.31757(8)\text{ cm}^{-1}$, $C''=0.30705\text{ cm}^{-1}$, $B'=0.31680(7)\text{ cm}^{-1}$, and $C'=0.30643(7)\text{ cm}^{-1}$. Morter *et al.*⁹ have directly probed the products and rate of propargyl + propargyl recombination using IR kinetic absorption spectroscopy in 1994, showing that propargyl radicals play a key role in the formation of benzene. Sumiyoshi *et al.*²³ and Tanaka *et al.*²⁴ have applied infrared diode laser spectroscopy to the propargyl radical produced by 193 nm excimer laser photolysis of allene, and the ν_6 CH_2 -wagging band origin was accurately determined to be $687.17603(62)\text{ cm}^{-1}$, consistent with the earlier matrix isolation study by Jacox and Milligan.¹⁵ Molecular constants including rotational, spin-rotation interaction, centrifugal distortion, and hyperfine coupling constants have also been reported for the $^2\text{B}_1$ ground vibrational state in the diode laser spectroscopy study²⁴ and Fourier-transform microwave (FTMW) spectroscopy study.²⁵ Yuan, DeSain, and Curl²⁶ extended the work of Tanaka *et al.*²⁴ by

analyzing the K-Subband structure of the ν_1 acetylenic CH stretch band of the propargyl radical and fitting its rotational constants of the upper state. In addition, Y. T. Lee and co-workers have performed cross molecular beam studies of the attack of carbon atoms on ethylene to give propargyl radical.²⁷ High-resolution infrared spectrum on the acetylenic C-D stretching fundamental of monodeuterated propargyl radical (CH_2CCD) have been observed by Eckhoff, Miller, Billera, Engel and Curl²⁸, in which a band origin at $2557.33(7) \text{ cm}^{-1}$ and several rotational constants were determined. The ultraviolet absorption spectrum and cross sections of propargyl radicals have been determined in the gas phase in the spectral range of 230-300 nm by Fahr, Hassanzadeh, Laszlo, and Huie.²⁹ Deyerl, Fischer, and Chen³⁰ studied the photodissociation dynamics of the propargyl radical upon UV excitation via time- and frequency-resolved detection of hydrogen atoms. Gilbert, Pfab, Fischer, and Chen³¹ have reported an ionization energy of 8.673 eV for propargyl radical and vibrational frequencies for the totally symmetric normal modes of the propargyl cation by means of zero kinetic energy photoelectron spectrum. Wyss, Riaplov, and Maier have observed bands in the electronic absorption spectra of the propargyl radical, its cation and their deuterated isotopomers in neon matrices.³² The permanent electric dipole moment of ground-state propargyl radical has been determined to be -0.150D by Kupper, Merritt, and Miller.³³

There have also been abundant theoretical studies on the propargyl radical. The early theoretical works^{17,19,34-36} are generally of low quality with small basis set such as 4-31G and methodologies that do not include electronic correlation effects. These calculations generally agreed upon the C_{2v} symmetry structure for X^2B_1 propargyl radical, and Honjou *et al*¹⁹ also computed the harmonic vibrational frequencies with 4-31G SCF method. In 1992 Melius, Miller and Evleth⁴ applied bond additivity corrected Moller-Plesset fourth-order perturbation theory

(BAC-MP4) to predict various reaction paths for the propargyl + propargyl reaction system. Botschwina and co-workers³⁷ conducted an early and extensive high-level *ab initio* investigation on the propargyl radical system with several correlation methods including multi-reference averaged coupled pair functional (MR-ACPF) and coupled electron pair approximation (CEPA-1) with a basis set of cc-pVTZ quality. Harmonic vibrational frequencies as well as anharmonic corrections to the five totally symmetric modes of propargyl radical were reported, and quartic centrifugal distortion constants have been derived. Their study confirmed the assignment of matrix absorption at 686.5 and 483.5 cm^{-1} to the CH_2 wagging and out-of-plane CCH bending vibrations, respectively.

Very recently, the production of propargyl radicals from reactive collisions of singlet methylene with acetylene has been observed by infrared kinetic spectroscopy,³⁸ and electronic structure theory has been used to map the surfaces for this process.³⁹ Vereecken, Pierloot, and Peeters⁴⁰ studied the potential energy surface of the reaction $\text{CH}(X^2\Pi)+\text{C}_2\text{H}_2$ which produces various C_3H_x ($x=1-3$) radicals using 6-31G** B3LYP methodology, and have obtained vibrational frequency wave numbers with scaling factors. Topological analysis of the electron localization function (ELF) was applied to the bonding in the propargyl radical by Krokidis, Moriarty, Lester, and Frenklach⁴¹, which proposed a resonance structure of almost equal contributions of propargyl and allenyl forms for propargyl radical and explained the anomalously high frequency for the in-plane C-C-H bending mode compared to the frequency of the out-of-plane C-C-H bending mode. In 2000, Botschwina and co-workers⁴² re-investigated the equilibrium structure and ionization potential of propargyl radical with a cc-pCVQZ basis set at the CCSD(T) level of theory, and arrived at an adiabatic ionization potential of 8.684 eV, in good agreement with the experimental value of 8.673 eV.³¹ Le, Mebel and Kaiser⁴³ have investigated

the potential energy surface for the reaction of the ground-state carbon atom with the propargyl radical using the G2M (rcc, MP2) method in 2001. The most recent study on propargyl radical was conducted by Jochnowitz *et al.*, who performed both infrared absorption spectroscopy and ANO CCSD(T) calculations on the vibrational spectrum of propargyl radical.⁴⁴ Nine of the twelve vibrational frequencies of propargyl radical have been identified from the infrared spectrum, and their assignments have been ascertained by the *ab initio* calculations.

2.3 THEORETICAL METHODS

Electronic energies of ground-state propargyl radical were determined by means of three electron-correlation procedures, which include the second-order Moller-Plesset perturbation theory (MP2),⁴⁵⁻⁴⁸ coupled-cluster singles and doubles method (CCSD),⁴⁹⁻⁵¹ and CCSD augmented by a quasiperturbative term arising from connected triple excitations [CCSD(T)].^{52,53} In each instance the reference electronic wave functions were constructed from single-configuration, restricted open-shell Hartree-Fock (ROHF) molecular orbitals.^{47,48,54} The atomic-orbital basis sets used in the electronic structure calculations were Dunning and coworkers⁵⁵⁻⁵⁷ correlation consistent families of basis sets denoted as (aug)-cc-p(C)VXZ.

CCSD(T) analytic gradient technique⁵⁸ was utilized to optimize the geometric structures to 10^{-6} Å or rad in the internal coordinate space. Since analytical second and higher-order derivatives are not available at the CCSD(T) level of theory, the complete set of quadratic, cubic, and quartic force constants were determined by finite difference method at the CCSD(T) level from analytic first derivatives. In all numerical differentiation schemes, displacement increments of ± 0.01 Å and ± 0.02 radius were employed for the various symmetry internal coordinates. A total of 580 displacements about the optimized geometry were computed to obtain the complete

quartic force field. Analytical first gradients were converged to 10^{-12} a.u./Å or a.u./rad at the CCSD(T) level of theory. The aug²-cc-pVTZ basis set, which refers to the combination of [C/H]=[aug-cc-pVTZ/cc-pVTZ], was used in the geometry optimization and quartic field computations. All electrons were correlated in the analytic gradient calculations. The electronic structure computations was performed with the program packages ACESII.⁵⁹

In addition, a complete basis set (CBS) limit quadratic force field was constructed by finite differences of energy points. Each of the energy points was extrapolated to the CBS limit using cc-pVXZ (X=T, Q, 5) CCSD(T) energy points based on the focal point analysis scheme developed by Allen and coworkers.⁶⁰ The functional form for the Hartree-Fock extrapolation is

$$E_{HF} = E_{HF}^{\infty} + ae^{-bX}$$

whereas the correlation energy was extrapolated via

$$E_{corr} = a + bX^{-3}$$

Additional core-correlation effects were computed by means of cc-pCVQZ CCSD(T) calculations. To further gauge the basis set dependency of vibrational modes, aug-cc-pVXZ (X=T, Q) basis sets, which include additional set of diffuse functions to the corresponding cc-pVXZ basis sets, were also used in the quadratic force field calculations. With each basis set, a new equilibrium geometry was determined and the quadratic and cubic force constants were shifted to the new r_e structure. The 1s core orbitals of the carbon atom were frozen in the correlation treatment except for the core-correlation effect calculation. All energy points were converged to 10^{-12} hartrees. The electronic structure computations for the complete basis set limit quadratic force field were performed with the program packages Molpro.⁶¹

Harmonic vibrational analysis was performed with the quadratic force field computed with different basis sets, and normal modes (Q_i) were quantitatively assigned in internal coordinates by means of the associated total energy distributions (TEDs).⁶²⁻⁶⁴

The anharmonic vibrational analysis of the propargyl radical was performed via application of second-order perturbation theory to the standard vibration-rotation Hamiltonian⁶⁵ containing a potential energy surface expansion through quartic terms. The use of *ab initio* anharmonic force fields in this approach has been investigated extensively in recent systematic studies of linear and asymmetric top molecules by Allen and co-workers⁶⁶⁻⁷² and other groups.⁷³⁻⁷⁶ The INTDER2000^{77,78} and ANHARM programs were utilized in the anharmonic vibrational analysis.

2.4 RESULTS AND DISCUSSIONS

A. EQUILIBRIUM GEOMETRY AND QUARTIC FORCE FIELD

Ground electronic state (X^2B_1) of propargyl radical is predicted to be in the C_{2v} symmetry at the aug'-cc-pVTZ CCSD(T) level of theory, consistent with early experimental and theoretical studies.^{13,14,37,44} The optimized equilibrium structure of propargyl radical is shown in Figure 1, and the geometrical parameters are summarized in Table 1. Our optimized equilibrium structure is in good agreement with recent *ab initio* works.^{37,42,44} The largest difference in bond length with the cc-pCVQZ CCSD(T) result is less than 0.004 Å and the bond angle differs by at most 0.08 degree, an expected outcome considering the high level of theory used in these studies.

Propargyl radical (C_3H_3) has twelve vibrational modes, including 5 a_1 , 3 b_1 , and 4 b_2 normal modes. In the complete quartic force field, it has 31 quadratic, 115 cubic, and 420 quartic symmetry-unique force constants. The numerical differentiation procedure shown in the APPENDIX was carried out in terms of the symmetry internal coordinate to obtain the full

quartic force field. The symmetry internal coordinate is depicted in Figure 1, with definitions and descriptions illustrated in Table 2.

To ensure the accuracy of the quartic force field, each higher order force constant of the final quartic force field was obtained by averaging over different numerical differentiation schemes from available analytical first derivative data. Due to the stringent convergence criteria employed in the analytic CCSD(T) analytical derivative computations, these higher order force constants show high degrees of internal consistency among different differentiation schemes. Some of the representative force constants and their corresponding differentiation schemes are: $F_{8,7,3,2}=\{0.149689 (2\ 3,7\ 8), 0.149836 (3\ 2,7\ 8), 0.149621 (7\ 2,3\ 8), 0.149572 (8\ 2,3\ 7)\}$ aJ Å⁻² rad⁻², $F_{11,10,4,3}=\{0.111419 (3\ 4,10\ 11), 0.111428 (4\ 3,10\ 11), 0.11139 (10\ 3,4\ 11), 0.111478 (11\ 3,4\ 10)\}$ aJ Å⁻¹ rad⁻³, $F_{11,9,4,1}=\{-0.0108557 (1\ 4, 9\ 11), -0.0108446 (4\ 1, 9\ 11), -0.0108648 (9\ 1, 4\ 11), -0.0109028 (11\ 1, 4\ 9)\}$ aJ Å⁻³ rad⁻¹, and $F_{9,9,4,3}=\{-0.459498 (3\ 4, 9\ 9), -0.459212 (4\ 3, 9\ 9), -0.458837 (9\ 3, 4\ 9)\}$ aJ Å⁻⁴.

In addition, quadratic force constants were obtained with different basis sets to assess their basis set dependence, and the CBS extrapolated quadratic force field with core-correlation effects was used in the final construction of the quartic force field. The full set of quadratic, cubic, and quartic force constants are given in supplementary materials (Tables S1 - S3).

Note that Botschwina and co-workers³⁷ have also reported the potential energy function terms for the ground electronic state of propargyl radical determined at the cc-pVTZ CEPA-1 level, but they have only reported the terms for the totally symmetric (*a*₁) vibrations. And even in the totally symmetric vibrational space, off-diagonal constants were obtained only to third order. Our complete and more accurate anharmonic force field includes the entire diagonal and off-diagonal elements for all vibrational modes (*a*₁, *b*₁, and *b*₂), which enables the determination

of more precise and comprehensive fundamental frequencies and spectroscopic constants as described in the following sections.

B. HARMONIC VIBRATIONAL FREQUENCIES

From the quadratic force field, harmonic vibrational frequencies were computed with different basis sets, and the results are shown in Table 3. The harmonic frequencies show internal consistency and convergence with increasing size of basis sets toward the CBS limit. It is of great interest to note the characteristic basis set dependence of different vibrational normal modes.

For all the a_1 vibrational modes, the basis set effect on the vibrational frequencies is relatively small. For example, there is essentially no change for the ω_2 C-H symmetric stretching mode when the basis is increased from cc-pVTZ basis set to the CBS limit. For the other four stretching and scissoring normal modes in the a_1 symmetry, the largest difference of harmonic vibrational frequencies between the cc-pVTZ and CBS limit is a decrease of 6 cm^{-1} for the ω_4 CH₂ scissoring mode. Diffuse functions introduced in the aug-cc-pVTZ basis set decreases ω_1 - ω_4 by an average of 8 cm^{-1} , with no effect on the ω_5 C-C stretching mode. Additional diffuse functions to the cc-pVQZ basis set have only decreased at most 2 cm^{-1} for all the a_1 harmonic vibrational frequencies. The core-correlation effects computed at the cc-pCVQZ CCSD(T) level add an average of 5 cm^{-1} to the theoretical harmonic frequencies for all the a_1 modes.

The situation changes, however, for the linear bending modes in b_1 symmetry. Although the ω_6 CH₂ wagging mode only records an 8 cm^{-1} increase from cc-pVTZ basis set to the CBS limit, the out-of-plane C-C-H and C-C-C linear bending modes have shown large changes with the increasing size of basis sets. More specifically, the ω_7 out-of-plane C-C-H linear bending mode

was computed as 447 cm⁻¹ with the cc-pVTZ basis set, 472 cm⁻¹ with the cc-pVQZ basis set, a significant increase of 25 cm⁻¹. The harmonic vibrational frequency is further increased by 10 cm⁻¹ to 482 cm⁻¹ with the cc-pV5Z basis set, and finally determined as 491 cm⁻¹ at the CBS limit. Similarly the ω_8 out-of-plane C-C-C linear bending mode is increased from 375 cm⁻¹ with the cc-pVTZ basis set, to 385 cm⁻¹ with the cc-pVQZ basis set, and finally reaches 389 cm⁻¹ at the CBS limit, a total increase of 24 cm⁻¹. Additional diffuse functions to the cc-pVTZ basis set also increases the ω_7 out-of-plane C-C-H linear bending mode by as much as 24 cm⁻¹, though they play a smaller role to the ω_8 out-of-plane C-C-C linear bending mode, with a slight increase of 3 cm⁻¹. Core-correlation effects again add an average of 5 cm⁻¹ to the CBS limit vibrational frequencies for the 3 b₁ modes.

Finally for the b₂ modes, the ω_9 C-H antisymmetric stretching mode sees a slight increase of 4 cm⁻¹ from cc-pVTZ basis set to the CBS limit, similar to the 6 cm⁻¹ increase for the ω_{12} in-plane C-C-C linear bending mode, whereas the ω_{10} CH₂ rocking mode were not affected at all by the size of the basis sets. Nonetheless, the basis set effect on the ω_{11} in-plane C-C-H linear bending mode is substantial, with a 20 cm⁻¹ increase going from cc-pVTZ to cc-pVQZ, and a further 9 cm⁻¹ increase toward the CBS limit. Diffuse functions only post an average of 4 cm⁻¹ decrease for the vibrational frequencies for the ω_9 , ω_{10} , and ω_{12} modes, while a large increase of 13 cm⁻¹ was recorded for the ω_{11} in-plane C-C-H linear bending mode when diffuse functions were added to the cc-pVTZ basis set. Core-correlation effect gains a similar 5 cm⁻¹ increase on average to the CBS limit vibrational frequencies of b₂ modes.

In brief summary, for the twelve harmonic vibrational frequencies of propargyl radical, nine of them show little or no change with the increasing size of basis sets, while the out-of-plane C-C-C linear bending mode shows a modest increased of 14 cm⁻¹, and the in-plane and

out-of-plane C-C-H linear bending modes were significantly increased by 29 and 44 cm^{-1} , respectively, when the basis set used in the calculation was increased from cc-pVTZ to the CBS limit. Diffuse functions supplemented to the cc-pVTZ basis set introduce rather large changes for most of the normal modes, but effect of additional diffuse functions to the cc-pVQZ basis set is almost negligible, with at most 2 cm^{-1} change to all but the out-of-plane C-C-H linear bending mode, in which an increase of 6 cm^{-1} was recorded. Core-correlation effects add an average of 5 cm^{-1} to the harmonic vibrational frequencies.

Several previous *ab initio* studies have also acknowledged the extreme sensitivity of linear bending modes to the basis set.^{79,80} For example, in the quartic force field investigation on acetylene by Martin, Lee, and Taylor,⁸⁰ the $\omega_7 \pi_g$ C-C-H linear bending vibrational frequency increases by 17 cm^{-1} when the basis set is increased from cc-pVTZ to cc-pVQZ, and another 17 cm^{-1} with the ANO basis set, while all other four vibrational modes have shown very little or no change with respect to the basis sets ranging from cc-pVTZ to ANO.

The final predicted harmonic frequencies were the CBS limit extrapolation frequencies with core-correlation effect, denoted as CBS-cc. Our harmonic vibrational frequencies are in good agreement with cc-pVTZ CEPA-1 results obtained by Botschwina *et al.*³⁷ and ANO CCSD(T) results computed by Jochnowitz and co-workers,⁴⁴ except for the out-of-plane and in-plane C-C-H linear bending frequencies, where the large discrepancy between different basis sets is a result of the extreme sensitivity of these modes to basis set used in the calculation.

C. FUNDAMENTAL VIBRATIONAL FREQUENCIES

In order to make direct comparison with experimental vibrational frequencies, anharmonic vibrational corrections were computed with the second-order perturbation theory to provide

theoretical fundamental vibrational frequencies. The diagonal and off-diagonal anharmonic constants are computed by the following formula:⁸¹

$$\chi_{ii} = \left(\frac{\phi_{iii}}{16}\right) + \left[-\frac{5}{48} \frac{\phi_{iii}^2}{\omega_i} - \frac{1}{16} \sum_j^* \frac{\phi_{ij}^2 (8\omega_i^2 - 3\omega_j^2)}{\omega_i (4\omega_i^2 - \omega_j^2)}\right]$$

$$\chi_{ij} = \left(\frac{\phi_{ijj}}{4}\right) + \left\{-\frac{1}{4} \sum_k \frac{\phi_{iik} \phi_{kjj}}{\omega_k} - \frac{1}{2} \sum_k^* \frac{\phi_{ijk}^2 \omega_k (\omega_k^2 - \omega_i^2 - \omega_j^2)}{[(\omega_i + \omega_j)^2 - \omega_k^2][(\omega_i - \omega_j)^2 - \omega_k^2]}\right\}$$

$$+ \left\{[A_e (\xi_{ij}^a)^2 + B_e (\xi_{ij}^b)^2 + C_e (\xi_{ij}^c)^2] \left(\frac{\omega_i}{\omega_j} + \frac{\omega_j}{\omega_i}\right)\right\}$$

where the diagonal anharmonic constants can be partitioned into quartic, cubic contributions, and the off-diagonal anharmonic constants also include Coriolis contributions. The computed anharmonic constants are listed in Table 4.

The final vibrational analysis is summarized in Table 5. This analysis includes vibrational mode assignments, harmonic frequencies, anharmonic corrections, fundamental frequencies, and total energy distributions (TEDs) for propargyl radical and its deuterated derivatives, as well as comparisons with previous theoretical and experimental studies. The total energy distribution result offers definitive assignments for the twelve fundamental frequencies.

In the cc-pVTZ CEPA-1 study by Botschwina and co-workers,³⁷ fundamental frequencies have been obtained only for the a_1 totally symmetric vibrations of propargyl radical and its deuterated derivatives. Because of the smaller basis set used in their study and the lack of treatment for higher order force constants and interactions from the b_1 and b_2 spaces, differences between our and their fundamental frequency predictions are expected. For example, our reported fundamental frequency for the ν_2 C-H symmetric stretching mode is 3045.0 cm^{-1} , 67 cm^{-1} less than the cc-pVTZ CEPA-1 value of 3112 cm^{-1} . Other large differences include the ν_3

C-C stretching vibrational frequency, where our value of 1928.4 cm^{-1} is more than 20 cm^{-1} smaller than the cc-pVTZ CEPA-1 result.

The agreement improves, however, when we compare our findings with ANO CCSD(T) results. Except for the in-plane and out-of-plane C-C-H linear bending modes which are extremely sensitive to basis set, the other ten modes agree with each other very well, with the largest difference of 15 cm^{-1} for the CH_2 scissor mode, and several other modes having almost the same fundamental frequencies. The large positive anharmonicity for the in-plane and out-of-plane C-C-H linear bending modes is mostly due to the Coriolis effect.

Of the twelve fundamental frequencies of propargyl radical, nine have been determined under different experimental conditions. The C-D stretching modes of the deuterated propargyl radical have also been determined by different groups.^{16,28}

To compare our *ab initio* fundamental frequencies with the experimental results, the acetylenic C-H stretching mode ascertained in this study is 3336.1 cm^{-1} , 14 cm^{-1} higher than recent high-resolution infrared laser kinetic spectroscopy value of $3322.287(2)\text{ cm}^{-1}$ obtained by Morter and co-workers²². Our predicted C-H symmetric stretching and CH_2 rocking vibrational frequencies are less than 20 cm^{-1} larger than the experimental results in cryogenic matrix, while the difference between the theoretical and experimental C-C stretching and CH_2 scissor vibrational frequencies are less than 10 cm^{-1} . Our computed ν_5 C-C stretching and ν_6 CH_2 wagging fundamental vibrational frequencies are almost the same as experimental values. However, the out-of-plane and in-plane C-C-H linear bending modes are 41 and 27 cm^{-1} greater than the corresponding experimental values, respectively. This indicates the deficiency of correlation consistent basis sets in predicting the linear bending modes, whereas the ANO basis sets have achieved much better agreement for these experimental vibrational frequencies. The

differences between our predictions on the C-D stretching modes with the experimental results are also less than 20 cm^{-1} .

Note that Jacox and Milligan have tentatively assigned the frequencies at 688 cm^{-1} and 484 cm^{-1} to the ν_7 out-of-plane C-C-H bending and ν_8 out-of-plane C-C-H bending modes, respectively in their matrix isolation study.¹⁵ However, based on our total energy distribution calculations, definitive conclusions can be drawn that these two bands should instead be assigned to the ν_6 CH₂ wagging mode and ν_7 out-of-plane C-C-H bending mode, respectively. In addition, Jacox and Milligan have attributed the 547.3 cm^{-1} band observed in matrix isolation study to the propargyl radical. However, no corresponding band was found for propargyl radical in the current work, which confirmed previous arguments^{16,18} that this band is actually due to triplet propargylene, a possible product in the photolysis process in the original matrix isolation study.

For out-of-plane and in-plane C-C-C linear bending modes and C-H antisymmetric stretching modes of propargyl radical, as well as other normal modes of deuterated propargyl radical where no experimental data are available, our predictions provide a basis for future experimental studies on these radicals.

D. SPECTROSCOPIC CONSTANTS

In order to establish the vibrational dependence of various spectroscopic constants, it is necessary to obtain the rotation-vibration interaction constants. The complete set of rotation-vibration interaction constants computed in the following formula⁸¹ are listed in Table 6:

$$\alpha_i^\beta = -\left(\frac{2B_e^2}{\omega_i}\right) \left[\sum_\gamma \frac{3(a_i^{b\gamma})^2}{4I_{\gamma\gamma}} + \sum_j^* \frac{(\xi_{ij}^b)^2 (3\omega_i^2 + \omega_j^2)}{\omega_i^2 - \omega_j^2} \right. \\ \left. + \pi \left(\frac{c}{h}\right)^{1/2} \sum_j \phi_{ij} a_j^{bb} \left(\frac{\omega_i}{\omega_j^{3/2}}\right) \right]$$

With the computed vibration-interaction constants, the vibrational dependence of the rotational constants B_β^v ($\beta=x, y, z$) can then be described in the quartic approximation by:⁸¹

$$B_\beta^v = B_\beta^e - \sum_i \alpha_i^\beta \left(v_i + \frac{1}{2}\right) + \dots$$

The zero-point corrected rotational constants and centrifugal distortion constants are summarized in Table 7.

The equilibrium rotational constants are reduced by less than 1% with zero-point correction. Our zero-point corrected rotational constants agree perfectly with previous infrared^{22,24} and Fourier-transform microwave studies.²⁵

The various centrifugal distortion constants determined here ($\Delta_J = 2.96$ kHz, $\Delta_{JK} = 396$ kHz, $\Delta_k = 21.51$ MHz, $\delta_J = 100$ Hz, $\delta_K = 215.1$ Hz) are also in excellent agreement with the experimental results²⁴ of $\Delta_J = 2.20(73)$ kHz, $\Delta_{JK} = 384(21)$ kHz, $\Delta_k = 22.62(41)$ MHz, $\delta_J = 103(50)$ Hz, and $\delta_K = 157.5$ Hz where the δ_K value is fixed at the previous *ab initio* value of 157.5 Hz.³⁷ The previous *ab initio* value of Δ_{JK} (283 kHz)³⁷ differed with the experimental value by almost 30%, whereas our value agrees within 3% of the experimental value because of a more thorough treatment of the vibrational dependency of the constants.

2.5 CONCLUSIONS

The complete quartic force field of ground electronic state propargyl radical has been constructed using [C/H]=[aug-cc-pVTZ/cc-pVTZ] CCSD(T) methodology. A complete basis set limit quadratic force field was also obtained via extrapolations using the cc-pVXZ (X=T, Q, 5) series of basis sets based on focal point analysis, and complemented with core-correlation effect computed at the cc-pCVQZ CCSD(T) level of theory. By means of vibrational perturbation theory, this full *ab initio* quartic force field provides accurate harmonic and fundamental vibrational frequencies and definitive assignments for all of the twelve vibrational normal modes for propargyl radical and its deuterated derivatives. Most of our harmonic and anharmonic vibrational frequency predictions are in good agreement with recent theoretical and experimental studies. The out-of-plane and in-plane C-C-H linear bending modes are found to be extremely sensitive to the basis set used in the calculations, similar to the conclusions from previous quartic force field study on acetylene.⁸⁰

Rotation-vibrational interaction constants, zero-pointed corrected rotational constants, and centrifugal distortion constants have also been computed with the quartic force field. Our complete treatment of the quartic force field enables the determination of highly-accurate molecular constants that are well within the error bars of experimental results, and provides a critical assessment of the spectroscopic constants determined over many years for this important soot formation intermediate molecule.

2.6 ACKNOWLEDGMENTS

This work was supported by the U.S. Department of Energy, Office of Basic Energy Sciences, through its Combustion Program (Grant No. DE-FG02-00ER14748) and the SciDAC

Computational Chemistry Research Program (Grant No. DE-FG02-01ER15226). G. Yan thanks Dr. Schuurman and Dr. Yamaguchi for many helpful discussions.

2.7 REFERENCES

- (1) Westmoreland, P. R.; Dean, A. M.; Howard, J. B.; Longwell, J. P. *J. Phys. Chem.* **1989**, *93*, 8171.
- (2) Miller, J. A.; Kee, R. J.; Westbrook, C. K. *Annu. Rev. Phys. Chem.* **1990**, *41*, 345.
- (3) Miller, J. A.; Melius, C. F. *Combust. Flame* **1992**, *91*, 21.
- (4) Melius, C. F.; Miller, J. A.; Evleth, E. M. In *Twenty-Fourth Symposium (International) on Combustion*; The Combustion Institute, 1992.
- (5) Wu, C. H.; Kern, R. D. *J. Phys. Chem.* **1987**, *91*, 6291.
- (6) Kern, R. D.; Xie, K. *Prog. Energy Combust. Sci.* **1991**, *17*, 191.
- (7) Kern, R. D.; Singh, H. J.; Wu, C. H. *Int. J. Chem. Kinet.* **1988**, *20*, 731.
- (8) Kiefer, J. H.; Mudipalli, P. S.; Sidhu, S. S.; Kern, R. D.; Jursic, B. S.; Xie, K.; Chen, H. *J. Phys. Chem. A* **1997**, *101*, 4057.
- (9) Morter, C. L.; Farhat, S. K.; Adamson, J. D.; Glass, G. P.; Curl, R. F. *J. Phys. Chem.* **1994**, *98*, 7029.
- (10) Alkemande, U.; Homann, K. H. *Z. Phys. Chem.* **1989**, *161*, 19.
- (11) Ramsay, D. A.; Thistlethwaite, P. *Can. J. Phys.* **1966**, *44*, 1381.
- (12) Fessenden, R. W.; Schuler, R. H. *J. Chem. Phys.* **1963**, *38*, 2147.
- (13) Kochi, J. K.; Krusic, P. J. *J. Am. Chem. Soc.* **1970**, *92*, 4110.
- (14) Kasai, P. H. *J. Am. Chem. Soc.* **1972**, *94*, 5950.
- (15) Jacox, M. E.; Milligan, D. E. *Chem. Phys.* **1974**, *4*, 45.

- (16) Huang, J. W.; Graham, W. R. M. *J. Chem. Phys.* **1990**, *93*, 1583.
- (17) Chipman, D. M.; Miller, K. E. *J. Am. Chem. Soc.* **1984**, *106*, 6236.
- (18) Maier, G.; Reisenauer, H. P.; Schwab, W.; Carsky, P.; Hess, B. A.; Schaad, L. J. *J. Chem. Phys.* **1989**, *91*, 4763.
- (19) Honjou, H.; Yoshimine, M.; Pacansky, J. *J. Am. Chem. Soc.* **1987**, *91*, 4455.
- (20) Lossing, F. P. *Can. J. Chem.* **1972**, *50*, 3973.
- (21) Minsek, D. W.; Chen, P. *J. Phys. Chem.* **1990**, *94*, 8399.
- (22) Morter, C. L.; Domingo, C.; Farhat, S. K.; Cartwright, E.; Glass, G. P.; Curl, R. F. *Chem. Phys. Lett.* **1992**, *195*, 316.
- (23) Sumiyoshi, Y.; Imajo, T.; Tanaka, K.; Tanaka, T. *Chem. Phys. Lett.* **1994**, *231*, 569.
- (24) Tanaka, K.; Harada, T.; Sakaguchi, K.; Harada, K.; Tanaka, T. *J. Chem. Phys.* **1995**, *103*, 6450.
- (25) Tanaka, K.; Sumiyoshi, Y.; Ohshima, Y.; Endo, Y.; Kawaguchi, K. *J. Chem. Phys.* **1997**, *107*, 2728.
- (26) Yuan, L.; DeSain, J.; Curl, R. F. *J. Mol. Spectrosc.* **1998**, *187*, 102.
- (27) Kaiser, R. I.; Lee, Y. T.; Suits, A. G. *J. Chem. Phys.* **1996**, *105*, 8705.
- (28) Eckhoff, W. C.; Miller, C. E.; Billera, C. F.; Engel, P. S.; Curl, R. F. *J. Mol. Spectrosc.* **1997**, *186*, 193.
- (29) Fahr, A.; Hassanzadeh, P.; Laszlo, B.; Huie, R. E. *Chem. Phys.* **1997**, *215*, 59.
- (30) Deyerl, H.-J.; Fischer, I.; Chen, P. *J. Chem. Phys.* **1999**, *111*, 3441.
- (31) Gilbert, T.; Pfab, R.; Fischer, I.; Chen, P. *J. Chem. Phys.* **2000**, *112*, 2575.
- (32) Wyss, M.; Riaplov, E.; Maier, J. P. *J. Chem. Phys.* **2001**, *114*, 10355.
- (33) Kupper, J.; Merritt, J. M.; Miller, R. E. *J. Chem. Phys.* **2002**, *117*, 647.

- (34) Bernardi, F.; Camaggi, C. M.; Tiecco, M. *J. Chem. Soc., Perkin Trans.* **1974**, 2, 518.
- (35) Hinchliffe, A. *J. Mol. Struct.* **1977**, 36, 162.
- (36) Hinchliffe, A. *J. Mol. Struct.* **1977**, 37, 295.
- (37) Botschwina, P.; Oswald, R.; Flugge, J.; Horn, M. *Z. Phys. Chem.* **1995**, 188, 29.
- (38) Adamson, J. D.; Morter, C. L.; DeSain, J. D.; Glass, G. P.; Curl, R. F. *J. Phys. Chem.* **1996**, 100, 2125.
- (39) Walch, S. P. *J. Chem. Phys.* **1995**, 103, 7064.
- (40) Vereecken, L.; Pierloot, K.; Peeters, J. *J. Chem. Phys.* **1998**, 108, 1068.
- (41) Krokidis, X.; W., M. N.; A., L. W.; Frenklach, M. *Chem. Phys. Lett.* **1999**, 314, 534.
- (42) Botschwina, P.; Horn, M.; Oswald, R.; Schmatz, S. *J. Electr. Spectrom. Rel. Phenom.* **2000**, 108, 109.
- (43) Le, T. N.; Mebel, A. M.; Kaiser, R. I. *J. Comp. Chem.* **2001**, 22, 1522.
- (44) Jochnowitz, E. B.; Zhang, X.; Nimlos, M. R.; Varner, M. E.; Stanton, J. F.; Ellison, G. B., Private communications.
- (45) Moller, C.; Plesset, M. S. *Phys. Rev.* **1934**, 46, 618.
- (46) Pople, J. A.; Binkley, J. S.; Seeger, R. *Int. J. Quantum Chem. Symp.* **1976**, 10, 1.
- (47) Hehre, W. J.; Radom, L.; Schleyer, P. v. R.; Pople, J. A. *Ab Initio Molecular Orbital Theory*; Wiley-Interscience: New York, 1986.
- (48) Szabo, A.; Ostlund, N. S. *Modern Quantum Chemistry*; McGraw-Hill: New York, 1989.
- (49) Bartlett, R. J. *Annu. Rev. Phys. Chem.* **1981**, 32, 359.
- (50) Purvis, G. D.; Bartlett, R. J. *J. Chem. Phys.* **1982**, 76, 1910.
- (51) Rittby, M.; Bartlett, R. J. *J. Phys. Chem.* **1988**, 92, 3033.

- (52) Raghavachari, K.; Trucks, G. W.; Pople, J. A.; Head-Gordon, M. *Chem. Phys. Lett.* **1989**, *157*, 479.
- (53) Scuseria, G. E. *Chem. Phys. Lett.* **1991**, *176*, 27.
- (54) Roothaan, C. C. J. *Rev. Mod. Phys.* **1951**, *23*, 69.
- (55) Dunning, T. H. *J. Chem. Phys.* **1989**, *90*, 1007.
- (56) Kendall, R. A.; Dunning, T. H.; Harrison, R. J. *J. Chem. Phys.* **1992**, *96*, 6769.
- (57) Basis sets were obtained from the Extensible Computational Chemistry Environment Basis Set Database, Version 12/03/03, as developed and distributed by the Molecular Science Computing Facility, Environmental and Molecular Sciences Laboratory which is part of the Pacific Northwest Laboratory, P.O. Box 999, Richland, Washington 99352, USA, and funded by the U.S. Department of Energy. The Pacific Northwest Laboratory is a multi-program laboratory operated by Battelle Memorial Institute for the U.S. Department of Energy under contract DE-AC06-76RLO 1830. Contact David Feller or Karen Schuchardt for further information.
- (58) Lee, T. J.; Rendell, A. P. *J. Chem. Phys.* **1991**, *94*, 6229.
- (59) ACES II is a program product of the Quantum Theory Project; University of Florida; Authors: J. F. Stanton, J. G., J. D. Watts, M. Nooijen, N. Oliphant, S. A. Perera, P. G. Szalay, W. J. Lauderdale, S. R. Gwaltney, S. Beck, A. Balkova D. E. Bernholdt, K.-K Baeck, P. Rozyczko, H. Sekino, C. Hober, and R.J. Bartlett. Integral packages included are VMOL (J. Almlöf and P. R. Taylor); VPROPS (P. Taylor); ABACUS (T. Helgaker, H.J. Aa. Jensen, P. Jorgensen, J. Olsen, and P. R. Taylor).
- (60) East, L. L. A.; Allen, W. D. *J. Chem. Phys.* **1993**, *99*, 4638.
- (61) MOLPRO is a package of ab initio programs written by H.-J. Werner, P. J. Knowles, M. Schütz, R. Lindh, P. Celani, T. Korona, G. Rauhut, F. R. Manby, R. D. Amos, A. Bernhardsson, A.

Berning, D. L. Cooper, M. J. O. Deegan, A. J. Dobbyn, F. Eckert, C. Hampel, G. Hetzer, A. W. Lloyd, S. J. McNicholas, W. Meyer, M. E. Mura, A. Nicklaß, P. Palmieri, R. Pitzer, U. Schumann, H. Stoll, A. J. Stone, R. Tarroni, and T. Thorsteinsson.

(62) Allen, W. D.; Csaszar, A. G.; Horner, D. A. *J. Am. Chem. Soc.* **1992**, *114*, 6834.

(63) Pulay, P.; Torok, F. *Acta Chim. Acad. Sci. Hungary* **1965**, *44*, 287.

(64) Keresztury, G.; Jalsovszky, G. *J. Mol. Struct.* **1971**, *10*, 304.

(65) Watson, J. K. G. *J. Chem. Phys.* **1968**, *48*, 4517.

(66) Clabo, D. A., Jr.; Allen, W. D.; Remington, R. B.; Yamaguchi, Y.; Schaefer III, H. F. *Chem. Phys.* **1988**, *123*, 187.

(67) Allen, W. D.; Yamaguchi, Y.; Csaszar, A. G.; Clabo, D. A., Jr.; Remington, R. B.; Schaefer III, H. F. *Chem. Phys.* **1990**, *145*, 427.

(68) Allen, W. D.; Csaszar, A. G. *J. Chem. Phys.* **1993**, *98*, 2983.

(69) East, A. L. L.; Johnson, C. S.; Allen, W. D. *J. Chem. Phys.* **1993**, *98*, 1299.

(70) Klepeis, N. E.; East, A. L. L.; Csaszar, A. G.; Allen, W. D.; Lee, T. J.; Schwenke, D. W. *J. Chem. Phys.* **1993**, *99*, 3865.

(71) East, A. L. L.; Allen, W. D.; Klippenstein, S. J. *J. Chem. Phys.* **1995**, *102*, 8506.

(72) Aarset, K.; Csaszar, A. G.; Sibert III, E. L.; Allen, W. D.; Schaefer III, H. F.; Klopper, W.; Noga, J. *J. Chem. Phys.* **2000**, *112*, 4053.

(73) Demainson, J.; Perrin, A.; Burger, H. *J. Mol. Spectrosc.* **2003**, *221*, 47.

(74) Burcl, R.; Handy, N. C.; Carter, S. *Spectrochimica Acta A: Mol. Biomol. Spectrosc.* **2003**, *59*, 1881.

(75) Breidung, J.; Constantin, L.; Demainson, J.; Margules, L.; Thiel, W. *Mol. Phys.* **2003**, *101*, 1113.

(76) Gambi, A. *J. Mol. Spectrosc.* **2002**, *216*, 508.

(77) INTDER2000 is a general program developed by Wesley D. Allen and co-workers which performs various vibrational analyses and higher-order nonlinear transformations among force field representations.

(78) Allen, W. D.; Cszaszar, A. G.; Szalay, V.; Mills, I. M. *Mol. Phys.* **1996**, *89*, 1213.

(79) Simandiras, E. D.; Rice, J. E.; Lee, T. J.; Amos, R. D.; Handy, N. C. *J. Chem. Phys.* **1988**, *88*, 3187.

(80) Martin, J. M.; Lee, T. J.; Taylor, P. R. *J. Chem. Phys.* **1998**, *108*, 676.

(81) Papousek, D.; Aliev, M. R. *Molecular Vibrational-Rotational Spectra*; Elsevier scientific publishing company: Amsterdam, 1982.

2.8 APPENDIX

The following equations were utilized to determine the force constants F_{ij} , F_{ijk} , and F_{ijkl} in the internal space from analytic first derivatives F_i computed at structures displaced from the reference geometry by $(\pm\Delta_i, \pm\Delta_j)$ in coordinate S_i and S_j :

$$F_{ii} = (12\Delta_i)^{-1} [F_i(-2\Delta_i) - 8F_i(-\Delta_i) + 8F_i(+\Delta_i) - F_i(+2\Delta_i)]$$

$$F_{ij} = (12\Delta_i)^{-1} [F_j(-2\Delta_i) - 8F_j(-\Delta_i) + 8F_j(+\Delta_i) - F_j(+2\Delta_i)]$$

$$F_{iii} = (\Delta_i)^{-2} [F_i(-\Delta_i) - 2F_i(0) + F_i(+\Delta_i)]$$

$$F_{iij} = (\Delta_i)^{-2} [F_j(-\Delta_i) + 2F_j(0) + F_j(+\Delta_i)]$$

$$F_{ijk} = (-2\Delta_j\Delta_k)^{-1} [-F_i(-\Delta_j, -\Delta_k) + F_i(-\Delta_j) + F_i(-\Delta_k) - 2F_i(0) + F_i(+\Delta_k) + F_i(+\Delta_j) - F_i(+\Delta_j, +\Delta_k)]$$

$$F_{iii} = (2\Delta_i)^{-3} [-F_i(-2\Delta_i) + 2F_i(-\Delta_i) - 2F_i(+\Delta_i) + F_i(+2\Delta_i)]$$

$$F_{iiij} = (2\Delta_i)^{-3} [-F_j(-2\Delta_i) + 2F_j(-\Delta_i) - 2F_j(+\Delta_i) + F_j(+2\Delta_i)]$$

$$F_{iijj} = (2\Delta_i\Delta_j^2)^{-1} [-F_i(-\Delta_i, -\Delta_j) + 2F_i(-\Delta_i) - F_i(-\Delta_i, +\Delta_j) + F_i(+\Delta_i, -\Delta_j) - 2F_i(+\Delta_i) + F_i(+\Delta_i, +\Delta_j)]$$

$$F_{ijkl} = (2\Delta_j\Delta_k\Delta_l)^{-1} [-F_i(-\Delta_j, -\Delta_k, -\Delta_l) + F_i(-\Delta_j, -\Delta_k) + F_i(-\Delta_j, -\Delta_l) - F_i(-\Delta_j) + F_i(-\Delta_k, -\Delta_l) - F_i(-\Delta_k) - F_i(-\Delta_l) + F_i(-\Delta_l) + F_i(+\Delta_k) - F_i(+\Delta_k, +\Delta_l) + F_i(+\Delta_j) - F_i(+\Delta_j, +\Delta_l) - F_i(+\Delta_j, +\Delta_k) + F_i(+\Delta_j, +\Delta_k, +\Delta_l)]$$

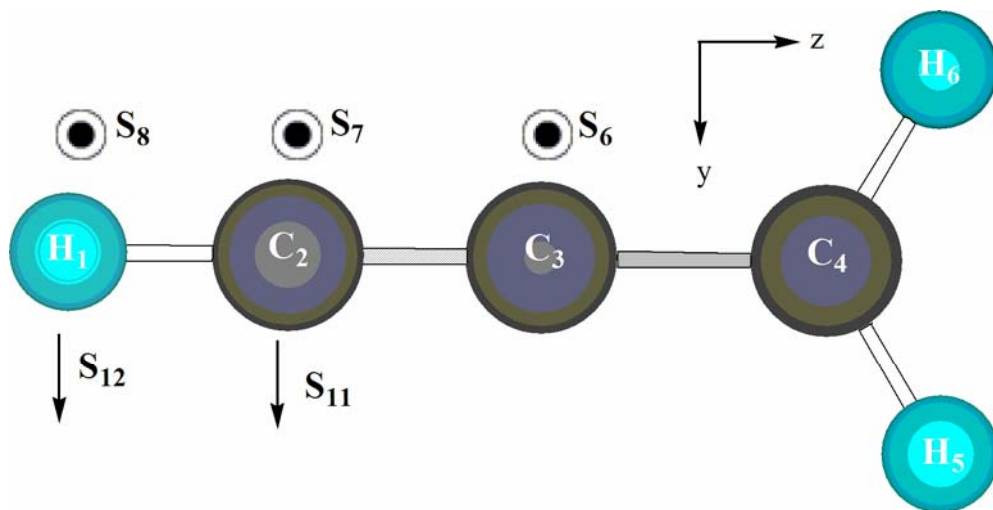


Figure 2.1. Propargyl radical, C_3H_3 , C_{2v} symmetry. Optimized equilibrium structure is given in Table 2.1. Symmetry internal coordinate definitions are given in Table 2.2.

TABLES

Table 2.1. Optimized geometry of propargyl radical (C_3H_3 , C_{2v}). Bond lengths are in Å and bond angles are in degrees.

	r(H ₁ -C ₂)	r(C ₂ -C ₃)	r(C ₃ -C ₄)	r(C ₄ -H ₅)	θ(H ₅ -C ₄ -H ₆)
<i>Ab initio</i> equilibrium data					
aug'-cc-pVTZ CCSD(T) ^a	1.0612	1.2245	1.3716	1.0780	119.01
cc-pVTZ CEPA-1 ^b	1.0627	1.2234	1.3829	1.0800	119.00
cc-pCVQZ CCSD(T) ^c	1.0618	1.2227	1.3752	1.0785	119.09
ANO CCSD(T) ^d	1.063	1.228	1.380	1.081	119.0

^aThis work.

^bReference 37.

^cReference 42.

^dReference 44.

Table 2.2. Symmetry internal coordinate definition for propargyl radical.^a

Coordinate	Irrep.	Description
$S_1=r(1,2)$	a_1	C-H stretch
$S_2=r(2,3)$	a_1	C-C stretch
$S_3=r(3,4)$	a_1	C-C stretch
$S_4=2^{-1/2}[r(4,5)+r(4,6)]$	a_1	C-H symmetric stretch
$S_5=\beta(5,4,6)$	a_1	CH ₂ scissor
$S_6=\gamma(3,4,5,6)$	b_1	CH ₂ wag
$S_7=2^{-1/2}[\theta_x(5,4,3,2)-\theta_x(6,4,3,2)]$	b_1	out-of-plane C-C-C linear bend
$S_8=2^{-1/2}[\theta_x(5,3,2,1)-\theta_x(6,3,2,1)]$	b_1	out-of-plane C-C-H linear bend
$S_9=2^{-1/2}[r(4,5)-r(4,6)]$	b_2	C-H antisymmetric stretch
$S_{10}=2^{-1/2}[\beta(3,4,5)-\beta(3,4,6)]$	b_2	CH ₂ rock
$S_{11}=2^{-1/2}[\theta_y(5,4,3,2)-\theta_y(6,4,3,2)]$	b_2	in-plane C-C-C linear bend
$S_{12}=2^{-1/2}[\theta_y(5,3,2,1)-\theta_y(6,3,2,1)]$	b_2	in-plane C-C-H linear bend

^aSee Fig. 2.1 for the numbering of atoms and sign conventions for the linear and out-of-plane bending modes. Definitions: $r(i,j)$ = i-j bond length; $\beta(i,j,k)$ = i-j-k valence bond angle; $\gamma(i,j,k,l)$ = angle of i-j bond vector out of j-k-l plane; $\theta_{x,y}(i,j,k,l)$ = x,y component of k->l unit vector in the local, right-handed coordinate system in which the k-j bond vector defines the z axis and atom i lies in the xz plane in the +x direction.

Table 2.3. Harmonic vibrational frequencies of propargyl radical computed with different basis sets.^a

Mode	Description	cVTZ	a'VTZ	aVTZ	cVQZ	aVQZ	cV5Z	CBS	cCVQZ	CBS-cc	cVTZ CEPA-1 ^b	ANO ^c
$\omega_1(a_1)$	C-H stretch	3456	3439	3442	3451	3449	3451	3452	3457	3458	3462	3460
ω_2	C-H symmetric stretch	3162	3163	3157	3163	3161	3163	3163	3169	3169	3172	3165
ω_3	C-C stretch	1979	2002	1972	1982	1980	1983	1984	1989	1992	2028	1983
ω_4	CH ₂ scissor	1471	1473	1464	1468	1466	1467	1465	1471	1468	1475	1465
ω_5	C-C stretch	1056	1073	1056	1060	1059	1060	1060	1064	1064	1068	1058
$\omega_6(b_1)$	CH ₂ wag	661	694	664	668	669	669	669	673	674	644	667
ω_7	out-of-plane C-C-H linear bend	447	465	471	472	478	482	491	478	498	476	477
ω_8	out-of-plane C-C-C linear bend	375	393	378	385	385	388	389	388	392	386	389
$\omega_9(b_2)$	C-H antisymmetric stretch	3262	3260	3257	3266	3264	3266	3266	3271	3272	3268	3266
ω_{10}	CH ₂ rock	1034	1029	1031	1034	1034	1034	1034	1037	1036	987	1034
ω_{11}	in-plane C-C-H linear bend	593	611	606	613	614	617	622	618	627	621	616
ω_{12}	in-plane C-C-C linear bend	325	335	320	330	329	331	331	333	334	351	330

^aa'VTZ represents the full-electron correlation CCSD(T) calculation with a [C/H]=[aug-cc-pVTZ/cc-pVTZ] basis set. cVXZ calculations use the respective cc-pVXZ basis sets in valence-electron correlation CCSD(T) calculations. Complete basis set (CBS)

limit is achieved by focal point extrapolation. cCVQZ represents full-electron correlation cc-pCVQZ CCSD(T) calculation. CBS-cc includes core-correlation effects computed with the cc-pCVQZ basis set in addition to the valence CBS result.

^bReference 37.

^cReference 44.

Table 2.4. Anharmonic constants (in cm^{-1}) of propargyl radical.

Q_i	Q_j	χ_{ij}	Q_i	Q_j	χ_{ij}	Q_i	Q_j	χ_{ij}
1	1	-52.22	7	6	-1.50	10	8	19.31
2	1	-0.17	7	7	0.13	10	9	42.49
2	2	-32.06	8	1	-0.12	10	10	8.78
3	1	-0.11	8	2	-20.38	11	1	-0.91
3	2	-114.08	8	3	-11.88	11	2	0.20
3	3	-27.64	8	4	6.90	11	3	1.63
4	1	-8.27	8	5	47.04	11	4	-5.18
4	2	-0.98	8	6	-7.81	11	5	1.41
4	3	-1.11	8	7	25.10	11	6	4.19
4	4	-12.16	8	8	-7.23	11	7	0.51
5	1	0.17	9	1	-14.64	11	8	-3.21
5	2	-21.01	9	2	-0.84	11	9	4.38
5	3	-2.33	9	3	-1.23	11	10	8.54
5	4	-1.65	9	4	-13.44	11	11	-0.54
5	5	-9.13	9	5	-1.82	12	1	0.19
6	1	-0.16	9	6	-1.07	12	2	-0.09
6	2	0.93	9	7	-4.01	12	3	1.99
6	3	0.19	9	8	-0.44	12	4	-7.78
6	4	-12.90	9	9	8.13	12	5	-0.05
6	5	-3.19	10	1	-19.00	12	6	2.65
6	6	-0.92	10	2	-3.46	12	7	-1.34
7	1	0.14	10	3	-3.07	12	8	2.42
7	2	-10.90	10	4	-27.57	12	9	6.60
7	3	-8.58	10	5	1.79	12	10	1.37
7	4	-3.31	10	6	11.37	12	11	18.18
7	5	-11.39	10	7	1.10	12	12	-1.30

Table 2.5. Final vibrational frequency (in cm^{-1}) analysis of HCCCH_2 , DCCCH_2 , HCCCD_2 , and DCCCD_2 .^a

Mode	Description	ω	Δ_{Anh}	ν	TED	cc-pVTZ CEPA-1 ^b	ANO CCSD(T) ^c	Expt.
HCCCH_2								
ν_1 (a_1)	C-H stretch	3458.2	-122.1	3336.1	$S_1(100)$	3462(3351)	3460(3322)	3308.5 ^c , 3310 ^d , 3308.8 ^e , 3322.287 ^f
ν_2	C-H symmetric stretch	3168.5	-123.5	3045.0	$S_4(100)$	3172(3112)	3165(3037)	3028.3 ^c
ν_3	C-C stretch	1991.5	-63.1	1928.4	$S_2(85)$ - $S_3(15)$	2028(1951)	1983(1923)	1935.4 ^c
ν_4	CH_2 scissor	1467.8	-18.4	1449.4	$S_5(96)$ + $S_3(4)$	1475(1458)	1465(1444)	1440.4 ^c
ν_5	C-C stretch	1064.1	-1.6	1062.4	$S_3(81)$ + $S_2(14)$ - $S_5(5)$	1068(1049)	1058(1055)	1061.6 ^c
ν_6 (b_1)	CH_2 wag	674.4	14.5	688.9	$S_6(100)$	644	667(689)	686.6 ^c , 688 ^d , 687.17603 ^g
ν_7	out-of-plane C-C-H linear bend	498.4	26.6	525.0	$S_8(96)$ + $S_7(4)$	476	477(482)	483.6 ^c , 484 ^d
ν_8	out-of-plane C-C-C linear bend	391.6	6.0	397.6	$S_7(96)$ + $S_8(4)$	386	389(398)	
ν_9 (b_2)	C-H antisymmetric stretch	3271.6	-147.4	3124.2	$S_9(100)$	3268	3266(3116)	
ν_{10}	CH_2 rock	1036.3	-6.2	1030.1	$S_{10}(93)$ + $S_{11}(7)$	987	1034(1018)	1016.7 ^c
ν_{11}	in-plane C-C-H linear bend	626.9	20.3	647.1	$S_{12}(96)$ + $S_{11}(4)$	621	616(612)	620 ^c
ν_{12}	in-plane C-C-C linear bend	334.2	6.7	340.9	$S_{11}(94)$ - $S_{10}(6)$	351	330(338)	
DCCCH_2								
ν_1 (a_1)	C-D stretch	2639.1	-74.2	2564.9	$S_1(82)$ - $S_2(18)$	(2580)		2547.2 ^c , 2557.33 ^h

ν_2	C-H symmetric stretch	3168.6	-123.3	3045.2	$S_4(100)$	(3112)	
ν_3	C-C stretch	1899.6	-50.9	1848.7	$S_2(67)-S_3(17)$ $+s_1(17)$	(1862)	
ν_4	CH ₂ scissor	1467.0	-18.5	1448.5	$S_5(96)$	(1457)	
ν_5	C-C stretch	1047.9	-2.2	1045.7	$S_3(80)+S_2(15)$ $-S_5(4)$	(1033)	
ν_6 (b ₁)	CH ₂ wag	674.3	12.8	687.0	$S_6(98)$		
ν_7	out-of-plane C-C-D linear bend	352.1	5.4	357.5	$S_8(54)+S_7(45)$		
ν_8	out-of-plane C-C-C linear bend	417.4	22.1	439.5	$S_7(53)-S_8(46)$		
ν_9 (b ₂)	C-H antisymmetric stretch	3271.6	-146.9	3124.7	$S_9(100)$		
ν_{10}	CH ₂ rock	1035.2	-5.7	1029.5	$S_{10}(94)+S_{11}(6)$		
ν_{11}	in-plane C-C-D linear bend	488.7	19.2	507.9	$S_{12}(102)$		
ν_{12}	in-plane C-C-C linear bend	322.5	4.2	326.7	$S_{11}(95)-S_{10}(6)$		
HCCCD ₂							
ν_1 (a ₁)	C-H stretch	3458.2	-122.1	3336.0	$S_1(97)$	(3351)	3308.8 ^e
ν_2	C-D symmetric stretch	2297.3	-89.5	2207.8	$S_4(98)$	(2249)	
ν_3	C-C stretch	1989.3	-60.0	1929.3	$S_2(83)-S_3(13)$	(1953)	
ν_4	CD ₂ scissor	1183.4	-17.0	1166.4	$S_5(49)+S_3(43)$ $-S_2(7)$	(1172)	
ν_5	C-C stretch	935.1	-14.3	920.8	$S_5(51)-S_3(42)$ $-S_2(6)$	(928)	
ν_6 (b ₁)	CD ₂ wag	548.8	8.8	557.6	$S_6(86)-S_7(13)$		
ν_7	out-of-plane C-C-H linear bend	498.2	21.1	519.3	$S_8(102)$		

ν_8	out-of-plane C-C-C linear bend	369.8	1.2	371.0	$S_7(89)+S_6(13)$		
ν_9 (b_2)	C-D antisymmetric stretch	2438.4	-83.2	2355.2	$S_9(100)$		
ν_{10}	CD ₂ rock	839.8	-4.4	835.4	$S_{10}(87)+S_{11}(13)$		
ν_{11}	in-plane C-C-H linear bend	626.5	16.9	643.4	$S_{12}(103)$		
ν_{12}	in-plane C-C-C linear bend	304.5	1.6	306.1	$S_{11}(91)-S_{10}(12)$		
DCCCD ₂							
ν_1 (a_1)	C-D stretch	2639.1	-74.4	2564.7	$S_1(82)-S_2(18)$	(2580)	2546.8 ^e
ν_2	C-D symmetric stretch	2297.2	-94.5	2202.7	$S_4(98)$	(2247)	
ν_3	C-C stretch	1897.0	-45.6	1851.4	$S_2(67)+S_1(17)$ $-S_3(16)$	(1867)	
ν_4	CD ₂ scissor	1175.4	-16.4	1159.0	$S_5(53)+S_3(38)$ $+S_2(7)$	(1165)	
ν_5	C-C stretch	926.3	-9.1	917.2	$S_5(48)-S_3(44)$ $-S_2(8)$	(919)	
ν_6 (b_1)	CD ₂ wag	548.0	8.7	556.7	$S_6(87)-S_7(13)$		
ν_7	out-of-plane C-C-D linear bend	409.2	16.7	425.9	$S_8(63)-S_7(32)$ $-S_6(5)$		
ν_8	out-of-plane C-C-C linear bend	338.7	-0.5	338.2	$S_7(55)+S_8(37)$ $+S_6(8)$		
ν_9 (b_2)	C-D antisymmetric stretch	2438.4	-83.0	2355.4	$S_9(100)$		
ν_{10}	CD ₂ rock	838.0	-3.5	834.5	$S_{10}(88)+S_{11}(13)$		
ν_{11}	in-plane C-C-D linear bend	488.0	14.4	502.4	$S_{12}(103)$		
ν_{12}	in-plane C-C-C linear bend	293.4	-0.3	293.1	$S_{11}(90)-S_{10}(12)$		

^aaug'-cc-pVTZ quartic force field with CBS-cc quadratic force field.

^bReference 37. Fundamental frequencies for the totally symmetric mode are listed in parentheses.

^cReference 44.

^dReference 15. Ar matrix. The 688 cm^{-1} and 484 cm^{-1} bands were originally assigned to ν_7 and ν_8 , respectively.

^eReference 16.

^fReference 22.

^gReference 24.

^hReference 28.

Table 2.6. Rotation-vibration interaction constants (in 10^{-3} cm^{-1}) of propargyl radical.

α_1^A	0.030	α_1^B	0.816	α_1^C	0.762
α_2^A	106.965	α_2^B	0.243	α_2^C	0.277
α_3^A	161.322	α_3^B	0.166	α_3^C	0.308
α_4^A	3.865	α_4^B	1.582	α_4^C	1.477
α_5^A	-105.041	α_5^B	-0.291	α_5^C	0.353
α_6^A	13.029	α_6^B	1.176	α_6^C	-0.049
α_7^A	-520.603	α_7^B	-0.178	α_7^C	1.521
α_8^A	436.165	α_8^B	0.561	α_8^C	-0.092
α_9^A	-2948.205	α_9^B	-0.483	α_9^C	-0.103
α_{10}^A	2947.222	α_{10}^B	-0.485	α_{10}^C	-0.874
α_{11}^A	-5528.674	α_{11}^B	-0.534	α_{11}^C	-1.088
α_{12}^A	5555.450	α_{12}^B	-1.454	α_{12}^C	-0.579

Table 2.7. Spectroscopic constants of propargyl radical.

Constant	<i>ab initio</i> results			Experimental results		Unit
	aug'-cc-pVTZ ^a	cc-pVTZ CEPA-1 ^b	cc-pCVQZ CCSD(T) ^c			
A _e	9.6844 ^a	9.6627	9.6758			cm ⁻¹
B _e	0.3183	0.31515	0.31781			cm ⁻¹
C _e	0.3081	0.30502	0.30770			cm ⁻¹
A ₀	9.6236				9.60847(36) ^e 9.60847(36) ^f	cm ⁻¹
B ₀	0.3177			0.31757(8) ^d	0.317674(24) 0.3176757(2)	cm ⁻¹
C ₀	0.3072			0.30705(8)	0.307098(24) 0.3071085(2)	cm ⁻¹
Δ _J	2.96	2.88			2.20(73) 3.44(63)	kHz
Δ _{JK}	396	283			384(21) 375.3(28)	kHz
Δ _K	21.51	21.43			22.62(41)	MHz
δ _J	100	97			103(50)	Hz
δ _K	215.1	157.5			157.5	kHz

^aThis work.^bReference 37.^cReference 43.^dReference 22. Infrared laser kinetic spectroscopy.^eReference 24. Infrared diode laser spectroscopy. δ_K was fixed at the *ab initio* value obtained in Reference 37.^fReference 25. Fourier-transform microwave (FTMW) spectroscopy. A₀ was fixed at the value obtained in Reference 24.

SUPPLEMENTARY MATERIALS

Table 2.8. Quadratic force constants (F_{ij}) extrapolation of propargyl radical.^a

i	j	cc-pVTZ	cc-pVQZ	cc-pV5Z	CBS	pCVQZ	CBS-cc
1	1	6.3939	6.3801	6.3810	6.3820	6.4030	6.4040
2	1	-0.1249	-0.1030	-0.1080	-0.1144	-0.1028	-0.1127
2	2	13.9299	13.9826	13.9944	14.0161	14.0935	14.1259
3	1	-0.0071	-0.0175	-0.0184	-0.0189	-0.0173	-0.0184
3	2	1.2391	1.2678	1.2674	1.2650	1.2821	1.2795
3	3	6.4263	6.4727	6.4779	6.4829	6.5162	6.5287
4	1	0.0014	0.0000	0.0000	-0.0012	0.0000	0.0000
4	2	-0.0380	-0.0411	-0.0422	-0.0435	-0.0415	-0.0439
4	3	0.1511	0.1605	0.1607	0.1603	0.1610	0.1608
4	4	5.7014	5.7058	5.7054	5.7032	5.7264	5.7239
5	1	0.0000	0.0000	0.0000	0.0000	0.0000	0.0000
5	2	-0.0443	-0.0457	-0.0465	-0.0471	-0.0453	-0.0467
5	3	-0.2758	-0.2748	-0.2739	-0.2730	-0.2740	-0.2724
5	4	0.0931	0.0896	0.0890	0.0886	0.0892	0.0882
5	5	0.6756	0.6710	0.6694	0.6676	0.6714	0.6680
6	6	0.1182	0.1198	0.1197	0.1194	0.1212	0.1210
7	6	0.0248	0.0231	0.0225	0.0218	0.0227	0.0214
7	7	0.1945	0.1951	0.1953	0.1955	0.1957	0.1971
8	6	0.0000	0.0011	0.0014	0.0016	0.0010	0.0015
8	7	0.0485	0.0448	0.0430	0.0414	0.0440	0.0407
8	8	0.0587	0.0643	0.0663	0.0681	0.0655	0.0695

9	9	5.6485	5.6596	5.6606	5.6599	5.6799	5.6801
10	9	0.1410	0.1416	0.1414	0.1414	0.1417	0.1414
10	10	0.5080	0.5062	0.5059	0.5056	0.5064	0.5058
11	9	0.0084	0.0089	0.0088	0.0087	0.0089	0.0089
11	10	0.0480	0.0493	0.0491	0.0490	0.0495	0.0493
11	11	0.1765	0.1777	0.1773	0.1769	0.1794	0.1788
12	9	0.0052	0.0049	0.0048	0.0048	0.0048	0.0047
12	10	0.0185	0.0186	0.0184	0.0182	0.0182	0.0178
12	11	0.0598	0.0566	0.0555	0.0546	0.0559	0.0538
12	12	0.1014	0.1066	0.1076	0.1086	0.1075	0.1098

^aThe units of the force constants are consistent with energy in aJ, bond lengths in Å, and bond angles in radians. The internal coordinates i, j for the F_{ij} values are defined in Table 2.2. cc-pVXZ (X=T, Q, 5) represents quadratic force constants F_{ij} computed with the corresponding correlation-consistent basis sets at the CCSD(T) level of theory. CBS represents the complete basis set limit of quadratic force constants extrapolated using the cc-pVXZ data via focal point analysis. CBS_CC includes additional core-correlation effects computed at the cc-pVQZ CCSD(T) level of theory.

Table 2.9. Cubic force constants (F_{ijk}) extrapolation of propargyl radical.^a

i	j	k	cc-pVTZ	cc-pVQZ	cc-pV5Z	CBS	pCVQZ	CBS-cc
1	1	1	-35.8209	-35.8438	-35.8998	-35.9543	-36.0925	-36.1979
2	1	1	0.0454	0.0505	0.0518	0.0531	0.0561	0.0581
2	2	1	0.0991	0.1024	0.1038	0.1050	0.1082	0.1105
2	2	2	-87.7550	-89.0158	-89.2978	-89.5668	-90.2311	-90.6712
3	1	1	-0.1511	-0.1528	-0.1534	-0.1540	-0.1556	-0.1567
3	2	1	-0.1157	-0.1159	-0.1161	-0.1163	-0.1169	-0.1173
3	2	2	1.8419	1.8382	1.8377	1.8368	1.8357	1.8349
3	3	1	0.0555	0.0572	0.0576	0.0579	0.0587	0.0593
3	3	2	-4.7167	-4.7275	-4.7303	-4.7323	-4.7388	-4.7431
3	3	3	-36.8000	-37.4684	-37.6263	-37.7594	-38.1402	-38.3837
4	1	1	-0.0031	-0.0031	-0.0030	-0.0030	-0.0030	-0.0030
4	2	1	-0.0241	-0.0246	-0.0248	-0.0249	-0.0252	-0.0254
4	2	2	-0.0639	-0.0631	-0.0629	-0.0627	-0.0623	-0.0618
4	3	1	-0.0400	-0.0408	-0.0410	-0.0412	-0.0417	-0.0420
4	3	2	0.1450	0.1473	0.1477	0.1481	0.1493	0.1500
4	3	3	-0.3155	-0.3076	-0.3055	-0.3038	-0.2985	-0.2952
4	4	1	-0.0127	-0.0130	-0.0130	-0.0131	-0.0131	-0.0131
4	4	2	-0.0155	-0.0150	-0.0148	-0.0147	-0.0142	-0.0140
4	4	3	0.2523	0.2594	0.2612	0.2626	0.2674	0.2701
4	4	4	-22.9210	-23.0208	-23.0526	-23.0744	-23.1861	-23.2353
5	1	1	0.0098	0.0098	0.0099	0.0099	0.0099	0.0099
5	2	1	0.0041	0.0041	0.0041	0.0041	0.0042	0.0042
5	2	2	-0.0106	-0.0109	-0.0110	-0.0110	-0.0112	-0.0113

5	3	1	-0.0140	-0.0142	-0.0143	-0.0144	-0.0144	-0.0145
5	3	2	-0.0417	-0.0416	-0.0415	-0.0414	-0.0417	-0.0414
5	3	3	0.1767	0.1793	0.1799	0.1804	0.1819	0.1827
5	4	1	0.0063	0.0064	0.0064	0.0064	0.0065	0.0066
5	4	2	0.0516	0.0514	0.0514	0.0514	0.0514	0.0513
5	4	3	0.1372	0.1366	0.1365	0.1364	0.1359	0.1358
5	4	4	-0.2006	-0.2007	-0.2007	-0.2008	-0.2006	-0.2007
5	5	1	0.0065	0.0067	0.0067	0.0067	0.0067	0.0068
5	5	2	-0.0423	-0.0428	-0.0429	-0.0431	-0.0432	-0.0435
5	5	3	-0.1091	-0.1096	-0.1098	-0.1100	-0.1097	-0.1101
5	5	4	-0.3717	-0.3717	-0.3716	-0.3715	-0.3716	-0.3715
5	5	5	-0.3256	-0.3244	-0.3241	-0.3238	-0.3234	-0.3229
6	6	1	-0.0058	-0.0057	-0.0057	-0.0057	-0.0056	-0.0056
6	6	2	0.1236	0.1241	0.1241	0.1241	0.1248	0.1247
6	6	3	-0.5470	-0.5468	-0.5465	-0.5463	-0.5470	-0.5465
6	6	4	-0.1442	-0.1443	-0.1443	-0.1442	-0.1444	-0.1444
6	6	5	0.1237	0.1227	0.1224	0.1221	0.1217	0.1212
7	6	1	-0.0001	-0.0001	-0.0001	-0.0001	-0.0001	-0.0001
7	6	2	0.0735	0.0734	0.0733	0.0733	0.0732	0.0732
7	6	3	-0.0196	-0.0193	-0.0192	-0.0192	-0.0190	-0.0189
7	6	4	0.0209	0.0210	0.0210	0.0210	0.0211	0.0211
7	6	5	-0.0371	-0.0370	-0.0369	-0.0369	-0.0369	-0.0368
7	7	1	-0.0121	-0.0119	-0.0118	-0.0118	-0.0117	-0.0117
7	7	2	-0.3238	-0.3244	-0.3245	-0.3246	-0.3249	-0.3250
7	7	3	-0.3393	-0.3408	-0.3411	-0.3414	-0.3423	-0.3429

7	7	4	0.0230	0.0228	0.0227	0.0227	0.0224	0.0223
7	7	5	0.0098	0.0097	0.0097	0.0097	0.0096	0.0095
8	6	1	0.0064	0.0064	0.0064	0.0064	0.0064	0.0064
8	6	2	0.0089	0.0087	0.0086	0.0086	0.0085	0.0084
8	6	3	-0.0011	-0.0011	-0.0012	-0.0012	-0.0012	-0.0012
8	6	4	0.0058	0.0057	0.0057	0.0057	0.0057	0.0057
8	6	5	-0.0061	-0.0060	-0.0060	-0.0060	-0.0060	-0.0059
8	7	1	0.0103	0.0103	0.0103	0.0103	0.0104	0.0105
8	7	2	0.0806	0.0809	0.0809	0.0810	0.0811	0.0812
8	7	3	0.0303	0.0303	0.0303	0.0303	0.0303	0.0303
8	7	4	-0.0072	-0.0072	-0.0072	-0.0072	-0.0073	-0.0073
8	7	5	-0.0058	-0.0058	-0.0058	-0.0058	-0.0058	-0.0058
8	8	1	-0.0580	-0.0582	-0.0583	-0.0583	-0.0584	-0.0584
8	8	2	-0.5584	-0.5585	-0.5585	-0.5585	-0.5586	-0.5585
8	8	3	0.2062	0.2071	0.2073	0.2074	0.2078	0.2080
8	8	4	-0.0196	-0.0198	-0.0199	-0.0200	-0.0202	-0.0203
8	8	5	0.0019	0.0019	0.0019	0.0019	0.0018	0.0018
9	9	1	-0.0183	-0.0189	-0.0190	-0.0191	-0.0194	-0.0196
9	9	2	-0.1086	-0.1087	-0.1087	-0.1087	-0.1090	-0.1089
9	9	3	0.2807	0.2868	0.2883	0.2894	0.2934	0.2955
9	9	4	-22.9027	-23.0069	-23.0400	-23.0628	-23.1770	-23.2282
9	9	5	0.3672	0.3673	0.3671	0.3667	0.3686	0.3680
10	9	1	0.0032	0.0034	0.0035	0.0035	0.0036	0.0037
10	9	2	-0.0212	-0.0208	-0.0208	-0.0207	-0.0204	-0.0203
10	9	3	-0.3388	-0.3405	-0.3410	-0.3414	-0.3420	-0.3428

10	9	4	0.0341	0.0342	0.0342	0.0342	0.0345	0.0345
10	9	5	0.0801	0.0811	0.0813	0.0816	0.0819	0.0824
10	10	1	0.0106	0.0109	0.0110	0.0111	0.0111	0.0113
10	10	2	-0.0764	-0.0776	-0.0780	-0.0783	-0.0785	-0.0791
10	10	3	-0.2288	-0.2296	-0.2298	-0.2300	-0.2301	-0.2305
10	10	4	-0.1712	-0.1717	-0.1718	-0.1720	-0.1719	-0.1722
10	10	5	0.4540	0.4558	0.4563	0.4567	0.4575	0.4582
11	9	1	-0.0019	-0.0018	-0.0018	-0.0018	-0.0018	-0.0018
11	9	2	-0.0637	-0.0639	-0.0640	-0.0640	-0.0641	-0.0642
11	9	3	-0.0386	-0.0396	-0.0399	-0.0401	-0.0406	-0.0411
11	9	4	0.0128	0.0128	0.0128	0.0128	0.0129	0.0129
11	9	5	0.0052	0.0054	0.0054	0.0055	0.0055	0.0056
11	10	1	-0.0107	-0.0107	-0.0107	-0.0107	-0.0107	-0.0107
11	10	2	-0.1089	-0.1089	-0.1090	-0.1090	-0.1090	-0.1090
11	10	3	-0.0170	-0.0169	-0.0169	-0.0170	-0.0168	-0.0169
11	10	4	-0.0406	-0.0410	-0.0411	-0.0412	-0.0413	-0.0415
11	10	5	0.0303	0.0308	0.0310	0.0311	0.0313	0.0316
11	11	1	-0.0079	-0.0077	-0.0076	-0.0076	-0.0074	-0.0074
11	11	2	-0.4462	-0.4464	-0.4465	-0.4466	-0.4466	-0.4467
11	11	3	-0.3131	-0.3158	-0.3165	-0.3170	-0.3186	-0.3196
11	11	4	0.0173	0.0165	0.0163	0.0162	0.0156	0.0153
11	11	5	0.0296	0.0298	0.0298	0.0299	0.0299	0.0300
12	9	1	-0.0021	-0.0021	-0.0021	-0.0021	-0.0021	-0.0021
12	9	2	0.0169	0.0170	0.0170	0.0170	0.0171	0.0171
12	9	3	-0.0105	-0.0105	-0.0104	-0.0104	-0.0104	-0.0104

12	9	4	-0.0012	-0.0012	-0.0012	-0.0012	-0.0012	-0.0012
12	9	5	0.0044	0.0045	0.0045	0.0045	0.0046	0.0046
12	10	1	0.0054	0.0054	0.0053	0.0053	0.0053	0.0053
12	10	2	0.0478	0.0478	0.0478	0.0477	0.0476	0.0476
12	10	3	-0.0021	-0.0020	-0.0020	-0.0020	-0.0020	-0.0019
12	10	4	-0.0057	-0.0057	-0.0057	-0.0057	-0.0057	-0.0058
12	10	5	0.0147	0.0146	0.0146	0.0145	0.0145	0.0145
12	11	1	-0.0084	-0.0084	-0.0084	-0.0084	-0.0084	-0.0083
12	11	2	0.1345	0.1346	0.1346	0.1346	0.1347	0.1347
12	11	3	-0.0153	-0.0150	-0.0150	-0.0149	-0.0147	-0.0146
12	11	4	-0.0100	-0.0101	-0.0101	-0.0101	-0.0101	-0.0101
12	11	5	-0.0001	0.0000	0.0001	0.0001	0.0001	0.0002
12	12	1	-0.0462	-0.0463	-0.0463	-0.0463	-0.0464	-0.0464
12	12	2	-0.4421	-0.4423	-0.4424	-0.4424	-0.4425	-0.4425
12	12	3	0.0377	0.0381	0.0382	0.0383	0.0384	0.0386
12	12	4	-0.0116	-0.0117	-0.0117	-0.0118	-0.0119	-0.0119
12	12	5	-0.0027	-0.0028	-0.0028	-0.0028	-0.0028	-0.0028

^aSee footnote a of Table 2.8 for the units of the force constants.

Table 2.10. Quartic force constants (F_{ijkl}) of propargyl radical.^a

$i j k l$	F_{ijkl}	$i j k l$	F_{ijkl}	$i j k l$	F_{ijkl}	$i j k l$	F_{ijkl}
1 1 1 1	195.3746	7 7 3 1	-0.0628	10 9 5 4	-0.0208	11 11 11 11	0.1408
2 1 1 1	-0.5645	7 7 3 2	-0.3132	10 9 5 5	0.1491	12 9 1 1	0.0032
2 2 1 1	-2.1897	7 7 3 3	0.7352	10 9 6 6	0.1621	12 9 2 1	0.0073
2 2 2 1	-0.6354	7 7 4 1	-0.0104	10 9 7 6	-0.0251	12 9 2 2	-0.0180
2 2 2 2	421.1054	7 7 4 2	-0.1317	10 9 7 7	-0.0223	12 9 3 1	-0.0010
3 1 1 1	1.0610	7 7 4 3	0.1394	10 9 8 6	-0.0015	12 9 3 2	-0.0349
3 2 1 1	0.4724	7 7 4 4	0.1566	10 9 8 7	-0.0029	12 9 3 3	0.0195
3 2 2 1	-0.3747	7 7 5 1	0.0075	10 9 8 8	-0.0026	12 9 4 1	-0.0102
3 2 2 2	6.6844	7 7 5 2	0.0436	10 9 9 9	-0.2929	12 9 4 2	0.0276
3 3 1 1	0.0433	7 7 5 3	-0.0274	10 10 1 1	0.0506	12 9 4 3	0.0015
3 3 2 1	0.3404	7 7 5 4	0.0376	10 10 2 1	-0.0355	12 9 4 4	-0.0395
3 3 2 2	-5.2638	7 7 5 5	0.0027	10 10 2 2	-0.1530	12 9 5 1	0.0050
3 3 3 1	-0.8826	7 7 6 6	0.1232	10 10 3 1	-0.0894	12 9 5 2	-0.0053
3 3 3 2	9.0408	7 7 7 6	-0.0024	10 10 3 2	0.5519	12 9 5 3	-0.0153
3 3 3 3	214.0445	7 7 7 7	0.5693	10 10 3 3	-0.3776	12 9 5 4	0.0020
4 1 1 1	-0.0208	8 6 1 1	0.0011	10 10 4 1	0.0238	12 9 5 5	-0.0081
4 2 1 1	-0.0125	8 6 2 1	0.0044	10 10 4 2	-0.0493	12 9 6 6	0.0063
4 2 2 1	-0.0582	8 6 2 2	0.0606	10 10 4 3	0.1857	12 9 7 6	0.0027
4 2 2 2	-0.1354	8 6 3 1	-0.0035	10 10 4 4	-0.0252	12 9 7 7	-0.0408
4 3 1 1	0.0238	8 6 3 2	-0.0009	10 10 5 1	0.0924	12 9 8 6	0.0066
4 3 2 1	0.2087	8 6 3 3	0.0238	10 10 5 2	-0.3128	12 9 8 7	0.0067
4 3 2 2	-0.0664	8 6 4 1	-0.0008	10 10 5 3	-0.2098	12 9 8 8	-0.0090
4 3 3 1	0.0397	8 6 4 2	0.0141	10 10 5 4	-0.1853	12 9 9 9	-0.0859

4 3 3 2	-0.7776	8 6 4 3	0.0025	10 10 5 5	0.1795	12 10 1 1	0.0161
4 3 3 3	-1.0449	8 6 4 4	0.0010	10 10 6 6	0.9535	12 10 2 1	-0.0009
4 4 1 1	-0.0351	8 6 5 1	-0.0064	10 10 7 6	-0.0232	12 10 2 2	0.0416
4 4 2 1	0.0591	8 6 5 2	-0.0146	10 10 7 7	0.0097	12 10 3 1	0.0136
4 4 2 2	-0.1430	8 6 5 3	-0.0058	10 10 8 6	-0.0092	12 10 3 2	-0.0043
4 4 3 1	0.0709	8 6 5 4	-0.0038	10 10 8 7	-0.0264	12 10 3 3	-0.0344
4 4 3 2	0.1414	8 6 5 5	0.0072	10 10 8 8	0.0183	12 10 4 1	-0.0017
4 4 3 3	-2.0065	8 6 6 6	-0.0297	10 10 9 9	-0.1753	12 10 4 2	-0.0090
4 4 4 1	-0.1192	8 7 1 1	-0.1163	10 10 10 9	0.2502	12 10 4 3	0.0294
4 4 4 2	-0.4328	8 7 2 1	0.0206	10 10 10 10	0.3677	12 10 4 4	-0.0218
4 4 4 3	-1.2067	8 7 2 2	-0.2699	11 9 1 1	-0.0001	12 10 5 1	-0.0220
4 4 4 4	85.9312	8 7 3 1	-0.0146	11 9 2 1	-0.0026	12 10 5 2	0.0481
5 1 1 1	-0.0192	8 7 3 2	0.1497	11 9 2 2	0.0517	12 10 5 3	-0.0023
5 2 1 1	-0.0138	8 7 3 3	-0.1418	11 9 3 1	-0.0066	12 10 5 4	-0.0148
5 2 2 1	0.0041	8 7 4 1	-0.0081	11 9 3 2	0.0473	12 10 5 5	-0.0024
5 2 2 2	-0.1239	8 7 4 2	0.0320	11 9 3 3	0.2570	12 10 6 6	0.0426
5 3 1 1	0.0088	8 7 4 3	-0.0006	11 9 4 1	-0.0109	12 10 7 6	0.0045
5 3 2 1	-0.0096	8 7 4 4	-0.0330	11 9 4 2	-0.0395	12 10 7 7	0.1408
5 3 2 2	0.1552	8 7 5 1	0.0045	11 9 4 3	0.0628	12 10 8 6	-0.0083
5 3 3 1	0.0844	8 7 5 2	-0.0049	11 9 4 4	-0.0885	12 10 8 7	-0.0468
5 3 3 2	-0.1452	8 7 5 3	-0.0073	11 9 5 1	-0.0005	12 10 8 8	-0.0182
5 3 3 3	-0.8666	8 7 5 4	0.0055	11 9 5 2	0.0055	12 10 9 9	-0.0210
5 4 1 1	0.0018	8 7 5 5	0.0042	11 9 5 3	-0.0704	12 10 10 9	0.0119
5 4 2 1	-0.0207	8 7 6 6	0.0350	11 9 5 4	0.0143	12 10 10 10	-0.0043
5 4 2 2	0.1108	8 7 7 6	0.0842	11 9 5 5	0.0333	12 11 1 1	-0.1140

5 4 3 1	-0.0163	8 7 7 7	0.2492	11 9 6 6	0.0403	12 11 2 1	0.0147
5 4 3 2	-0.0658	8 8 1 1	-0.1155	11 9 7 6	0.0046	12 11 2 2	0.0118
5 4 3 3	0.2475	8 8 2 1	-0.1751	11 9 7 7	-0.0082	12 11 3 1	0.0113
5 4 4 1	-0.0094	8 8 2 2	-0.5556	11 9 8 6	0.0027	12 11 3 2	-0.0388
5 4 4 2	-0.0027	8 8 3 1	0.2089	11 9 8 7	0.0366	12 11 3 3	-0.0765
5 4 4 3	0.0285	8 8 3 2	0.6049	11 9 8 8	-0.0058	12 11 4 1	-0.0045
5 4 4 4	-0.0140	8 8 3 3	-0.9297	11 9 9 9	-0.1926	12 11 4 2	0.0109
5 5 1 1	0.0125	8 8 4 1	0.0827	11 10 1 1	-0.0137	12 11 4 3	0.0209
5 5 2 1	-0.0074	8 8 4 2	-0.0065	11 10 2 1	-0.0186	12 11 4 4	-0.0369
5 5 2 2	-0.0712	8 8 4 3	0.0815	11 10 2 2	0.0399	12 11 5 1	0.0017
5 5 3 1	-0.0361	8 8 4 4	-0.0135	11 10 3 1	0.0191	12 11 5 2	-0.0181
5 5 3 2	0.2371	8 8 5 1	0.0036	11 10 3 2	-0.0532	12 11 5 3	-0.0196
5 5 3 3	-0.1259	8 8 5 2	0.0084	11 10 3 3	-0.0404	12 11 5 4	0.0102
5 5 4 1	0.0104	8 8 5 3	0.0014	11 10 4 1	0.0049	12 11 5 5	0.0081
5 5 4 2	-0.0175	8 8 5 4	0.0054	11 10 4 2	0.0554	12 11 6 6	0.0414
5 5 4 3	0.0680	8 8 5 5	0.0113	11 10 4 3	0.1114	12 11 7 6	0.0126
5 5 4 4	-0.1378	8 8 6 6	0.1146	11 10 4 4	-0.0791	12 11 7 7	-0.1031
5 5 5 1	0.0272	8 8 7 6	0.1172	11 10 5 1	-0.0086	12 11 8 6	0.0430
5 5 5 2	-0.0776	8 8 7 7	0.2195	11 10 5 2	-0.0290	12 11 8 7	0.0951
5 5 5 3	-0.3642	8 8 8 6	-0.0086	11 10 5 3	-0.1188	12 11 8 8	-0.0472
5 5 5 4	0.1250	8 8 8 7	-0.1260	11 10 5 4	-0.0562	12 11 9 9	-0.0494
5 5 5 5	0.1010	8 8 8 8	0.3047	11 10 5 5	0.0746	12 11 10 9	-0.0138
6 6 1 1	0.0018	9 9 1 1	-0.0053	11 10 6 6	0.0824	12 11 10 10	0.0300
6 6 2 1	-0.0170	9 9 2 1	0.0701	11 10 7 6	-0.0286	12 11 11 9	-0.0369
6 6 2 2	0.2835	9 9 2 2	-0.1745	11 10 7 7	-0.0049	12 11 11 10	-0.0173

6 6 3 1	-0.0119	9 9 3 1	0.1421	11 10 8 6	0.0032	12 11 11 11	-0.1396
6 6 3 2	-0.4828	9 9 3 2	0.2614	11 10 8 7	-0.0315	12 12 1 1	-0.0304
6 6 3 3	0.4422	9 9 3 3	-2.1304	11 10 8 8	-0.0059	12 12 2 1	-0.0713
6 6 4 1	0.0028	9 9 4 1	-0.0438	11 10 9 9	-0.0124	12 12 2 2	-0.0389
6 6 4 2	0.0949	9 9 4 2	-0.1223	11 10 10 9	0.0823	12 12 3 1	0.0658
6 6 4 3	-0.0423	9 9 4 3	-0.4592	11 10 10 10	0.1230	12 12 3 2	0.1072
6 6 4 4	-0.0304	9 9 4 4	86.8350	11 11 1 1	0.0701	12 12 3 3	-0.2492
6 6 5 1	0.0008	9 9 5 1	0.0065	11 11 2 1	-0.0191	12 12 4 1	0.0870
6 6 5 2	-0.2481	9 9 5 2	0.1337	11 11 2 2	0.0249	12 12 4 2	0.0147
6 6 5 3	0.5301	9 9 5 3	-0.1086	11 11 3 1	-0.0603	12 12 4 3	0.0217
6 6 5 4	0.0853	9 9 5 4	-0.3346	11 11 3 2	0.0874	12 12 4 4	-0.0231
6 6 5 5	-0.1935	9 9 5 5	-0.9670	11 11 3 3	0.7336	12 12 5 1	-0.0097
6 6 6 6	0.3744	9 9 6 6	0.0725	11 11 4 1	-0.0410	12 12 5 2	-0.0043
7 6 1 1	0.0050	9 9 7 6	-0.0020	11 11 4 2	-0.0462	12 12 5 3	0.0183
7 6 2 1	-0.0001	9 9 7 7	-0.0805	11 11 4 3	0.2119	12 12 5 4	-0.0052
7 6 2 2	0.1179	9 9 8 6	0.0008	11 11 4 4	0.2292	12 12 5 5	-0.0260
7 6 3 1	-0.0006	9 9 8 7	-0.0062	11 11 5 1	0.0035	12 12 6 6	0.0614
7 6 3 2	-0.0525	9 9 8 8	0.0038	11 11 5 2	-0.0365	12 12 7 6	0.1834
7 6 3 3	-0.0293	9 9 9 9	87.8679	11 11 5 3	-0.0406	12 12 7 7	0.4692
7 6 4 1	-0.0022	10 9 1 1	0.0264	11 11 5 4	0.0607	12 12 8 6	0.0038
7 6 4 2	-0.0154	10 9 2 1	-0.0179	11 11 5 5	0.0287	12 12 8 7	-0.0319
7 6 4 3	-0.0210	10 9 2 2	-0.0537	11 11 6 6	0.1790	12 12 8 8	0.1087
7 6 4 4	0.0138	10 9 3 1	-0.0455	11 11 7 6	-0.0081	12 12 9 9	0.0015
7 6 5 1	0.0028	10 9 3 2	-0.0463	11 11 7 7	0.1646	12 12 10 9	-0.0034
7 6 5 2	-0.0231	10 9 3 3	0.5422	11 11 8 6	0.1024	12 12 10 10	-0.0569

7 6 5 3	-0.0078	10 9 4 1	-0.0134	11 11 8 7	0.2659	12 12 11 9	-0.0253
7 6 5 4	-0.0030	10 9 4 2	-0.0376	11 11 8 8	-0.0340	12 12 11 10	-0.0039
7 6 5 5	0.0150	10 9 4 3	0.1163	11 11 9 9	-0.0850	12 12 11 11	-0.0419
7 6 6 6	-0.0872	10 9 4 4	-0.2652	11 11 10 9	-0.0299	12 12 12 9	-0.0038
7 7 1 1	0.0331	10 9 5 1	0.0234	11 11 10 10	0.1002	12 12 12 10	-0.0073
7 7 2 1	0.0020	10 9 5 2	-0.0435	11 11 11 9	0.0165	12 12 12 11	-0.1255
7 7 2 2	0.5712	10 9 5 3	-0.2732	11 11 11 10	0.0315	12 12 12 12	0.3681

^aSee footnote a of Table 2.8 for the units of the force constants.

CHAPTER 3

STRUCTURES AND ENERGETICS OF HOCO RADICAL, ANION, AND CATION: HIGH-ACCURACY AB INITIO INVESTIGATION VIA FOCAL POINT ANALYSIS

¹Yan, G.; Allen, W. D.; Schaefer, H. F.; *To be submitted*

3.1 ABSTRACT

Accurate equilibrium structures and energetics of *trans*- and *cis*-HOCO anion, radical, and cation have been determined via systematic *ab initio* calculations. Electron affinities and ionization potentials of *trans*- and *cis*-HOCO radicals have been predicted. State-of-the-art *ab initio* electronic structure theory, including MP2 (second order Møller-Plesset perturbation theory), CCSD (coupled cluster single and double excitations), CCSD(T) (CCSD with perturbative triples), and CCSDT (CCSD with full triple excitations), in combination with correlation basis sets of the form aug-cc-p(C)VXZ (X=2-6), have been utilized to extrapolate to the complete basis set full configuration interaction limit via the focal point analysis method developed by Allen and co-workers. Core-correlation effects, special relativity, zero-point vibrational energy, and diagonal Born-Oppenheimer corrections were explicitly incorporated in the results to provide accuracy to the level of 0.1 kcal mol⁻¹. The final proposals for the adiabatic electron affinities are: 1.3712 eV (*trans*-HOCO) and 1.5038 eV (*cis*-HOCO). The vertical detachment energies are necessarily larger: 1.9618 eV (*trans*-HOCO) and 2.0809 eV (*cis*-HOCO). The predicted adiabatic and vertical radical ionization potentials of the *trans*-HOCO are 8.1077 eV and 9.7771 eV, respectively.

3.2 INTRODUCTION

The hydroxyformyl radical, HOCO, is one of the most important radicals in the combustion process. It has long been shown as a critical intermediate in the reaction $\text{OH} + \text{CO} \rightarrow \text{H} + \text{CO}_2$, a key reaction for the production of CO₂ in combustion.¹⁻⁴

HOCO neutral radical has been the subject of extensive experimental and theoretical studies. Milligan and Jacox first identified *trans*- and *cis*-HOCO radicals by vacuum-ultraviolet

photolysis of H₂O in a CO matrix, and assigned vibrational frequencies to them.⁵ Vibrational spectra of *trans*-HOCO free radical have also been obtained later in argon matrix,⁶ neon matrix,⁷ and gas phase.⁸⁻¹⁰ Rotational spectra of *trans*-HOCO and DOCO were recorded by Radford, Wei, and Sears using millimeter-wave spectroscopy.¹¹ Numerous *ab initio* computations have also been performed on HOCO radical.¹²⁻²¹ Most recent high-level theoretical studies include coupled cluster theory determination of the heats of formation for *trans*-HOCO radical by Feller, Dixon, and Francisco,¹⁸ and the applications of G3MP2B3 and CCSD(T)-CBS methods to the thermochemical properties of HOCO radicals by Fabian and Janoschek.¹⁹

HOCO⁻ and HOCO⁺, on the other hand, were less studied. HOCO⁻ anion was characterized for the first time in 2002 by Clements, Continetti, and Francisco via dissociative photodetachment spectroscopy.²² Later Dixon, Feller, and Francisco performed high-level coupled cluster calculations on *trans*- and *cis*-HOCO anions, and predicted the electron affinities of the two isomers as 1.36 and 1.42 eV, respectively.¹⁷ HOCO⁺ cation was first studied with photoionization spectroscopy in 1989 by Ruscic, Schwarz, and Berkowitz,²³ and the adiabatic ionization potential of *trans*-HOCO was determined as 8.486 ± 0.012 eV, but this value was later revised to a tentatively suggested value of 8.06 ± 0.03 eV in a renewed photoionization study by Ruscic and Litorja in 2000.²⁴ Francisco applied CCSD(T) 6-311++G(3df, 3pd)//CCSD(T) 6-311G(3df,3pd) methodology to *trans*-HOCO⁺ and proposed an adiabatic ionization potential of 8.01 eV,²⁵ in good agreement with the renewed experimental results. ν_1 fundamental band of *trans*-HOCO⁺ cation was determined by difference-frequency spectroscopy²⁶, and recently Jacox and Thompson identified three vibrational modes of this cation via infrared spectroscopy in Ne matrix.²⁷ Complete rotational constants were also obtained by submillimeter wave spectroscopy.²⁸

With the important role of the HOCO families of molecules in combustion chemistry and recent advent of latest experimental discoveries, it is of great interest to provide improved and highly accurate *ab initio* data on the geometrical structures and energetics of the relevant species to assist further experimental studies. In the continuing pursuit of subchemical accuracy for computational methods in our group, the focal point analysis scheme proposed by Allen and co-workers have been applied to different systems to consistently achieve subchemical accuracy to the level of 0.1 kcal/mol, which will be utilized in this study to make critical assessment of current experimental and theoretical data.

3.3 COMPUTATIONAL METHODS

In this investigation, the focal point approach developed by Allen and co-workers²⁹⁻³² were employed to extrapolate total and relative energies of relevant species toward the complete basis set (CBS) full configuration interaction (FCI) limit. Focal-point analysis aims at a two-dimensional extrapolation scheme for the basis set and correlation method dependence of electronic energies. Supplemented with core correlation, special relativity, diagonal Born-Oppenheimer, and zero-point vibrational energy corrections, it has been successfully applied to a variety of molecular systems achieving subchemical accuracies to the level of 0.1 kcal mol⁻¹.

In the focal point scheme, the aug-cc-p(C)VXZ families of basis sets developed by Dunning and co-workers³³⁻³⁷ were utilized exclusively for the electronic structure calculations in this study.

We begin with the determination of a set of high quality r_e structural parameters for *trans*- and *cis*-HOCO neutral radicals, anions, and cations at the aug-cc-pVQZ CCSD(T) level of theory,

freezing the 1s orbitals of carbon and oxygen. The reference electronic wave functions were determined by single-reference spin-restricted Hartree-Fock theory.^{38,39} Geometry optimizations were carried out via finite differences of energy points.

With the optimal equilibrium geometries, total energies of *trans*- and *cis*-HOCO radicals, anions, and cations were first extrapolated under the frozen-core approximation. For this primary extrapolation, valence correlation consistent basis sets of the form aug-cc-pVXZ (X=2,3,4,5,6) were utilized to determine energies at the Hartree-Fock, MP2 (second-order Møller-Plesset perturbation theory),³⁹⁻⁴¹ CCSD (coupled-cluster singles and doubles),⁴²⁻⁴⁴ CCSD(T) (CCSD with perturbative triples),^{45,46} and CCSDT (full couple cluster with singles, doubles, and triples)⁴⁷⁻⁵⁰ levels of theory. In the second set of extrapolation, the core correlation effects were extrapolated utilizing the core-valence basis set aug-cc-pCVXZ (X=2,3,4).

The functional form adopted for the Hartree-Fock extrapolation is

$$E_{HF} = E_{HF}^{\infty} + ae^{-bX}$$

whereas the correlation energy was extrapolated via

$$E_{corr} = a + bX^{-3}$$

Auxiliary effects, including diagonal Born-Oppenheimer correction (DBOC)⁵¹⁻⁵⁴ and special relativistic effects⁵⁵⁻⁵⁸ were necessarily included in the results to ensure subchemical accuracy. The DBOC was computed at the aug-cc-pVTZ SCF level of theory with PSI3.⁵⁹ Special relativity corrections were carried out in aug-cc-pVTZ CCSD(T) with ACESII.⁶⁰ Harmonic vibrational frequency were computed at the aug-cc-pVTZ CCSD(T) level of theory by finite differences of energy points to provide zero-point vibrational energy (ZPVE) corrections. All energy points in the frequency calculation were converged to at least 10^{-10} hartrees.

Ionization potential (IP), electron affinity (EA) and vertical detachment energies (VDE) were evaluated as differences in total energies between relevant molecular species. The classical adiabatic IPs are defined as

$$IP_a = E_{(\text{optimized cation})} - E_{(\text{optimized radical})};$$

the classical adiabatic IPs with zero-point corrections are

$$IP_a = E_{(\text{zero-point corrected cation})} - E_{(\text{zero-point corrected radical})};$$

the vertical IPs are determined by

$$IP_v = E_{(\text{cation at optimized radical geometry})} - E_{(\text{optimized radical})};$$

the classical adiabatic EAs are defined as

$$EA_a = E_{(\text{optimized radical})} - E_{(\text{optimized anion})};$$

the classical adiabatic EAs with zero-point corrections are

$$EA_a = E_{(\text{zero-point corrected radical})} - E_{(\text{zero-point corrected anion})};$$

and the vertical detachment energies are computed via

$$VDE = E_{(\text{radical at optimized anion geometry})} - E_{(\text{optimized anion})}.$$

Except for the DBOC and special relativity effects, all electronic structure calculations were performed using Molpro⁶¹ and NWChem^{62,63} suite of software packages.

3.4 RESULTS AND DISCUSSIONS

A. OPTIMIZED GEOMETRIES

High quality equilibrium structures for *trans*- and *cis*-HOCO anion, radical, and cation determined at the aug-cc-pVQZ CCSD(T) level of theory are shown in Figure 1,. Theoretical and experimental geometrical parameters for these molecular systems are summarized in Table 1.

All molecules possess C_s symmetries in their ground electronic states. Agreement between our equilibrium geometry and previous experimental and high level theoretical results are very good. For all five species investigated in this study, the differences in bond lengths are less than 0.002 Å and that in bond angles are less than 0.4° between our aug-cc-pVQZ CCSD(T) results and earlier high level *ab initio* studies.^{17,25} Experimental rotational constants are only available for the *trans*-HOCO radical and cation,^{11,26,28} where our equilibrium rotational constants are in excellent agreement with the experimental values. The 35 GHz difference for the A value of *trans*-HOCO⁺ is typical between the calculated equilibrium and experimentally determined zero-point rotational constants.

The geometry changes caused by the addition or removal of an electron from the neutral radicals are significant. For *trans*-HOCO radical, with the addition of an electron, the O-C bond length is increased by 0.168 Å, the H-O-C angle is decreased by 7.3° and the O-C-O' angle is decreased by as much as 16.3° to *trans*-HOCO⁻. The geometry change from *trans*-HOCO radical to cation is even more dramatic, with a 0.117 Å decrease for the O-C bond length, a 10.1° increase for the H-O-C angle, and a huge increase of 47.3° for the O-C-O' angle. The O-C-O' angle in *trans*-HOCO⁺ is almost flat, and no *cis*-HOCO⁺ structure can be located on the potential energy surface.

Similar structural alterations are also observed for the *cis* isomer. For *cis*-HOCO⁻ anion, the O-C bond length is 0.1213 Å longer, whereas the H-O-C and O-C-O' bond angles are 5.7° and 18.4° smaller than the corresponding *cis*-HOCO radical.

B. VIBRATIONAL FREQUENCIES

Harmonic vibrational frequencies for *trans*-HOCO anion, radical, cation and *cis*-HOCO anion and radical are computed at the aug-cc-pVTZ CCSD(T) level of theory in this work. A comprehensive list of available experimental and high level theoretical vibrational frequencies is collected in Table 2.

For vibrational study, *trans*-HOCO neutral radical is the most studied one among the five molecules. Its vibrational spectrum has been obtained experimentally in CO, Ne, and Ar matrices and gas phase.⁵⁻⁷ The O-H stretching mode in CO matrix is 150 cm⁻¹ or more lower than in other matrices or in gas phase, a result of the strong interaction between the CO matrix and the radical. Our predicted harmonic vibrational frequencies are in good agreement with other *ab initio* methods as well as experimental fundamental frequencies, where anharmonic corrections are needed to make direct comparisons.

The only available experimental vibrational study for *cis*-HOCO radical is performed in CO matrix by Milligan and Jacox.⁵ Similarly as the *trans*-HOCO radical, the O-H stretching mode has been significantly perturbed by the CO matrix.

No experimental study has been reported for the vibrational spectra of *trans*- and *cis*-HOCO anions. Dixon *et al.* reported harmonic vibrational frequencies for the two anions based on aug-cc-pVDZ CCSD(T) study,¹⁷ which are in reasonable agreement with our results via aug-cc-pVTZ CCSD(T) computations.

For the *trans*-HOCO cation, its ν_1 O-H stretching mode has been reported in gas phase,²⁶ and the O-H stretching, C-O stretching, and C-O' stretching modes were recently reported in the Ne matrix,²⁷ which agree with *ab initio* calculations nicely.

Based on the vibrational frequencies, zero-point vibrational energy corrections can be made to the various energetics under investigation in the following discussions.

C. ELECTRON AFFINITIES

The theoretical determination of adiabatic electron affinity of *trans*- and *cis*-HOCO radicals is listed in Table 3, 6, and 7.

In the valence focal point analysis in Table 3, explicit computations have been performed with up to aug-cc-pV6Z basis set and correlation method up to the CCSDT level of theory. One of the remarkable features of the extrapolation data is the rapid convergence of the RHF and incremental correlation energies with respect to one- and many-particle basis. For example, the explicitly computed aug-cc-pV6Z RHF energies are essentially the same as the extrapolated CBS RHF energies, whereas the explicitly computed MP2 and CCSD incremental energies with the aug-cc-pV6Z basis set are within 0.014 eV of the extrapolated CBS limit. The increment with the aug-cc-pV5Z CCSD(T) computation is within 0.0015 eV of the CBS CCSD(T) limit. In addition, all of the coupled-cluster correlation increments are less than 0.12 eV in magnitude. An interesting characteristic of the extrapolation is the mutually canceling effect of CCSD and CCSD(T) incremental corrections, whose composite effect results in almost no post-MP2 corrections for *trans*-HOCO and less than 0.02 eV correction for *cis*-HOCO.

The extrapolated core correlation effect shown in Table 7 gives rise to less than 0.018 eV corrections to adiabatic electron affinity of both *trans*- and *cis*-HOCO radicals. Zero-point vibrational energy corrections contribute to less than 0.07 eV for both radicals. DBOC and relativistic corrections are less than 0.003 eV. The final adiabatic electron affinities combining valence and core correlation extrapolations, ZPVE, DBOC, and relativistic corrections are

1.3712 and 1.5038 eV for *trans*- and *cis*-HOCO radicals, respectively. This final summary is listed in Table 6.

Our renewed AEA for *trans*- and *cis*-HOCO are 0.01 eV and 0.08 eV larger than the value obtained by Dixon *et al.*¹⁷ While the previous work did an impressive job in the extrapolation of relative energies toward the CBS CCSD(T) limit using aug-cc-pVXZ (X=D, T, Q) basis sets, inclusion of core correlation effects with cc-pCVTZ CCSD(T) calculation and ZPVE corrections with aug-cc-pVDZ CCSD(T) harmonic vibrational frequency computation, our focal point analysis with larger basis set and complete treatment for the correlation effects should yield more accurate results.

The vertical detachment energy (VDE) is computed as the difference between the radical and anion, where the radical is assumed to possess the anion geometry. Focal point analysis for VDE is shown in Table 4, 6, and 7. Similar rapid convergence toward the one-particle basis is observed throughout the table, although the CCSD and CCSD(T) increments do not cancel out each other, and composite post-MP2 corrections contribute to more than 0.03 eV in magnitude to the final predictions. Final predictions of VDE are 1.9618 and 2.0809 eV for *trans*- and *cis*-HOCO radicals, respectively.

D. IONIZATION POTENTIALS

Adiabatic and vertical ionization potential data are only available to *trans*-HOCO radical, as *cis*-HOCO cation is found non-existent from our calculations due to the nearly linear structure of *trans*-HOCO cation. Valence-electron extrapolations of adiabatic and vertical ionization potentials of *trans*-HOCO radical are listed in Table 5, core correlations extrapolations are shown

in Table 7, and the final predictions are summarized in Table 6. Our final predictions for the ionization potentials for *trans*-HOCO radical are 8.1077 eV (AIP) and 9.7771 eV (VIP).

In an early photoionization study of COOH species,²³ the adiabatic ionization potential of HOCO was determined as 8.486±0.012 eV. A rather steep descent is followed by a more gradual decline in the photoionization spectrum, consistent with the substantial geometry change between the *trans*-HOCO neutral radical and cation. However, at a recent *ab initio* study at the 6-311++G(3df, 3pd)//CCSD(T) 6-311G(3df,3pd) level of theory, Francisco *et al.* reported an adiabatic ionization potential of *trans*-HOCO as 8.01 eV,²⁵ a surprisingly large deviation from the experimental value considering the high level of theory used in the computation. Soon after, Ruscic and Litorja reexamined the photoionization threshold of HOCO radical with higher resolution.²⁴ Although the unfavorable Franck-Condon factors make the experimental detection quite difficult, they were able to conclude for a strict upper limit of 8.195±0.022 eV, and a tentative value of 8.056±0.026 eV for the adiabatic ionization potential of *trans*-HOCO radical, in excellent agreement with theoretical results.

3.5 SUMMARY

In this work, fully optimized geometries were obtained for *trans*- and *cis*-HOCO neutral radicals, cations, and anions at the aug-cc-pVQZ CCSD(T) level of theory. Significant geometry changes are observed between radicals, anions, and cations, where the O-C-O angle in the *trans*-HOCO is almost linear. Harmonic vibrational frequencies determined at the aug-cc-pVTZ CCSD(T) level of theory are comparable to previous theoretical and spectroscopic studies. Based on the focal point analysis scheme developed by Allen and coworkers, adiabatic electron affinities, vertical detachment energies, adiabatic and vertical ionization potentials of the radicals were extrapolated

to the complete basis set (CBS) full configuration interaction (FCI) limit with aug-cc-p(C)VXZ (X=2-6) basis sets, and core correlation effects, DBOC, relativistic and zero-point vibrational energy corrections were explicitly included in the results to achieve subchemical accuracy in our predictions.

Our final theoretical predictions are: AEA 1.3712 eV (*trans*-HOCO), 1.5038 eV (*cis*-HOCO); VDE 1.9618 eV (*trans*-HOCO), 2.0809 eV (*cis*-HOCO); AIP 8.1077 eV (*trans*-HOCO); VIP 9.7771 eV (*trans*-HOCO). The adiabatic ionization potential derived in this work is in excellent agreement with recent result from photoionization experiment.

3.6 ACKNOWLEDGMENTS

This work was supported by the U.S. Department of Energy, Office of Basic Energy Sciences, through its Combustion Program (Grant No. DE-FG02-00ER14748) and the SciDAC Computational Chemistry Research Program (Grant No. DE-FG02-01ER15226). This research was performed in part using the Molecular Science Computing Facility (MSCF) in the William R. Wiley Environmental Molecular Sciences Laboratory, a national scientific user facility sponsored by the U.S. Department of Energy's Office of Biological and Environmental Research and located at the Pacific Northwest National Laboratory. Pacific Northwest is operated for the Department of Energy by Battelle.

3.7 REFERENCES

- (1) Smith, I. W. M. *Chem. Phys. Lett.* **1977**, *49*, 112.
- (2) Fulle, D.; Hamann, H. F.; Hippler, H.; Troe, J. *J. Chem. Phys.* **1996**, *105*, 983.
- (3) Valero, R.; McCormack, D. A.; Kroes, G.-J. *J. Chem. Phys.* **2004**, *120*, 4263.

- (4) Lester, M. L.; Pond, B. V.; Anderson, D. T.; Harding, L. B.; Wagner, A. F. *J. Chem. Phys.* **2000**, *113*, 9889.
- (5) Milligan, D. E.; Jacox, M. E. *J. Chem. Phys.* **1971**, *54*, 927.
- (6) Jacox, M. E. *J. Chem. Phys.* **1988**, *88*, 4598.
- (7) Forney, D.; Jacox, M. E.; Thompson, W. E. *J. Chem. Phys.* **2003**, *119*, 10814.
- (8) Petty, J. T.; Moore, C. B. *J. Mol. Spectrosc.* **1993**, *161*, 149.
- (9) Sears, T. J.; Fawzy, W. M.; Johnson, P. M. *J. Chem. Phys.* **1992**, *97*, 3996.
- (10) Petty, J. T.; Moore, C. B. *J. Chem. Phys.* **1993**, *99*, 47.
- (11) Radford, H. E.; Wei, W.; Sears, T. J. *J. Chem. Phys.* **1992**, *97*, 3989.
- (12) McLean, A. D.; Ellinger, Y. *Chem. Phys.* **1985**, *94*, 25.
- (13) Aoyagi, M.; Kato, S. *J. Chem. Phys.* **1988**, *88*, 6409.
- (14) Duncan, T. V.; Miller, C. E. *J. Chem. Phys.* **2000**, *113*, 5138.
- (15) Li, Y.; Francisco, J. S. *J. Chem. Phys.* **2000**.
- (16) Yu, H.-G.; Muckerman, J. T.; Sears, T. J. *Chem. Phys. Lett.* **2001**, *349*, 547.
- (17) Dixon, D. A.; Feller, D.; Francisco, J. S. *J. Phys. Chem. A* **2003**, *107*, 186.
- (18) Feller, D.; Dixon, D. A.; Francisco, J. S. *J. Phys. Chem. A* **2003**, *107*, 1604.
- (19) Fabian, W. M. F.; Janoschek, R. *J. Mol. Struct.* **2005**, *713*, 227.
- (20) Zhang, D. H.; Zhang, J. Z. H. *J. Chem. Phys.* **1995**, *103*, 6512.
- (21) McCormack, D. A.; Kroes, G.-J. *J. Chem. Phys.* **2002**, *116*, 4184.
- (22) Clements, T. G.; Continetti, R. E.; Francisco, J. S. *J. Chem. Phys.* **2002**, *117*, 6478.
- (23) Ruscic, B.; Schwarz, M.; Berkowitz, J. *J. Phys. Chem.* **1989**, *91*, 6780.
- (24) Ruscic, B.; Litorja, M. *Chem. Phys. Lett.* **2000**, *316*, 45.
- (25) Francisco, J. S. *J. Chem. Phys.* **1997**, *107*, 9039.

- (26) Amano, T.; Tanaka, K. *J. Chem. Phys.* **1985**, *83*, 3721.
- (27) Jacox, M. E.; Thompson, W. E. *J. Chem. Phys.* **2003**, *119*, 10824.
- (28) Bogey, M.; Demuyneck, C.; Destombes, J. L.; Krupnor, A. *J. Mol. Struct.* **1988**, *190*, 465.
- (29) East, L. L. A.; Allen, W. D. *J. Chem. Phys.* **1993**, *99*, 4638.
- (30) Kenny, J. P.; Allen, W. D.; Schaefer, H. F. *J. Chem. Phys.* **2003**, *118*, 7353.
- (31) Allen, W. D.; East, L. L. A.; Csaszar, A. G. In *Structures and Conformations of Non-Rigid Molecules*; Oberhammer, H., Ed.; Kluwer: Dordrecht, 1993, p 343.
- (32) Csaszar, A. G.; Allen, W. D.; Schaefer, H. F. *J. Chem. Phys.* **1998**, *108*, 9751.
- (33) Dunning, T. H. *J. Chem. Phys.* **1989**, *90*, 1007.
- (34) Kendall, R. A.; Dunning, T. H.; Harrison, R. J. *J. Chem. Phys.* **1992**, *96*, 6796.
- (35) Woon, D. E.; Dunning, T. H. *J. Chem. Phys.* **1995**, *103*, 4572.
- (36) Wilson, A. K.; Mourik, T. v.; Dunning, T. H. *J. Mol. Struct.: THEOCHEM* **1996**, *388*, 339.
- (37) Basis sets were obtained from the Extensible Computational Chemistry Environment Basis Set Database, V., as developed and distributed by the Molecular Science Computing Facility, Environmental and Molecular Sciences Laboratory which is part of the Pacific Northwest Laboratory, P.O. Box 999, Richland, Washington 99352, USA, and funded by the U.S. Department of Energy. The Pacific Northwest Laboratory is a multi-program laboratory operated by Battelle Memorial Institute for the U.S. Department of Energy under contract DE-AC06-76RLO 1830. Contact David Feller or Karen Schuchardt for further information.
- (38) Roothaan, C. C. *J. Rev. Mod. Phys.* **1951**, *23*, 69.

- (39) Szabo, A.; Ostlund, N. S. *Modern Quantum Chemistry*; McGraw-Hill: New York, 1989.
- (40) Moller, C.; Plesset, M. S. *Phys. Rev.* **1934**, *46*, 618.
- (41) Pople, J. A.; Binkley, J. S.; Seeger, R. *Int. J. Quantum Chem. Symp.* **1976**, *10*, 1.
- (42) Bartlett, R. J. *Annu. Rev. Phys. Chem.* **1981**, *32*, 359.
- (43) Purvis, G. D.; Bartlett, R. J. *J. Chem. Phys.* **1982**, *76*, 1910.
- (44) Rittby, M.; Bartlett, R. J. *J. Phys. Chem.* **1988**, *92*, 3033.
- (45) Raghavachari, K.; Trucks, G. W.; Pople, J. A.; Head-Gordon, M. *Chem. Phys. Lett.* **1989**, *157*, 479.
- (46) Scuseria, G. E. *Chem. Phys. Lett.* **1991**, *176*, 27.
- (47) Noga, J.; Bartlett, R. J. *J. Chem. Phys.* **1987**, *86*, 7041.
- (48) Noga, J.; Bartlett, R. J. *J. Chem. Phys.* **1988**, *89*, 3401.
- (49) Watts, J. D.; Bartlett, R. J. *J. Chem. Phys.* **1990**, *93*, 6104.
- (50) Scuseria, G. E.; Schaefer, H. F. *Chem. Phys. Lett.* **1988**, *152*, 382.
- (51) Handy, N. C.; Yamaguchi, Y.; Schaefer, H. F. *J. Chem. Phys.* **1986**, *84*, 4481.
- (52) Ioannou, A. G.; Amos, R. D.; Handy, N. C. *Chem. Phys. Lett.* **1996**, *251*, 52.
- (53) Handy, N. C.; Lee, A. M. *Chem. Phys. Lett.* **1996**, *252*, 425.
- (54) Kutzelnigg, W. *Mol. Phys.* **1997**, *90*, 909.
- (55) Perera, S. A.; Bartlett, R. J. *Chem. Phys. Lett.* **1993**, *216*, 606.
- (56) Cowan, R. D.; Griffin, D. C. *J. Opt. Soc. Am.* **1976**, *66*, 1010.
- (57) Tarczay, G.; Csaszar, A. G.; Klopper, W.; Quiney, H. M. *Mol. Phys.* **2001**, *99*, 1769.
- (58) Balasubramanian, K. *Relativistic Effects in Chemistry*; Wiley: New York, 1997. (59)
- T. Daniel Crawford, C. David Sherrill, Edward F. Valeev, Justin T. Fermann, Rollin A. King,

Matthew L. Leininger, Shawn T. Brown, Curtis L. Janssen, Edward T. Seidl, Joseph P. Kenny, and Wesley D. Allen, PSI 3.2, 2003.

(60) ACES II is a program product of the Quantum Theory Project, University of Florida. Authors: J. F. Stanton, J. Gauss, J. D. Watts, M. Nooijen, N. Oliphant, S. A. Perera, P. G. Szalay, W. J. Lauderdale, S. R. Gwaltney, S. Beck, A. Balkova D. E. Bernholdt, K.-K Baeck, P. Rozyczko, H. Sekino, C. Hober, and R.J. Bartlett. Integral packages included are VMOL (J. Almlöf and P. R. Taylor); VPROPS (P. Taylor); ABACUS (T. Helgaker, H.J. Aa. Jensen, P. Jørgensen, J. Olsen, and P. R. Taylor).

(61) MOLPRO is a package of ab initio programs written by H.-J. Werner, P. J. Knowles, M. Schütz, R. Lindh, P. Celani, T. Korona, G. Rauhut, F. R. Manby, R. D. Amos, A. Bernhardsson, A. Berning, D. L. Cooper, M. J. O. Deegan, A. J. Dobbyn, F. Eckert, C. Hampel, G. Hetzer, A. W. Lloyd, S. J. McNicholas, W. Meyer, M. E. Mura, A. Nicklaß, P. Palmieri, R. Pitzer, U. Schumann, H. Stoll, A. J. Stone, R. Tarroni, and T. Thorsteinsson.

(62) Straatsma, T.P.; Aprà, E.; Windus, T.L.; Bylaska, E.J.; de Jong, W.; Hirata, S.; Valiev, M.; Hackler, M. T.; Pollack, L.; Harrison, R. J.; Dupuis, M.; Smith, D.M.A; Nieplocha, J.; Tipparaju V.; Krishnan, M.; Auer, A. A.; Brown, E.; Cisneros, G; Fann, G. I.; Fruchtl, H.; Garza, J.; Hirao, K.; Kendall, R.; Nichols, J.; Tsemekhman, K.; Wolinski, K.; Anchell, J.; Bernholdt, D.; Borowski, P.; Clark, T.; Clerc, D.; Dachsel, H.; Deegan, M.; Dyll, K.; Elwood, D.; Glendenning, E.; Gutowski, M.; Hess, A.; Jaffe, J.; Johnson, B.; Ju, J.; Kobayashi, R.; Kutteh, R.; Lin, Z.; Littlefield, R.; Long, X.; Meng, B.; Nakajima, T.; Niu, S.; Rosing, M.; Sandrone, G.; Stave, M.; Taylor, H.; Thomas, G.; van Lenthe, J.; Wong, A.; Zhang, Z.; "NWChem, A Computational Chemistry Package for Parallel Computers, Version 4.6" (2004), Pacific Northwest National Laboratory, Richland, Washington 99352-0999, USA.

(63) Kendall, R.A.; Aprà, E.; Bernholdt, D.E.; Bylaska, E.J.; Dupuis, M.; Fann, G.I.; Harrison, R.J.; Ju, J.; Nichols, J.A.; Nieplocha, J.; Straatsma, T.P.; Windus, T.L.; Wong, A.T. *Computer Phys. Comm.*, **2000**, *128*, 260

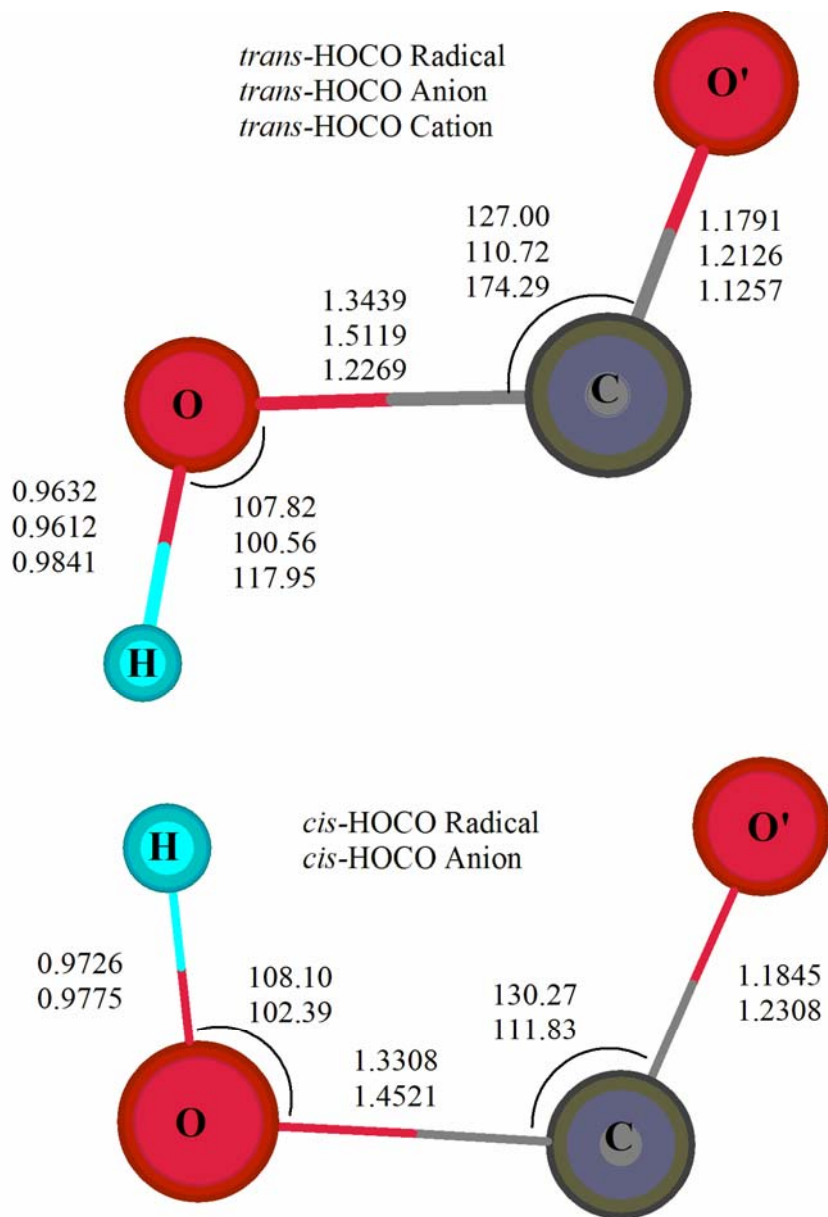


Figure 3.1: Equilibrium geometries for *trans*- and *cis*-isomers of HOCO species, C_s symmetry. Optimized geometrical parameters are given in Table 3.1.

TABLES

Table 3.1. The optimized geometrical parameters and rotational constants of *trans*- and *cis*-HOCO radical, anion, and cation. Bond lengths are in Å, bond angles are in degrees, and rotational constants are in GHz.^a

Molecule	Method	r(H-O)	r(O-C)	r(C-O')	θ(H-O-C)	θ(O-C-O')	A	B	C
<i>trans</i> -HOCO	aVQZ CCSD(T)	0.9632	1.3439	1.1791	107.82	127.00	166.251	11.455	10.717
	6-311G(3df,3pd) CCSD(T) ^b	0.962	1.345	1.179	107.4	126.8	164.962	11.470	10.724
	millimeter wave ^c						167.8478	11.43311	10.68676
<i>cis</i> -HOCO	aVQZ CCSD(T)	0.9726	1.3308	1.1845	108.10	130.27	141.085	11.767	10.861
<i>trans</i> -HOCO ⁻	aVQZ CCSD(T)	0.9612	1.5119	1.2126	100.56	110.72	94.563	11.508	10.259
	aVQZ QCISD(T) ^d	0.961	1.515	1.214	100.5	110.7	94.242	11.473	10.228
<i>cis</i> -HOCO ⁻	aVQZ CCSD(T)	0.9775	1.4521	1.2308	102.39	111.83	83.972	12.459	10.849
	aVQZ QCISD(T) ^d	0.978	1.454	1.232	102.3	111.8	83.763	12.435	10.828
<i>trans</i> -HOCO ⁺	aVQZ CCSD(T)	0.9841	1.2269	1.1257	117.95	174.29	754.826	10.742	10.592
	6-311G(3df,3pd) CCSD(T) ^b	0.983	1.228	1.126	117.7	174.3	751.500	10.736	10.585
	difference frequency ^e						789.9385	10.773636	10.609502
	submillimeter wave ^f						789.951154	10.7746768	10.6103741

^aaVQZ CCSD(T) represents the aug-cc-pVQZ CCSD(T) equilibrium geometries determined in this work.

^bReference 25.

^cReference 11.

^dReference 17.

^eReference 26.

^fReference 28.

Table 3.2. Vibrational frequencies of *trans*- and *cis*-HOCO anion, radical, and cation.^a

Molecule	Method	O-H stretch	C-O stretch	HOC bend	C-O' stretch	O'CO bend	Torsion
	<i>Symmetry</i>	<i>a'</i>	<i>a'</i>	<i>a'</i>	<i>a'</i>	<i>a'</i>	<i>a''</i>
<i>trans</i> -HOCO							
	aVTZ CCSD(T)	3805	1882	1253	1075	613	532
	6-31G(d) CCSD(T) ^b	3728	1903	1279	1084	605	538
	VTZ CCSD(T) ^c	3830	1898	1262	1087	620	533
	VTZ B3LYP ^d	3794	1903	1243	1084	622	546
	Ne matrix ^e	3628.0	1848.0	1210.4	1050.4		
	Ar matrix ^f	3602.9	1843.6	1211.2	1064.6		515
	CO matrix ^g	3456	1833	1261	1077	615	
	Gas Phase	3635.7 ^h	1852.57 ⁱ				
<i>cis</i> -HOCO							
	aVTZ CCSD(T)	3639	1843	1308	1071	600	571
	VTZ CCSD(T) ^c	3662	1860	1319	1077	608	578
	VTZ B3LYP ^d	3571	1867	1299	1074	600	594
	CO matrix ^g	3316	1797	1261	1088	620	
<i>trans</i> -HOCO ⁻							
	aVTZ CCSD(T)	3795	1654	1108	647	467	504
	aVDZ CCSD(T) ^j	3762	1639	1083	612	380	485
<i>cis</i> -HOCO ⁻							
	aVTZ CCSD(T)	3521	1572	1186	701	563	643
	aVDZ CCSD(T) ^j	3514	1551	1170	661	510	624
<i>trans</i> -HOCO ⁺							
		O-H stretch	C-O' stretch	C-O stretch	HOC bend	O'CO bend	Torsion
	aVTZ CCSD(T)	3549	2419	1237	1070	531	583

6-31G(d) CCSD(T) ^b	3479	2428	1240	1055	517	566
Gas Phase ^k	3375.37413					
Ne matrix ^l	3280.9	2400.4		1019.9		

^aaVTZ CCSD(T) represents aug-cc-pVTZ CCSD(T) harmonic vibrational frequencies determined in his work.

^bReference 25.

^cReference 16.

^dReference 19.

^eReference 7.

^fReference 6.

^gReference 5.

^hReference 8.

ⁱReference 9.

^jReference 17.

^kReference 26.

^lReference 27.

Table 3.3. Valence focal point analysis for adiabatic electron affinity (in eV) of *trans*- and *cis*-HOCO radicals.^a

Basis Set	ΔE_e [RHF]	+ δ [MP2]	+ δ [CCSD]	+ δ [CCSD(T)]	+ δ [CCSDT]	ΔE_e [CCSDT]
<i>trans</i> -HOCO						
aug-cc-pVDZ	0.2670	0.9420	-0.0077	0.0808	-0.0026	[1.2796]
aug-cc-pVTZ	0.2012	1.0623	-0.0540	0.0944	[-0.0026]	[1.3012]
aug-cc-pVQZ	0.1862	1.1032	-0.0723	0.0975	[-0.0026]	[1.3120]
aug-cc-pV5Z	0.1841	1.1211	-0.0832	0.0987	[-0.0026]	[1.3181]
aug-cc-pV6Z	0.1838	1.1307	-0.0892	[0.0992]	[-0.0026]	[1.3220]
CBS Limit	[0.1838]	[1.1439]	[-0.0974]	[0.1000]	[-0.0026]	[1.3276]
<i>cis</i> -HOCO						
aug-cc-pVDZ	0.3488	1.0076	-0.0205	0.0825	-0.0039	[1.4146]
aug-cc-pVTZ	0.2803	1.1360	-0.0671	0.0975	[-0.0039]	[1.4429]
aug-cc-pVQZ	0.2644	1.1787	-0.0861	0.1010	[-0.0039]	[1.4542]
aug-cc-pV5Z	0.2621	1.1970	-0.0970	0.1022	[-0.0039]	[1.4605]
aug-cc-pV6Z	0.2617	1.2064	-0.1029	[0.1028]	[-0.0039]	[1.4642]
CBS Limit	[0.2617]	[1.2195]	[-0.1110]	[0.1036]	[-0.0039]	[1.4698]
Extrapolation Scheme	$a+be^{-cX}$	$a+bX^{-3}$	$a+bX^{-3}$	$a+bX^{-3}$	additive	
Points (X=)	4,5,6	5,6	5,6	4,5		

^aThe symbol δ denotes the incremental correlation energy with respect to the previous level of theory in the hierarchy RHF->MP2->CCSD->CCSD(T)->CCSDT. Values in brackets are extrapolated according to the fitting formula in the last rows of the tables, while all other results were explicitly computed. Final predictions are in boldface.

Table 3.4. Valence focal point analysis for vertical detachment energy (in eV) of *trans*- and *cis*-HOCO radicals.^a

Basis Set	ΔE_c [RHF]	+ δ [MP2]	+ δ [CCSD]	+ δ [CCSD(T)]	+ δ [CCSDT]	ΔE_c [CCSDT]
<i>trans</i> -HOCO						
aug-cc-pVDZ	1.3355	0.3319	0.0971	-0.0054	-0.0068	[1.7523]
aug-cc-pVTZ	1.3379	0.4864	0.0719	-0.0037	[-0.0068]	[1.8857]
aug-cc-pVQZ	1.3356	0.5410	0.0617	-0.0031	[-0.0068]	[1.9285]
aug-cc-pV5Z	1.3353	0.5635	0.0535	-0.0029	[-0.0068]	[1.9425]
aug-cc-pV6Z	1.3354	0.5750	0.0484	[-0.0028]	[-0.0068]	[1.9491]
CBS Limit	[1.3353]	[0.5907]	[0.0414]	[-0.0027]	[-0.0068]	[1.9580]
<i>cis</i> -HOCO						
aug-cc-pVDZ	1.3292	0.5473	0.0131	0.0055	-0.0096	[1.8856]
aug-cc-pVTZ	1.3241	0.7066	-0.0175	0.0075	[-0.0096]	[2.0111]
aug-cc-pVQZ	1.3207	0.7596	-0.0289	0.0083	[-0.0096]	[2.0501]
aug-cc-pV5Z	1.3198	0.7813	-0.0373	0.0085	[-0.0096]	[2.0627]
aug-cc-pV6Z	1.3198	0.7920	-0.0420	[0.0086]	[-0.0096]	[2.0687]
CBS Limit	[1.3198]	[0.8067]	[-0.0486]	[0.0087]	[-0.0096]	[2.0769]

^aSee footnote “a” of Table 3.3.

Table 3.5. Valence focal point analysis for adiabatic and vertical ionization potential (in eV) of *trans*-HOCO radical.^a

Basis Set	ΔE_c [RHF]	+ δ [MP2]	+ δ [CCSD]	+ δ [CCSD(T)]	+ δ [CCSDT]	ΔE_c [CCSDT]
Adiabatic IP						
aug-cc-pVDZ	7.6412	0.2465	0.1543	-0.0011	0.0096	[8.0505]
aug-cc-pVTZ	7.5574	0.3524	0.1491	0.0095	[0.0096]	[8.0780]
aug-cc-pVQZ	7.5438	0.3813	0.1424	0.0128	[0.0096]	[8.0898]
aug-cc-pV5Z	7.5433	0.3936	0.1374	0.0140	[0.0096]	[8.0978]
aug-cc-pV6Z	7.5430	0.3993	0.1345	[0.0145]	[0.0096]	[8.1010]
CBS Limit	[7.5427]	[0.4072]	[0.1307]	[0.0152]	[0.0096]	[8.1053]
Vertical IP						
aug-cc-pVDZ	10.0113	-0.6274	0.2754	-0.1446	0.0072	[9.5219]
aug-cc-pVTZ	10.0066	-0.4938	0.3045	-0.1513	[0.0072]	[9.6733]
aug-cc-pVQZ	10.0064	-0.4457	0.3099	-0.1517	[0.0072]	[9.7261]
aug-cc-pV5Z	10.0066	-0.4266	0.3078	-0.1519	[0.0072]	[9.7430]
aug-cc-pV6Z	10.0066	-0.4172	0.3058	[-0.1520]	[0.0072]	[9.7505]
CBS Limit	[10.0067]	[-0.4042]	[0.3031]	[-0.1521]	[0.0072]	[9.7607]

^aSee footnote “a” of Table 3.3.

Table 3.6. Determination of adiabatic electron affinity (AEA), vertical detachment energy (VDE), adiabatic and vertical ionization potentials (AIP, VIP) of *trans*- and *cis*-HOCO radicals.

	$\Delta E_{\text{fp}}(\text{valence})$	$\Delta E_{\text{fp}}(\text{core})$	$\Delta Z\text{PVE}$	ΔDBOC	ΔREL	$\Delta E_{\text{e}}(\text{final})$
<i>trans</i> -HOCO						
AEA	1.3276	-0.0175	0.0610	-0.0012	0.0013	1.3712
VDE	1.9580	0.0061		-0.0006	-0.0017	1.9618
AIP	8.1053	-0.0093	0.0142	-0.0020	-0.0005	8.1077
VIP	9.7607	0.0213		-0.0009	-0.0040	9.7771
<i>cis</i> -HOCO						
AEA	1.4698	-0.0172	0.0524	-0.0027	0.0015	1.5038
VDE	2.0769	0.0048		-0.0009	0.0001	2.0809

Supplemental Materials

Table 3.7. Focal point analysis of core-correlation effects (in eV) for adiabatic electron affinity, vertical detachment energy, and ionization potentials of *trans*- and *cis*-HOCO radicals.^a

Basis Set	$\Delta E_{\text{fp}}(\text{core})[\text{MP2}]$	$+\delta[\text{CCSD}]$	$+\delta[\text{CCSD(T)}]$	$\Delta E_{\text{fp}}(\text{core})[\text{CCSD(T)}]$
AEA of <i>trans</i> -HOCO				
aug-cc-pCVDZ	-0.0046	-0.0039	0.0006	[-0.0079]
aug-cc-pCVTZ	-0.0082	-0.0056	0.0009	[-0.0129]
aug-cc-pCVQZ	-0.0104	-0.0061	0.0009	[-0.0156]
CBS Limit	[-0.0120]	[-0.0064]	[0.0010]	[-0.0175]
AEA of <i>cis</i> -HOCO				
aug-cc-pCVDZ	-0.0039	-0.0041	0.0007	[-0.0073]
aug-cc-pCVTZ	-0.0076	-0.0058	0.0010	[-0.0124]
aug-cc-pCVQZ	-0.0099	-0.0064	0.0011	[-0.0152]
CBS Limit	[-0.0116]	[-0.0068]	[0.0011]	[-0.0172]
VDE of <i>trans</i> -HOCO				
aug-cc-pCVDZ	0.0047	-0.0026	-0.0001	[0.0019]
aug-cc-pCVTZ	0.0108	-0.0044	-0.0012	[0.0051]
aug-cc-pCVQZ	0.0119	-0.0048	-0.0015	[0.0057]
CBS Limit	[0.0128]	[-0.0050]	[-0.0017]	[0.0061]
VDE of <i>cis</i> -HOCO				
aug-cc-pCVDZ	0.0051	-0.0034	0.0000	[0.0018]
aug-cc-pCVTZ	0.0098	-0.0048	-0.0010	[0.0039]
aug-cc-pCVQZ	0.0109	-0.0052	-0.0013	[0.0044]
CBS Limit	[0.0116]	[-0.0054]	[-0.0014]	[0.0048]

<i>AIP of trans-HOCO</i>				
aug-cc-pCVDZ	-0.0076	-0.0008	-0.0006	[-0.0089]
aug-cc-pCVTZ	-0.0047	-0.0020	-0.0012	[-0.0079]
aug-cc-pCVQZ	-0.0046	-0.0026	-0.0016	[-0.0087]
CBS Limit	[-0.0045]	[-0.0030]	[-0.0019]	[-0.0093]
<i>VIP of trans-HOCO</i>				
aug-cc-pCVDZ	0.0043	0.0028	-0.0026	[0.0045]
aug-cc-pCVTZ	0.0189	0.0024	-0.0057	[0.0156]
aug-cc-pCVQZ	0.0233	0.0022	-0.0067	[0.0189]
CBS Limit	[0.0265]	[0.0022]	[-0.0074]	[0.0213]
Extrapolation Scheme	$a+bX^{-3}$	$a+bX^{-3}$	$a+bX^{-3}$	
Points (X=)	3,4	3,4	3,4	

^aSee footnote a of Table 3.3.

CHAPTER 4

ENERGETICS AND STRUCTURES OF ADAMANTANE AND THE 1- AND 2-ADAMANTYL RADICALS, CATIONS AND ANIONS¹

¹Yan, G.; Brinkmann, N. R.; Schaefer, H. F.; *Journal of Physical Chemistry A.*; 2003; 107(44); 9479-9485. Reprinted by permission of the American Chemical Society.

4.1 ABSTRACT

Equilibrium structures and harmonic vibrational frequencies were computed for adamantane (Ad), the 1- and 2-adamantyl radicals (1-Ad \cdot , 2-Ad \cdot), cations (1-Ad $^+$, 2-Ad $^+$), and anions (1-Ad $^-$, 2-Ad $^-$). Ionization potentials and electron affinities of Ad, 1-Ad \cdot and 2-Ad \cdot have been predicted using four different density functional and hybrid Hartree–Fock/density functional methods. The equilibrium structure of adamantane (T_d symmetry) is in excellent agreement with electron diffraction experiments. 1-Ad \cdot and 1-Ad $^-$ are predicted to lie about 4 kJ mol $^{-1}$ below their 2-isomers, while 1-Ad $^+$ is predicted to lie 47 kJ mol $^{-1}$ below 2-Ad $^+$. For 1-Ad \cdot , 1-Ad $^+$, and 1-Ad $^-$, C_{3v} structures are found to be the minima, while a C_s structure lies lowest for 2-Ad \cdot , 2-Ad $^+$, and 2-Ad $^-$. The final predicted adiabatic ionization potentials for the radicals are 6.22 (1-Ad \cdot) and 6.70 eV (2-Ad \cdot). The vertical radical ionization potentials are necessarily larger: 6.85 (1-Ad \cdot) and 7.08 eV (2-Ad \cdot). The predicted adiabatic electron affinities are all negative: -0.13 (1-Ad \cdot) and -0.13 eV (2-Ad \cdot). The vertical electron affinities are: -0.28 (1-Ad \cdot) and -0.37 eV (2-Ad \cdot). The vertical detachment energies are 0.07 (1-Ad $^-$) and 0.22 eV (2-Ad $^-$).

4.2 INTRODUCTION

Adamantane has been the subject of much chemical interest because of its highly symmetric cage structure. Schleyer's 1957 synthesis¹ transformed adamantane from an exotic species into one of the staples of organic chemistry. Adamantane and its derivatives have a broad range of chemical,^{2,3} polymer^{4,5} and pharmaceutical⁶⁻⁹ applications. Compounds containing adamantyl radicals are useful catalysts for many chemical reactions,^{2,3} such as the refining of halogen atoms and preparation of heterogeneous bimetallic catalysts. The rigid, spherical structure of adamantane reduces interchain interaction in polymers and helps the synthesis of polymers,^{4,5}

such as MAE-PPV. Adamantane-containing molecules have also been found to have antiviral activity. They have been used in the treatment of influenza,⁶ HIV-1,⁷ leukemia and deafness,⁸ and many other diseases.⁹

Adamantane and its derivatives have been the subject of many studies, both experimental and theoretical. The molecular structure of adamantane was determined by Hargittai, et al. in 1972 using gas-phase electron diffraction.¹⁰ Adamantane has also been studied with two-dimensional Penning ionization electron spectroscopy,¹¹ by which the adiabatic (IP_a) and vertical (IP_v) ionization potentials were reported as 9.40 and 9.67 eV, respectively. Valuable information concerning the 1- and 2-adamantyl radicals (1-Ad \cdot and 2-Ad \cdot) was obtained by Kruppa and Beauchamp using photoelectron spectroscopy,¹² and the IP_a and IP_v were found for each system (IP_a : 6.21 ± 0.03 eV, IP_v : 6.36 ± 0.05 eV for 1-Ad \cdot , IP_a : 6.73 ± 0.03 eV, IP_v : 6.99 ± 0.05 eV for 2-Ad \cdot). ESR studies have been performed on 2-Ad \cdot ,¹³ and a planar radical site was suggested. Electron impact appearance energies were used to measure the heats of formation of the 1- and 2-adamantyl cations (1- and 2-Ad $^+$) and 2-Ad \cdot ,¹⁴ and these were recently computed using the G2(MP2) methodology.¹⁵ The Raman and IR spectra of adamantane and 2-adamantanone were computed using density functional theory.¹⁶ Dutler, Rauk, Sorensen, and Whitworth used the MP2/6-31G* method to study 2-Ad $^+$ and proposed that the ground electronic state has C_s symmetry.¹⁷ However, very little experimental research has been reported for the adamantyl anions, because of their apparent general instability. Complete molecular structures for the adamantyl radicals and anions are not available. Theoretical predictions on the properties of these species can thus provide valuable information concerning their relative stabilities and reactivities.

Density functional theory (DFT) has been shown to be a relatively inexpensive and reliable theoretical method for predicting ionization potentials (IPs) as well as electron affinities (EAs).^{18,19} Using a moderate DZP++ basis set, DFT has been exhaustively tested and shown to predict molecular EAs to within 0.15 eV of the experimentally reported values on average.¹⁹ In the present study we predicted the structures, vibrational frequencies, and relative energies of adamantane, 1- and 2-Ad[•], 1- and 2-Ad⁺, and 1- and 2-Ad⁻ as well as IPs and EAs of 1- and 2-Ad[•] to investigate the relative stabilities and reactivity of these species.

4.3 METHODS

The DFT quantum chemical computations were performed on Ad, 1- and 2-Ad[•], 1- and 2-Ad⁺ and 1- and 2-Ad⁻ using the Gaussian 94 program package.²⁰ Several gradient-corrected functionals, denoted B3LYP, BHLYP, BLYP and BP86, were used to compute the geometries, energies, and harmonic vibrational frequencies. Energies were converged to at least 10^{-6} hartrees in the self-consistent-field procedures, although the absolute accuracy may be somewhat lower, due to errors inherent in the numerical integration procedures.

The different functionals used may be described as follows. B3LYP is a hybrid Hartree-Fock and density functional theory (HF/DFT) method using Becke's three-parameter gradient-corrected exchange functional (B3)²¹ with the Lee-Yang-Parr's correlation functional (LYP).²² The BHLYP functional combines Becke's half-and-half exchange functional²³ (BH) with the LYP correlation functional and is a HF/DFT method. BLYP uses Becke's 1988 exchange function (B)²⁴ and the LYP functional, and BP86 is formed from the Becke's exchange functional (B) and the 1986 correlation correction of Perdew (P86).²⁵ Geometries were optimized for each molecular species with each functional using analytic gradient technique. Residual

Cartesian gradients were less than 1.5×10^{-5} hartrees/Bohr. Stationary points found in optimizations were confirmed as minimum by computing the harmonic vibrational frequencies using analytic second derivatives with each functional.

A double- ζ basis set with polarization and diffuse functions, denoted DZP++, was utilized in this study. The basis set was constructed from the Huzinaga-Dunning^{26,27} set of contracted double- ζ Gaussian functions. Added to this was one set of p -type polarization functions for each H atom and one set of d -type polarization functions for each C atom [$\alpha_p(\text{H})=0.75$ and $\alpha_d(\text{C})=0.75$]. To complete the DZP++ basis, the above set of functions was augmented with an “even-tempered” s diffuse function for each H atom and “even-tempered” s and p diffuse functions for each C atom with orbital exponents determined by the formula expressed by Lee and Schaefer²⁸ [$\alpha_s(\text{H})=0.04415$, $\alpha_s(\text{C})=0.04302$, and $\alpha_p(\text{H})=0.03629$]. The final contraction scheme for this basis is H [5s1p/3s1p] and C [10s6p1d/5s3p1d].

IPs and EAs were evaluated as differences in total energies between molecular species. The classical adiabatic IPs are defined as

$$\text{IP}_a = E_{(\text{optimized cation})} - E_{(\text{optimized radical})};$$

the classical adiabatic IPs with zero-point corrections are

$$\text{IP}_a = E_{(\text{zero-point corrected cation})} - E_{(\text{zero-point corrected radical})};$$

the vertical IPs are determined by

$$\text{IP}_v = E_{(\text{cation at optimized radical geometry})} - E_{(\text{optimized radical})};$$

The classical adiabatic EAs are defined as

$$\text{EA}_a = E_{(\text{optimized radical})} - E_{(\text{optimized anion})};$$

the vertical EAs are

$$\text{EA}_v = E_{(\text{optimized radical})} - E_{(\text{anion at optimized radical geometry})};$$

and the vertical detachment energies computed via

$$\text{VDE} = E_{\text{(radical at optimized anion geometry)}} - E_{\text{(optimized anion)}}$$

4.4 RESULTS AND DISCUSSION

A. STRUCTURES AND ENERGETICS

Optimized structures of Ad, 1- and 2-Ad[•], Ad⁺ and Ad⁻ with all functionals are shown in Figures 1-3, and geometrical parameters are summarized in Tables I to VII. The total and relative ground state energies of Ad, 1- and 2-Ad[•], Ad⁺, Ad⁻ are summarized in Tables VIII and IX.

The theoretical geometry of the T_d symmetry adamantane (Table I) is in excellent agreement with the electron diffraction experiments. The B3LYP predicted geometry is the closest to experimental values, with C-C and C-H bond lengths of 1.544 Å and 1.100 Å, respectively, and the C-C_{sec}-C and C-C_{ter}-C bond angles of 109.7° and 109.4°, respectively.

For the molecular anion 1-Ad⁻ (Table IV), the ground state is found to possess C_{3v} symmetry. The geometry change at the formal anionic center is rather small compared to neutral adamantane. At the DZP++ B3LYP level, The C⁻-C_α bond length was shortened by 0.019 Å and the C_α-C⁻-C_α angle is decreased by 0.5° upon the removal of the proton from Ad. The C_α-C_β bond length is increased by 0.014 Å and the C⁻-C_α-C_β angle is decreased by 1.5°.

In the case of 2-Ad⁻ (Table VII), C_s symmetry is found for the ground state rather than the more symmetrical C_{2v} structure. The vibrational frequency analysis shows a C_{2v} imaginary frequency (553i cm⁻¹ with the B3LYP method) for the out-of-plane bending mode of the C⁻-H bond for the 2-Ad⁻ structure, leading to the C_s minimum. The potential energy surface is found to be rather flat, with an energy difference of 20.0 kJ mol⁻¹ between the C_{2v} and C_s structures at the DZP++/B3LYP level. The geometry change at the formal anionic site is similar to that of 1-Ad⁻.

The C⁻-C_α bond length was shortened by 0.010 Å and the C_α-C⁻-C_α angle is decreased by 1.5°, while the C_α-C_β bond length is increased by 0.019 Å and the C⁻-C_α-C_β angle decreased by 3.3°. The 1-Ad⁻ anion is 2.6 (B3LYP), -2.1 (BHLYP), 6.6 (BLYP), and 5.5 (BP86) kJ mol⁻¹ lower in energy than the 2-isomer, respectively.

For the radical 1-Ad[·] (Table II), the ground state is found to have C_{3v} symmetry. The geometry change at the radical site with respect to the neutral Ad is quite substantial. At the DZP++/B3LYP level, The C[·]-C_α bond length was shortened by 0.044 Å and the C_α-C[·]-C_α angle is increased by 3.6° upon the removal of one proton from the neutral Ad, whereas the C_α-C_β bond length is increased by 0.019 Å and C[·]-C_α-C_β angle decreased by 3.7°.

The ground state of 2-Ad[·] is also found in C_s symmetry (Table V). At the DZP++/B3LYP level, The C[·]-C_α bond length was shortened by 0.029 Å and the C_α-C[·]-C_α angle is increased by 5.9° upon the removal of one electron from the formal anionic site of 2-Ad[·]. The potential energy surface near the minimum is rather flat, with only a 0.23 kJ mol⁻¹ energy difference between the C_s and C_{2v} isomers with the B3LYP functional. Bond lengths and bond angles for the two structures are quite similar. However, the dihedral angle between the C_α-C[·]-C_α plane and the α-H of the C_s structure was decreased by 19.3° from the 180° value for the C_{2v} structure. The 1-Ad[·] radical is 3.0 (B3LYP), 1.2 (BHLYP), 4.4 (BLYP), and 4.7 (BP86) kJ mol⁻¹ lower in energy than the 2-isomer, respectively.

The ground state of the cation 1-Ad⁺ is found to possess C_{3v} symmetry (Table III). The geometry change at what was the radical site prior to ionization is quite substantial. At the DZP++/B3LYP level, the C⁺-C_α bond length is shorter by 0.048 Å and the C_α-C⁺-C_α angle is increased by 4.9° upon the removal of the electron from the radical site of 1-Ad[·]. The C_α-C_β bond length is increased by 0.063 Å and C⁺-C_α-C_β angle decreased by 7.3°.

For the 2-Ad⁺ cation, Dutler, *et al.* used the MP2/6-31G* method and suggested a ground electronic state with C_s symmetry rather than the more symmetric C_{2v} symmetry.¹⁷ This is confirmed by the present research (Table VI). The energy difference between the C_{2v} and C_s structures is 7.1 kJ mol⁻¹ at the DZP++/B3LYP level. The geometry change at the formal cationic site is similar to that of the 1-Ad⁺. A natural bond orbital analysis has been performed on the 2-Ad⁺ cation and a positive natural charge of 0.270 was found at what was the radical site prior to ionization. Compared with 2-Ad[·], the C⁺-C_α bond length is shorter by 0.060 Å and the C_α-C⁺-C_α angle has increased by 5.9° upon the removal of the electron from the radical site, and the C_α-C_β bond length is lengthened by 0.078 Å and the C⁺-C_α-C_β angle decreased by 10.8°. The 1-Ad⁺ cation is found to be 47.4 (B3LYP), 46.3 (BHLYP), 47.5 (BLYP), and 49.0 (BP86) kJ mol⁻¹ lower in energy than the 2-isomer, respectively.

At the DZP++/B3LYP level, 1-Ad[·] was found to be lowest in energy among 1-Ad[·], Ad⁺ and Ad⁻ (Table VIII). The energy difference between 1-Ad[·] and 1-Ad⁻ is quite small, with 1-Ad⁻ predicted to lie only 12.9 kJ mol⁻¹ higher than 1-Ad[·]. 1-Ad⁺ is of course much higher in energy than the neutral radical, lying 591.6 kJ mol⁻¹ above the neutral. These energy differences are similar for the case of the 2-Ad series (Table IX), with 2-Ad⁻ lying 12.5 kJ mol⁻¹ higher in energy than 2-Ad[·], and 2-Ad⁺ 636.0 kJ mol⁻¹ above 2-Ad[·]. This energy ordering is consistent with the predicted ordering at the BHLYP and BLYP levels of theory. However, using DZP++/BHLYP level of theory, much larger energy differences between the anions and the neutral radicals are predicted. Both 1-Ad⁻ and 2-Ad⁻ were both found to lie about 50 kJ mol⁻¹ above that of their radical counterparts. It is clear that the electron affinities of both the 1- and 2-adamantyl radicals are close to zero, explaining the difficulty observed in preparing the anions.

B. IONIZATION POTENTIALS

Adiabatic and vertical ionization potentials (IP_a , IP_v) were computed and are shown in Table X. For 1-Ad', the IP_a predicted by four different functionals range from 5.84 eV (BLYP) to 6.13 eV (B3LYP). Zero-point vibrational energy (ZPVE) corrections by the B3LYP method added 0.03 eV to the results. With the ZPVE corrections, all but the BLYP functional are within 0.02 eV of the photoelectron spectroscopy result reported by Kruppa and Beauchamp,¹² which is 6.21 ± 0.03 eV. BLYP underestimates the ionization potentials by 0.34 eV, and B3LYP gives the closest agreement with the experimental result. The IP_v of 1-Ad' is larger than the IP_a by as much as 0.60 (B3LYP), 0.66 (B3LYP), 0.53 (BLYP), and 0.54 (BP86) eV, respectively. This is attributed to the significant differences between the geometries of 1-Ad' and 1-Ad⁺. B3LYP overestimates the IP_a of 1-Ad' by almost 0.5 eV, and BLYP (6.37 eV) gives the best agreement with experiment (6.36 ± 0.05 eV).¹²

For 2-Ad', the B3LYP result of 6.70 eV (6.66 eV without ZPVE corrections) was found to give the best agreement with the experimental IP_a of 6.73 ± 0.03 eV. The B3LYP and BP86 values are both within 0.20 eV of the experimental value, while BLYP underestimates the IP_a by 0.41 eV. The B3LYP and BP86 results are within 0.1 eV of the experimental IP_v of 2-Ad' (6.99 ± 0.05 eV). BP86 underestimates the IP_v by 0.16 eV, and BLYP underestimates it by almost 0.40 eV.

C. ELECTRON AFFINITIES

Adiabatic and vertical electron affinities and vertical detachment energies (EA_a , EA_v , VDE) of the adamantyl radicals are shown in Table XI. For 1-Ad', the predicted adiabatic EAs range from -0.55 (B3LYP) to 0.07 eV (BP86). Only the BP86 functional gives a positive EA. ZPVE

corrections increase the EA_a by as much as 0.14 eV. This is an expected result of the anions being more loosely held together entities. Rienstra-Kiracofe, Barden, Brown, and Schaefer²⁹ used DFT to study the EAs of several polycyclic aromatic hydrocarbons including benzene, naphthalene, anthracene, tetracene, and perinaphthenyl radical, and comparable ZPVE corrections were found for their systems.

The EA_v differs considerably from the EA_a for 1-Ad⁻. This is attributed to the significant geometry difference between 1-Ad⁻ and 1-Ad⁻. All four functionals predicted a negative EA_v , with the most negative value (-0.77 eV) reported by the BHLYP functional and the least negative value (-0.04 eV) by the BP86 functional. The geometry difference between 1-Ad⁻ and 1-Ad⁻ also leads to VDEs that are quite different from the adiabatic EAs. Only BHLYP predicted a negative value (-0.24 eV) for the VDE of 1-Ad⁻ while the other three functionals predicted positive VDEs, with the largest value (0.23 eV) reported by the BP86 functional. The dipole moment of 1-Ad⁻ at the 1-Ad⁻ equilibrium geometry is predicted to be 1.1 debye; thus the 1-Ad⁻ anion would not be dipole bound.

The adiabatic EAs of 2-Ad⁻ are quite similar to those of 1-Ad⁻. BHLYP gives the lowest value of -0.51 eV, followed by B3LYP (-0.13 eV) and BLYP (-0.07 eV). BP86 is the only functional to give a positive EA_a (0.06 eV). The B3LYP ZPVE correction is 0.09 eV. The vertical EAs are also negative for 2-Ad⁻ using each functional. BHLYP gives the lowest EA_v , -0.82 eV, while BP86 gives the highest value, -0.15 eV. For the VDEs, only BHLYP predicted a negative value of -0.09 eV, while the other three functionals predicted positive VDEs.

D. VIBRATIONAL FREQUENCIES

The observed and computed vibrational frequencies of Ad are given in Table XII. The vibrational frequencies of 1- and 2- Ad[•], Ad⁺, and Ad⁻ computed by the B3LYP method are given in Tables XIII and XIV. Bistričić, Baranović, and Mlinarić-Majerski have reported Raman and infrared spectra, as well as a scaled semiempirical force field based on the vibrational assignments for Ad.³⁰ In our reported DFT harmonic vibrational frequencies without scaling factors, the qualitative agreement with the experiment is good. The B3LYP, BLYP, and BP86 functionals all give mean absolute errors of less than 50 cm⁻¹. The BHLYP functional is the worst in predicting the vibrational frequencies, with the largest mean absolute error (98 cm⁻¹), as one might expect because BHLYP includes 50% Hartree-Fock exchange. No experimental vibrational spectra for 1- and 2- Ad[•], Ad⁺, or Ad⁻ have been reported, and we have predicted their harmonic vibrational frequencies using the B3LYP method. The vibrational frequencies of the adamantyl anions are generally smaller than those of the radicals, while the adamantyl cations have the largest vibrational frequencies for the same modes, compared with the anions and neutral radicals.

4.5 CONCLUSIONS

In the extensive review of Rienstra-Kiracofe, Tschumper, and Schaefer¹⁹ on the electron affinities from photoelectron experiments and theoretical computations, it was found that DFT EA results tend to overestimate experimental values for all but the BHLYP functional. Rienstra-Kiracofe *et al.*¹⁹ also found that for the EAs in closed-shell anion to open-shell neutral systems (like 1- and 2- Ad[•] to Ad[•]), the B3LYP functional gives the smallest average absolute errors compared to experimental results. Therefore it is reasonable to argue that the true electron

affinities for the systems studied here should lie between the predicted values of B3LYP and the other functionals and should be closest to the B3LYP predicted values. Also we have found that the ZPVE corrections are as large as 0.13 eV for the 1-Ad \cdot and 0.10 eV for the 2-Ad \cdot . However, the negative EAs suggested non-bound anions, and ZPVE corrections are not necessary for these cases. Therefore it is reasonable to give theoretical predictions for EAs from the B3LYP results without ZPVE corrections. Our final predicted values are: EA_a -0.13 eV(1- and 2-Ad \cdot); EA_v -0.28 eV(1-Ad \cdot), -0.37 eV(2-Ad \cdot); VDE 0.07 eV(1-Ad \cdot), 0.22 eV(2-Ad \cdot). It is clear that the adamantyl radicals do not readily attract an electron. Of course, suitable substituted adamantyl radicals are expected to have positive electron affinities.

4.6 ACKNOWLEDGMENTS

This work was supported by the Department of Energy, through its Combustion and SciDAC Research Programs.

4.7 REFERENCES

- (1) Schleyer, P. v. R. *J. Am. Chem. Soc.* **1957**, *79*, 3292.
- (2) Beller, M.; Ehrentraut, A.; Fuhrmann, C.; Zapf, A. *PCT Int. Appl.* **2002**, 41.
- (3) Taoufik, M.; Santini, C. C.; Basset, J.-M. *J. Organomet. Chem.* **1999**, *580*, 128.
- (4) Jeong, H. Y.; Lee, Y. K.; Talaie, A.; Kim, K. M.; Kwon, Y. D.; Jang, Y. R.; Yoo, K. H.; Choo, D. J.; Jang, J. *Thin Solid Films* **2002**, *417*, 171.
- (5) Mathias, L. J.; Jensen, J. J.; Reichert, V. R.; Lewis, C. M.; Tullos, G. L. *Polym. Prepr: (Am. Chem. Soc., Div. Polym. Chem.)* **1995**, *36*, 741.

- (6) Stotskaya, L. L.; Serbin, A. V.; Munshi, K.; Kozeletskaya, K. N.; Sominina, A. A.; Kiselev, O. I.; Zaitseva, K. V.; Natochin, Y. V. *Khimiko-Farmatsevticheski Zhurnal* **1995**, *29*, 19.
- (7) Boukrinskaia, A. G.; Serbin, A. V.; Bogdan, O. P.; Stotskaya, L. L.; Alymova, I. V.; Klimochkin, Y. N. *PCT Int. Appl.* **1995**, 32.
- (8) Ruppertsberg, J. P.; Fakler, B. P. *PCT Int. Appl.* **2002**, 31.
- (9) Spasov, A. A.; Khamidova, T. V.; Bugaeva, L. I.; Morozov, I. S. *Pharm. Chem. J. (Translation of Khim.-Farm. Zh.)* **2000**, *34*, 1.
- (10) Hargittai, I.; Hedberg, K. In *Molecular Structures and Vibrations*; Cyvin, S. J., Ed.; Elsevier, 1972, p 340.
- (11) Tian, S. X.; Kishimoto, N.; K., H. *J. Phys. Chem. A* **2002**, *106*, 6541.
- (12) Kruppa, G. H.; Beauchamp, J. L. *J. Am. Chem. Soc.* **1985**, *108*, 2162.
- (13) Kira, M.; Akiyama, M.; Ichinose, M.; Sakurai, H. *J. Am. Chem. Soc.* **1989**, *111*, 8256.
- (14) Aubry, C.; Holmes, J. L.; Walton, J. C. *J. Phys. Chem. A* **1998**, *102*, 1389.
- (15) Abboud, J.-L. M.; Castano, O.; Davalos, J. Z.; Gomperts, R. *Chemical Physics Letters* **2001**, *337*, 327.
- (16) Bisticic, L.; Pejov, L.; Baranovic, G. *J. Molecular Structure (Theochem)* **2002**, *594*, 79.
- (17) Dutler, R.; Rauk, A.; Sorensen, T. S.; Whitworth, S. M. *J. Am. Chem. Soc.* **1989**, *111*, 9024.
- (18) Proft, F. D.; Geerlings, P. *J. Chem. Phys.* **1997**, *106*, 3270.

- (19) Rienstra-Kiracofe, J. C.; Tschumper, G. S.; Schaefer, H. F.; Nandi, S.; Ellison, G. B. *Chem. Rev.* **2002**, *102*, 231.
- (20) Gaussian 94; Revision C.3.; Frisch, M. J.; Trucks, G. W.; Schlegel, H. B.; Gill, P. M. W.; Johnson, B. G.; Robb, M. A.; Cheeseman, J. R.; Keith, T.; Petersson, G. A.; Montgomery, J. A.; Raghavachari, K.; Al-Laham, M. A.; Zakrzewski, V. G.; Ortiz, J. V.; Foresman, J. B.; Cioslowski, J.; Stefanov, B. B.; Nanayakkara, A.; Challacombe, M.; Peng, C. Y.; Ayala, P. Y.; Chen, W.; Wong, M. W.; Andres, J. L.; Replogle, E. S.; Gomperts, R.; Martin, R. L.; Fox, D. J.; Binkley, J. S.; Defrees, D. J.; Baker, J.; Stewart, J. P.; Head-Gordon, M.; Gonzalez, C.; Pople, J. A.; Gaussian, Inc.: Pittsburgh, PA, U.S.A., 1995.
- (21) Becke, A. D. *J. Chem. Phys.* **1993**, *98*, 5648.
- (22) Lee, C.; Yang, W.; Parr, R. G. *Phys. Rev. B.* **1988**, *37*, 785.
- (23) Becke, A. D. *J. Chem. Phys.* **1993**, *98*, 1372.
- (24) Becke, A. D. *Phys. Rev. A.* **1988**, *38*, 3098.
- (25) Perdew, J. P. *Phys. Rev. B.* **1986**, *33*, 8822.
- (26) Huzinaga, S. *J. Chem. Phys.* **1965**, *42*, 1293.
- (27) Dunning, T. H. *J. Chem. Phys.* **1970**, *53*, 2823.
- (28) Lee, T. J.; Schaefer, H. F. *J. Chem. Phys.* **1985**, *83*, 1784.
- (29) Rienstra-Kiracofe, J. C.; Barden, C. J.; Brown, S. T.; Schaefer, H. F. *J. Phys. Chem. A* **2001**, *105*, 524.
- (30) Bisticic, L.; Baranovic, G.; Mlinaric-Majerski, K. *Spectrochim. Acta A* **1995**, *51*, 1643.

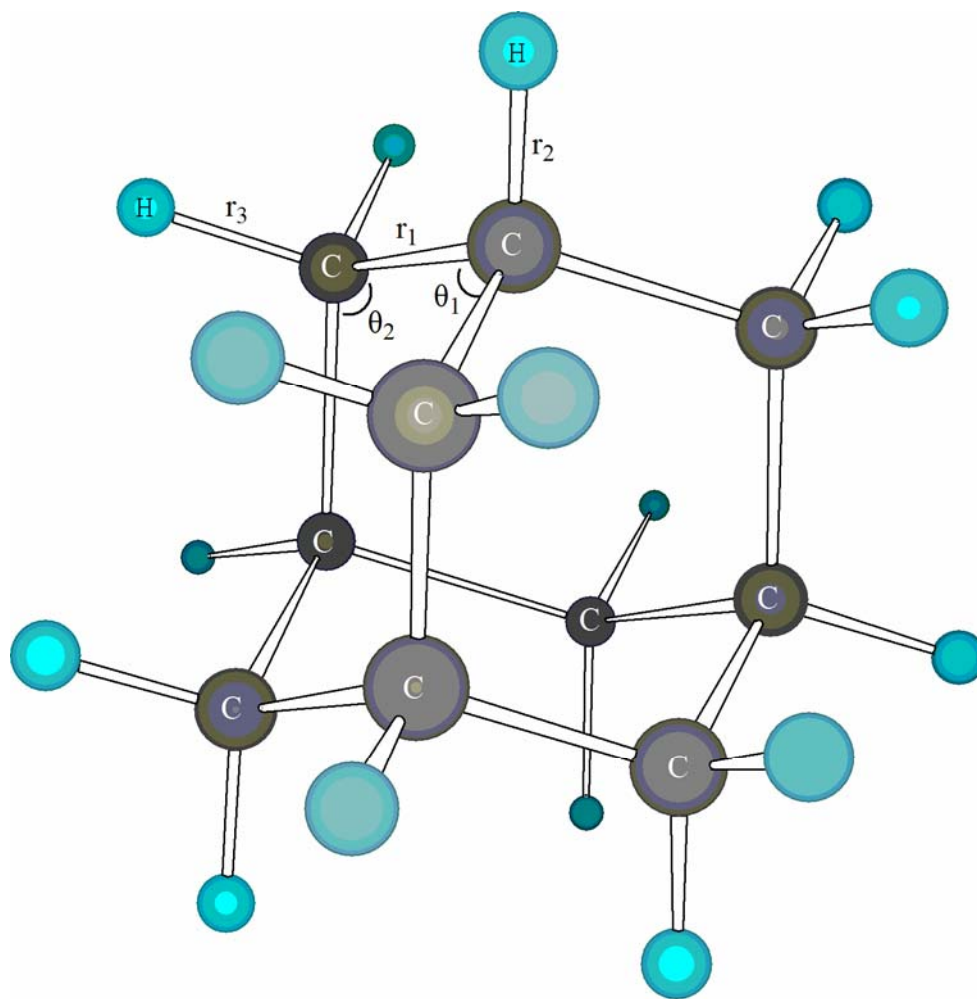


Figure 4.1. Adamantane ($C_{10}H_{16}$), T_d symmetry. Optimized geometrical parameters are given in Table 4.1.

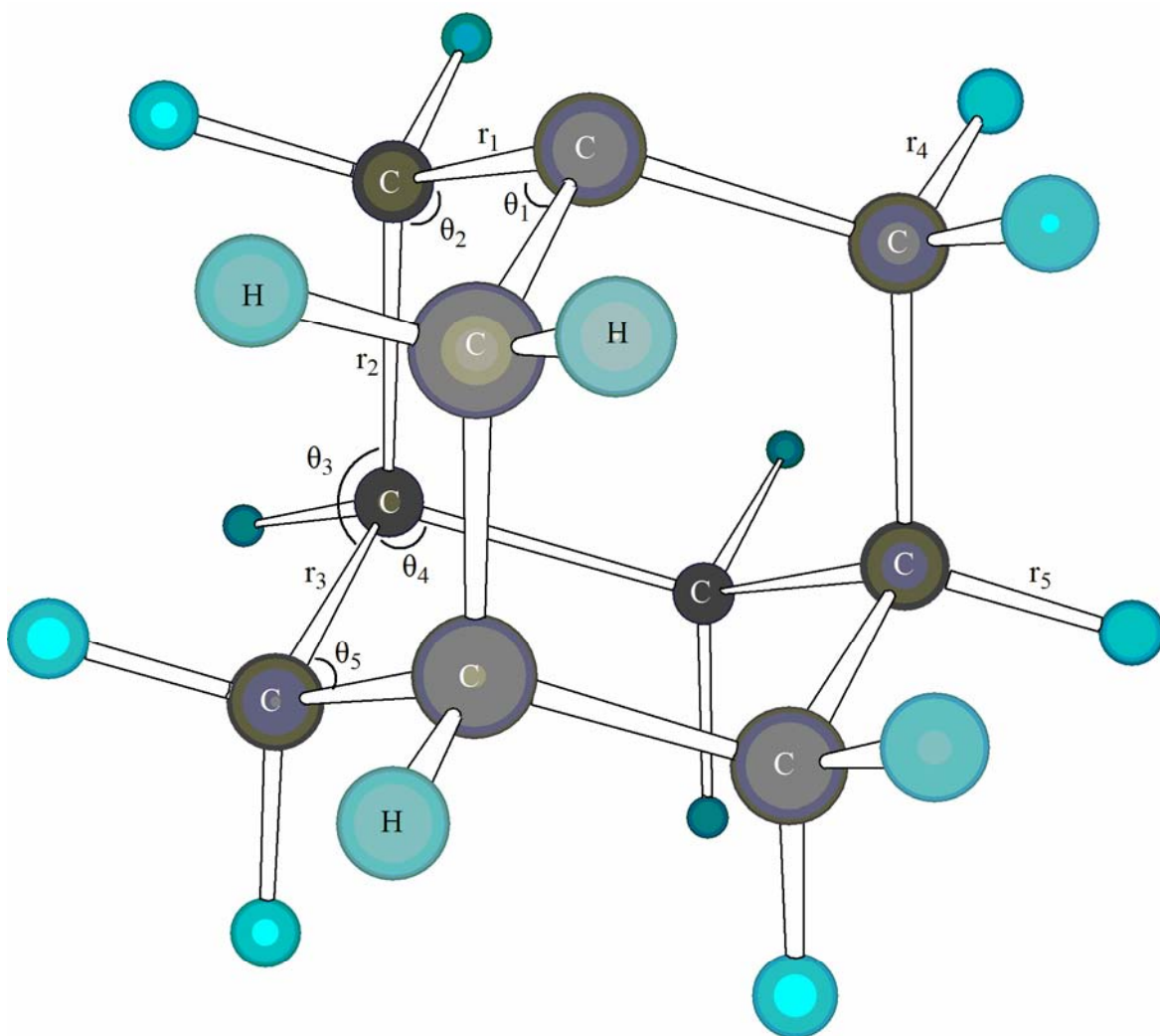


Figure 4.2. 1-Adamantyl radical, 1-adamantyl cation, and 1-adamantyl anion ($C_{10}H_{15}$), C_{3v} symmetry. Optimized geometrical parameters are given in Tables 4.2 - 4.4, respectively.

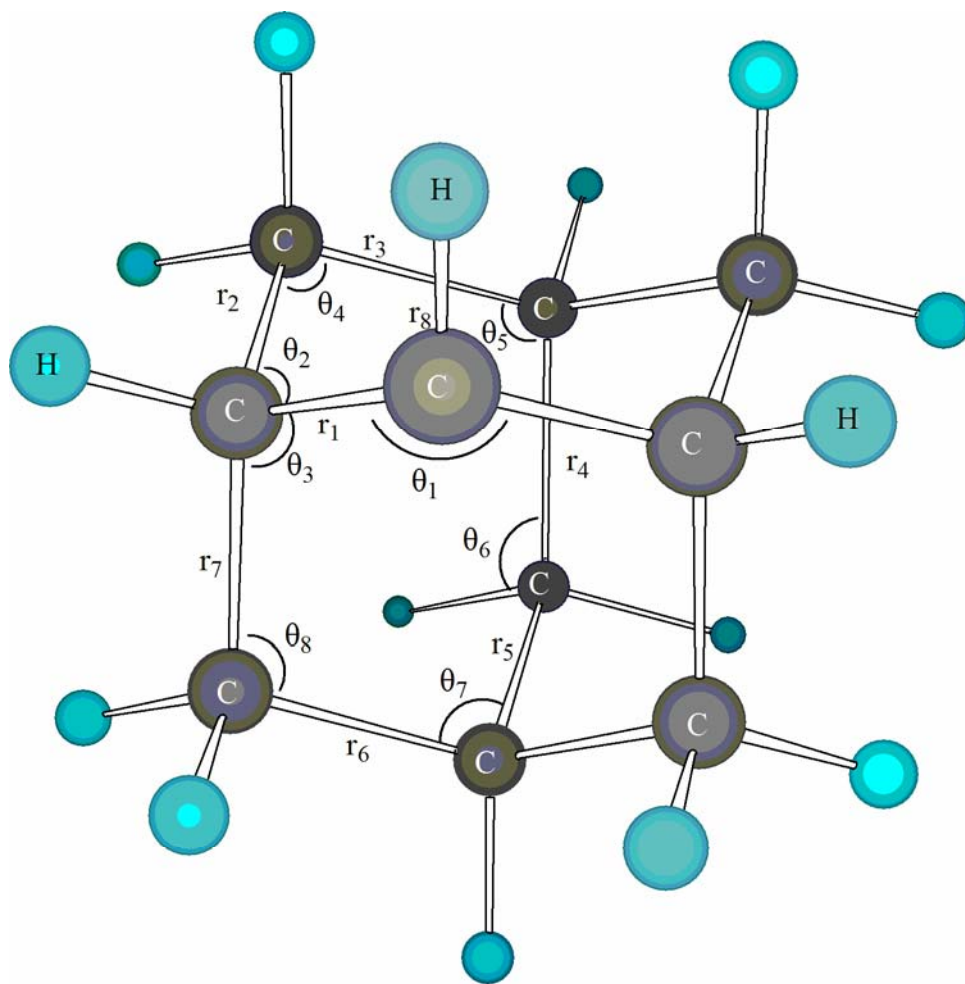


Figure 4.3. 2-Adamantyl radical, 2-adamantyl cation, and 2-adamantyl anion ($C_{10}H_{15}$), C_s symmetry. Optimized geometrical parameters are given in Tables 4.5- 4.7, respectively.

TABLES

Table 4.1. Optimized geometry of adamantane ($C_{10}H_{16}$, T_d). Bond lengths are in Å and bond angles are in degrees. Geometric parameters correspond to those labeled in Figure 4.1.

method	B3LYP	BHLYP	BLYP	BP86	Experiment ^a
r_1	1.544	1.533	1.557	1.549	1.540±0.002
r_2	1.100	1.091	1.108	1.109	1.112±0.004
r_3	1.101	1.092	1.108	1.109	1.112±0.004
θ_1	109.4	109.3	109.4	109.4	109.8±0.5
θ_2	109.7	109.7	109.7	109.7	108.8±1

^aReference 10.

Table 4.2. Optimized structures of the 1-adamantyl radical ($C_{10}H_{15}$, C_{3v}). Bond lengths are in Å and bond angles are in degrees.

Geometric parameters correspond to those labeled in Figure 4.2.

method	B3LYP	BHLYP	BLYP	BP86
r_1	1.509	1.502	1.518	1.512
r_2	1.563	1.548	1.579	1.569
r_3	1.545	1.534	1.558	1.550
r_4	1.100	1.091	1.107	1.109
r_5	1.101	1.091	1.109	1.110
θ_1	113.0	112.9	113.1	113.1
θ_2	106.0	106.1	106.0	105.9
θ_3	108.9	109.0	108.8	108.8
θ_4	109.6	109.5	109.7	109.6
θ_5	110.2	110.2	110.1	110.2

Table 4.3. Optimized structures of the 1-adamantyl cation ($C_{10}H_{15}$, C_{3v}). Bond lengths are in Å and bond angles are in degrees.

Geometric parameters correspond to those labeled in Figure 4.2.

method	B3LYP	BHLYP	BLYP	BP86
r_1	1.461	1.454	1.470	1.465
r_2	1.626	1.604	1.648	1.634
r_3	1.537	1.527	1.548	1.540
r_4	1.093	1.085	1.100	1.102
r_5	1.096	1.087	1.104	1.105
θ_1	117.9	117.9	117.8	117.8
θ_2	98.7	98.5	99.0	98.8
θ_3	108.2	108.4	108.0	108.0
θ_4	111.4	111.1	111.7	111.7
θ_5	109.8	109.7	109.9	109.9

Table 4.4. Optimized structures of the 1-adamantyl anion ($C_{10}H_{15}$, C_{3v}). Bond lengths are in Å and bond angles are in degrees.

Geometric parameters correspond to those labeled in Figure 4.2.

method	B3LYP	BHLYP	BLYP	BP86
r_1	1.525	1.524	1.530	1.525
r_2	1.558	1.547	1.569	1.561
r_3	1.545	1.533	1.558	1.550
r_4	1.109	1.099	1.117	1.118
r_5	1.112	1.100	1.122	1.123
θ_1	108.8	107.6	109.9	109.6
θ_2	111.2	112.3	110.0	110.4
θ_3	108.7	108.9	108.6	108.6
θ_4	109.3	109.2	109.5	109.5
θ_5	110.0	109.8	110.2	110.2

Table 4.5. Optimized structures of the 2-adamantyl radical ($C_{10}H_{15}$, C_s). Bond lengths are in Å and bond angles are in degrees.

Geometric parameters correspond to those labeled in Figure 4.3.

method	B3LYP	BHLYP	BLYP	BP86
r_1	1.505	1.499	1.512	1.507
r_2	1.560	1.545	1.567	1.558
r_3	1.545	1.534	1.558	1.549
r_4	1.544	1.532	1.557	1.549
r_5	1.544	1.533	1.557	1.548
r_6	1.545	1.533	1.558	1.549
r_7	1.552	1.538	1.575	1.565
r_8	1.090	1.081	1.097	1.098
θ_1	114.1	113.8	114.3	114.2
θ_2	108.6	108.0	109.1	109.0
θ_3	109.1	109.0	108.3	108.2
θ_4	108.1	109.5	109.5	109.5
θ_5	109.4	109.3	109.4	109.4

θ_6	109.6	109.7	109.6	109.6
θ_7	109.9	109.4	109.4	109.3
θ_8	109.3	109.7	109.4	109.4

Table 4.6. Optimized structures of the 2-adamantyl cation ($C_{10}H_{15}$, C_s). Bond lengths are in Å and bond angles are in degrees.

Geometric parameters correspond to those labeled in Figure 4.3.

method	B3LYP	BHLYP	BLYP	BP86
r_1	1.445	1.439	1.454	1.450
r_2	1.638	1.613	1.662	1.647
r_3	1.530	1.522	1.539	1.532
r_4	1.544	1.532	1.557	1.548
r_5	1.543	1.532	1.556	1.548
r_6	1.540	1.530	1.552	1.544
r_7	1.547	1.535	1.562	1.551
r_8	1.095	1.086	1.102	1.103
θ_1	119.9	120.0	119.7	119.7
θ_2	97.7	97.4	98.6	97.7
θ_3	114.6	114.3	114.5	114.8
θ_4	108.2	108.6	107.9	108.0
θ_5	111.2	110.9	111.4	111.5

θ_6	109.8	109.9	109.5	109.5
θ_7	109.8	109.8	109.8	109.7
θ_8	109.9	109.9	109.9	109.9

Table 4.7. Optimized structures of the 2-adamantyl anion ($C_{10}H_{15}$, C_s). Bond lengths are in Å and bond angles are in degrees.

Geometric parameters correspond to those labeled in Figure 4.3.

method	B3LYP	BHLYP	BLYP	BP86
r_1	1.534	1.530	1.540	1.535
r_2	1.563	1.549	1.576	1.567
r_3	1.547	1.535	1.561	1.553
r_4	1.545	1.534	1.557	1.549
r_5	1.545	1.534	1.558	1.550
r_6	1.546	1.534	1.559	1.551
r_7	1.549	1.537	1.563	1.554
r_8	1.110	1.093	1.108	1.110
θ_1	108.2	107.5	109.2	108.8
θ_2	112.6	113.0	111.9	112.3
θ_3	109.5	109.4	109.7	109.5
θ_4	109.2	109.4	109.0	109.1
θ_5	108.9	109.0	108.9	108.9

θ_6	109.6	109.6	109.6	109.6
θ_7	109.1	109.0	109.1	109.0
θ_8	109.4	109.5	109.4	109.4

TABLE 4.8. Total electronic energies in hartrees and relative electronic energies in kJ mol^{-1} of the 1-adamantyl cation, anion, and radical. Total energies of each system are followed by the relative energies.

method	B3LYP		BHLYP		BLYP		BP86	
1-Ad ⁺	-389.89031	591.6	-389.65228	597.1	-389.65106	563.1	-389.87865	583.2
1-Ad ⁻	-390.11070	12.9	-389.85967	52.6	-389.86373	4.7	-390.10341	-6.9
1-Ad [·]	-390.11563	0.0	-389.87971	0.0	-389.86551	0.0	-390.10080	0.0

TABLE 4.9. Total electronic energies in hartrees and relative electronic energies in kJ mol^{-1} of the 2-adamantyl cation, anion, and radical. Total energies of each system are followed by the relative energies.

method	B3LYP		BHLYP		BLYP		BP86	
2-Ad ⁺	-389.87227	636.0	-389.63465	642.2	-389.63298	606.1	-389.86001	627.5
2-Ad ⁻	-390.10973	12.5	-389.86047	49.3	-389.86121	6.9	-390.10131	-6.0
2-Ad [·]	-390.11449	0.0	-389.87925	0.0	-389.86384	0.0	-390.09901	0.0

TABLE 4.10. Adiabatic ionization potentials (in eV) of the 1- and 2-adamantyl radicals. Zero-point energy corrected values are listed in parentheses. Vertical ionization potentials are listed in boldface.

molecule	B3LYP	BHLYP	BLYP	BP86	Experiment ^a
1-Ad [•]	6.13	6.19	5.84	6.04	
	(6.16)	(6.22)	(5.87)	(6.08)	6.21 ± 0.03
	6.73	6.85	6.37	6.58	6.36 ± 0.05
2-Ad [•]	6.59	6.66	6.28	6.50	
	(6.63)	(6.70)	(6.32)	(6.55)	6.73 ± 0.03
	6.97	7.08	6.60	6.83	6.99 ± 0.05

^aReference 11.

TABLE 4.11. Adiabatic electron affinities (in eV) of the 1- and 2-adamantyl radicals. Zero-point energy corrected values are listed in parentheses. Vertical electron affinities are listed in bold face, and vertical detachment energy are in italics.

molecule	B3LYP	BHLYP	BLYP	BP86
1-Ad [•]	-0.13	-0.55	-0.05	0.07
	(0.00)	(-0.41)	(0.08)	(0.21)
	-0.28	-0.77	-0.14	-0.04
	<i>0.07</i>	<i>-0.24</i>	<i>0.08</i>	<i>0.23</i>
2-Ad [•]	-0.13	-0.51	-0.07	0.06
	(-0.04)	(-0.42)	(0.01)	(0.16)
	-0.37	-0.82	-0.27	-0.15
	<i>0.22</i>	<i>-0.09</i>	<i>0.20</i>	<i>0.37</i>

TABLE 4.12. Observed and computed vibrational wavenumbers ω_e (in cm^{-1}) for adamantane. Infrared intensities (in km mol^{-1}) larger than 1 km mol^{-1} are shown in parenthesis following the wavenumbers.

mode	Symmetry	Experiment ^a	B3LYP	BHLYP	BLYP	BP86
ω_1	A ₁	2950	3048	3147	2964	2972
ω_2	A ₁	2913	3013	3109	2930	2937
ω_3	A ₁	1472	1519	1573	1480	1467
ω_4	A ₁	990	1049	1093	1015	1015
ω_5	A ₁	756	755	787	726	741
ω_6	A ₂	1189	1124	1165	1092	1088
ω_7	E	2900	3015	3109	2934	2941
ω_8	E	1439	1483	1536	1446	1429
ω_9	E	1370	1401	1464	1351	1356
ω_{10}	E	1217	1228	1277	1190	1189
ω_{11}	E	953	922	959	887	906
ω_{12}	E	402	412	422	403	402
ω_{13}	T ₁	-	3054	3149	2971	2984

ω_{14}	T ₁	1321	1341	1399	1299	1291
ω_{15}	T ₁	1288	1317	1380	1266	1276
ω_{16}	T ₁	-	1125	1170	1091	1086
ω_{17}	T ₁	1043	1060	1103	1018	1035
ω_{18}	T ₁	-	901	932	876	871
ω_{19}	T ₁	-	340	341	335	338
ω_{20}	T ₂	2940	3060 (109)	3156 (109)	2976 (117)	2987 (102)
ω_{21}	T ₂	2910	3037 (179)	3135 (163)	2952 (207)	2962 (186)
ω_{22}	T ₂	2850	3015 (38)	3109 (43)	2933 (26)	2939 (47)
ω_{23}	T ₂	1455	1497 (11)	1550 (11)	1459 (10)	1444 (12)
ω_{24}	T ₂	1359	1380	1440	1336	1331
ω_{25}	T ₂	1310	1340	1408	1284	1292
ω_{26}	T ₂	1101	1115 (3)	1159 (3)	1081 (3)	1081 (3)
ω_{27}	T ₂	970	981 (1)	1018 (1)	948 (1)	957 (2)
ω_{28}	T ₂	800	817 (1)	846 (1)	788	805 (1)
ω_{29}	T ₂	638	657	678	639	639

ω_{30}	T_2	444	458	467	449	447
---------------	-------	-----	-----	-----	-----	-----

^aReference 30.

TABLE 4.13 Harmonic vibrational wavenumbers ω_e (in cm^{-1}) for the 1-adamantyl radical, anion, and cation by the B3LYP method. Infrared intensities (in km mol^{-1}) larger than 1 km mol^{-1} are shown in parenthesis following the wavenumbers.

mode	Symmetry	1-Ad \cdot	1-Ad $^-$	1-Ad $^+$
ω_1	A $_1$	3060 (105)	2984 (28)	3109 (6)
ω_2	A $_1$	3044 (15)	2969 (86)	3106 (1)
ω_3	A $_1$	3023 (99)	2910 (9)	3099 (1)
ω_4	A $_1$	3012 (7)	2869 (238)	3063 (1)
ω_5	A $_1$	1509	1492 (1)	1540 (3)
ω_6	A $_1$	1491 (12)	1448	1496 (15)
ω_7	A $_1$	1349	1334 (9)	1320 (4)
ω_8	A $_1$	1266 (5)	1242 (14)	1203 (61)
ω_9	A $_1$	1097 (5)	1085	1081 (29)
ω_{10}	A $_1$	1028 (1)	997 (28)	1010 (10)
ω_{11}	A $_1$	924 (1)	918 (37)	882 (3)
ω_{12}	A $_1$	778 (3)	761 (45)	826 (1)
ω_{13}	A $_1$	757 (1)	742 (27)	766 (3)

ω_{14}	A ₁	636 (6)	556 (220)	682 (16)
ω_{15}	A ₁	439	404 (62)	468
ω_{16}	A ₂	3065	2942	3169
ω_{17}	A ₂	1337	1332	1335
ω_{18}	A ₂	1303	1302	1290
ω_{19}	A ₂	1124	1114	1130
ω_{20}	A ₂	1110	1108	1087
ω_{21}	A ₂	1048	1048	1050
ω_{22}	A ₂	901	874	927
ω_{23}	A ₂	311	328	289
ω_{24}	E	3071 (89)	2989 (133)	3175 (2)
ω_{25}	E	3054 (12)	2958 (272)	3104 (11)
ω_{26}	E	3034 (196)	2945 (149)	3102 (4)
ω_{27}	E	3018 (6)	2905 (778)	3096 (1)
ω_{28}	E	3013 (14)	2880 (324)	3059 (8)
ω_{29}	E	1487 (11)	1476 (2)	1520 (23)

ω ₃₀	E	1476	1447 (2)	1475 (12)
ω ₃₁	E	1387	1377 (12)	1411 (2)
ω ₃₂	E	1362	1353 (2)	1381 (1)
ω ₃₃	E	1333	1313 (21)	1351 (6)
ω ₃₄	E	1294 (1)	1274 (19)	1276 (5)
ω ₃₅	E	1260	1242 (1)	1210 (18)
ω ₃₆	E	1173	1161 (3)	1135
ω ₃₇	E	1113 (3)	1100 (36)	1095 (13)
ω ₃₈	E	1041	1034 (22)	1020 (16)
ω ₃₉	E	984 (2)	976 (28)	983 (9)
ω ₄₀	E	920	909 (8)	895
ω ₄₁	E	890	888 (5)	859 (17)
ω ₄₂	E	799	787 (26)	737 (5)
ω ₄₃	E	638 (1)	651	569 (19)
ω ₄₄	E	447	447	460 (1)
ω ₄₅	E	395	406	358 (8)

ω_{46}	E	320	315 (2)	337 (4)
---------------	---	-----	---------	---------

TABLE 4.14. Harmonic vibrational wavenumbers ω_e (in cm^{-1}) for the 2-adamantyl radical, anion, and cation by the B3LYP method. Infrared intensities (in km mol^{-1}) are shown in parenthesis following the wavenumbers.

mode	Symmetry	2-Ad \cdot	2-Ad $^-$	2-Ad $^+$
ω_1	A'	3178 (35)	3054 (47)	3160
ω_2	A'	3068 (79)	3031 (97)	3129 (12)
ω_3	A'	3063 (94)	2991 (167)	3116 (4)
ω_4	A'	3057 (2)	2977 (89)	3113 (14)
ω_5	A'	3042 (127)	2966 (28)	3087 (14)
ω_6	A'	3036 (128)	2959 (109)	3074 (7)
ω_7	A'	3017 (4)	2941 (26)	3066 (8)
ω_8	A'	3014 (19)	2916 (281)	3058 (17)
ω_9	A'	3012 (20)	2865 (771)	3045 (4)
ω_{10}	A'	1508 (2)	1494 (2)	1518 (2)
ω_{11}	A'	1485 (10)	1467 (25)	1497 (16)
ω_{12}	A'	1482 (4)	1466 (15)	1487 (7)
ω_{13}	A'	1394	1374 (1)	1440 (11)

ω ₁₄	A'	1377	1361 (1)	1380
ω ₁₅	A'	1375	1349 (9)	1369 (1)
ω ₁₆	A'	1337	1326 (1)	1345 (4)
ω ₁₇	A'	1326	1311 (19)	1322
ω ₁₈	A'	1318	1296 (3)	1318
ω ₁₉	A'	1271	1261 (6)	1228 (17)
ω ₂₀	A'	1225	1201 (8)	1180 (9)
ω ₂₁	A'	1124	1110	1128 (2)
ω ₂₂	A'	1103 (2)	1090 (4)	1108 (5)
ω ₂₃	A'	1063 (1)	1066 (2)	1077 (7)
ω ₂₄	A'	1046	1041 (1)	1056 (2)
ω ₂₅	A'	1023 (1)	1016 (1)	1018 (4)
ω ₂₆	A'	964 (2)	959 (3)	982 (11)
ω ₂₇	A'	947 (2)	933 (1)	948 (4)
ω ₂₈	A'	911	900	929 (2)
ω ₂₉	A'	816 (1)	804 (5)	875 (19)

ω ₃₀	A'	799 (1)	787 (10)	810 (1)
ω ₃₁	A'	759	749 (2)	791 (1)
ω ₃₂	A'	681 (2)	731 (129)	742 (3)
ω ₃₃	A'	652	647 (5)	667 (16)
ω ₃₄	A'	535 (10)	628 (105)	619 (1)
ω ₃₅	A'	438	461 (8)	443
ω ₃₆	A'	406	441 (6)	435 (6)
ω ₃₇	A'	349 (4)	393 (36)	372 (4)
ω ₃₈	A'	214 (17)	317 (12)	326 (7)
ω ₃₉	A''	3066 (26)	3049	3127
ω ₄₀	A''	3060 (5)	3026 (6)	3117 (1)
ω ₄₁	A''	3056 (152)	3009 (99)	3111 (11)
ω ₄₂	A''	3055 (24)	2966 (461)	3102 (12)
ω ₄₃	A''	3018 (78)	2946 (18)	3070 (3)
ω ₄₄	A''	3013 (31)	2869 (617)	3064 (15)
ω ₄₅	A''	1486 (11)	1465	1515 (32)

ω ₄₆	A''	1470	1452 (6)	1480
ω ₄₇	A''	1381	1381	1465 (2)
ω ₄₈	A''	1374	1349 (1)	1387
ω ₄₉	A''	1341	1321	1346
ω ₅₀	A''	1333	1316	1325 (12)
ω ₅₁	A''	1321	1306 (1)	1307
ω ₅₂	A''	1304	1258 (13)	1292 (6)
ω ₅₃	A''	1261	1244 (8)	1201 (12)
ω ₅₄	A''	1161	1153	1178 (1)
ω ₅₅	A''	1125 (1)	1112 (1)	1160
ω ₅₆	A''	1122	1102 (7)	1111
ω ₅₇	A''	1112 (3)	1094 (4)	1098 (2)
ω ₅₈	A''	1069	1049 (11)	1063 (15)
ω ₅₉	A''	1050	1026 (17)	990 (35)
ω ₆₀	A''	983 (1)	977 (3)	976 (5)
ω ₆₁	A''	906	899	896

ω_{63}	A''	896	895 (2)	877
ω_{63}	A''	884	862 (1)	844 (22)
ω_{64}	A''	797	786	666 (18)
ω_{65}	A''	644	646 (1)	581 (26)
ω_{66}	A''	446	447	441 (1)
ω_{67}	A''	401	406	353 (5)
ω_{68}	A''	313	322	301
ω_{69}	A''	305	317 (1)	169 (27)

CHAPTER 5

CONCLUDING REMARKS

Development of modern quantum mechanical methods and advent of faster computers have revolutionized the way chemists understand the world. Scientific computations performed on laboratory computer clusters and national supercomputing centers have yielded abundant theoretical results of various qualities, from qualitative description of reaction pathways, to accurate determinations of relative energies. Computational data have already played an important role in predicting, confirming, or even challenging experimental discoveries.

In carrying out computational chemistry research work, a sensible choice of computational methods is essential to achieve proper balance between chemical accuracy and computational cost. In this work, three molecular systems of different sizes have been investigated by different theoretical methods to illustrate the accuracy and applicability of modern quantum mechanical methods to real world problems.

In the first two investigations, two small yet fundamental systems have been studied with highly accurate *ab initio* methods. For these two molecular systems, propargyl and hydroxyformyl radicals, only three non-hydrogen heavy atoms are present, which enable accurate theoretical computations with high level computational methods within a reasonable amount of period. Such high accuracy computations usually employ correlated methods such as MP2, CCSD, CCSD(T) and even CCSDT, where the scaling factor can be as high as N^8 , with N being the number of basis functions. Large basis sets such as aug-cc-pVXZ ($X=2-6$) are routinely used in such studies to provide a more accurate and complete description of molecular orbitals. Theoretical results from such calculations are usually of chemical or even subchemical accuracy due to the extensive and rigorous treatment of correlation energies, and agreement between *ab initio* and available experimental results are usually excellent.

For larger systems, however, high level *ab initio* methods will be inapplicable due to

extremely expensive computational cost. In Chapter 4, we have examined the geometries and energetics of adamantane and several of its derivatives. For such large systems which contain ten heavy atoms, high level *ab initio* computations such as the coupled cluster methods will take tremendous amount of time to finish. As such, methods based on density functional theory (DFT) are usually employed in these cases. As a method depends on electron density instead of wave function, DFT is much faster than highly correlated *ab initio* methods with a N^4 scaling factor, yet it yields adequately accurate results that still provide many useful insights into large chemical systems out of reach by *ab initio* method with current computing power, therefore it becomes the natural choice for computational studies of larger molecules.

Through these three studies, the importance of computational chemistry in modern chemistry has been clearly demonstrated. With properly chosen theoretical methods, detailed information about chemical systems can be accurately determined from informed computations. As the computing power continuously to increase, computational chemistry will play an even more important role in broad areas of modern chemistry.